Broadband Rotor Noise Analyses

NASA

NASA Contractor Report 3797

Broadband Rotor Noise Analyses

Albert R. George and Shau-Tak Chou
Cornell University
Ithaca, New York

Prepared for
Langley Research Center
under Grant NAG1-107

NASA
National Aeronautics
and Space Administration

**Scientific and Technical
Information Office**

1984

BROADBAND ROTOR NOISE ANALYSES

TABLE OF CONTENTS

SUMMARY

A study is made of the various mechanisms which generate broadband noise on a range of rotors. The sources considered are load fluctuations due to inflow turbulence, due to turbulent boundary layers passing the blades' trailing edges, and due to tip vortex formation. Our past work had been the first to identify and present analyses of these mechanisms. In the present work we review these and other investigators' prediction mechanisms, determine their limitations, and make significant extensions to allow more accurate prediction of rotor noise spectra. Our analyses, although evaluated by computer programs, are primarily analytical and thus helpful in understanding the nature of the noise generation. Comparisons to more numerically based approaches show that our analyses are accurate but restricted to advance ratios of less than approximately 0.4 (which include all cases of practical interest). All present broadband analyses leave out in-plane force mechanisms and are thus restricted to angles which are not too close to the rotor plane. Vortex shedding noise due to laminar boundary layers and blunt trailing edges are not considered as they can be prevented in most cases.

An extensive search was made of existing experiments and then calculations based on the various prediction methods were made for comparison purposes. This study shows that present analyses are adequate to predict the spectra from a wide variety of experiments on fans, full scale and model scale helicopter rotors, wind turbines, and propellers to within about 5 to 10 dB. Better knowledge of the inflow turbulence improves the accuracy of the predictions.

The results of this study indicate that inflow turbulence noise depends strongly on ambient conditions and dominates at low frequencies. Trailing edge noise and tip vortex noise are important at higher frequencies if inflow turbulence is weak. Boundary layer trailing edge noise is important, especially for large sized rotors. This noise increases slowly with angle of attack but not as rapidly as tip vortex noise, which can be important at high angles of attack for wide chord, square edge tips.

INTRODUCTION

Despite extensive research over the past fifty years and particularly over the last fifteen years, the relative importances of various rotor noise mechanisms are only now becoming understood. The accuracies of the existing analyses are also hard to document. The primary reason for these difficulties is that there are a large number of noise mechanisms on rotors which can be important in different parts of the acoustic frequency spectrum, depending upon the rotor parameters and operating environment. The wide variety of source mechanisms is due to various aeroacoustic effects: boundary layers, separated flow, and inflow turbulence; high Mach numbers, including nonlinear effects; blade-vortex interactions; non-uniform inflow; etc. (1). In general, the mechanisms each affect different parts of the acoustic spectrum. Then, on craft with either tandem or main and tail rotors, many of these mechanisms can interact with each other and between rotors. Thus, in many cases, it is not clear which mechanisms are dominant in many operating conditions for full scale helicopters, propellers, etc. This study addresses a part of the problem - broadband noise. It reviews and extends broadband noise analyses and compares calculations based on various analyses of broadband noise mechanisms to each other and to available experimental data. The aims of this work are to help understand which broadband noise mechanisms are important under which circumstances, to identify a number of satisfactory, existing , and well-documented experimental measurements, and to evaluate the various analytical approaches by comparing them to each other and to the chosen experiments. It will be seen that several satisfactory analytical approaches are available and their limitations will be delineated. These approaches can show which mechanisms are important in which cases and are able to predict absolute spectra to within about five dB for clean experiments.

The frequencies of interest in rotor noise are usually determined by human annoyance (or detection, in some cases). The common measures of annoyance, such as the perceived noise level (PNdB) or A-weighted sound level (dBA), account for the fact that humans find low frequencies, say below a few hundred Hertz, much less annoying. On the other hand, if long distance propagation is a factor for the rotor in question, then high frequencies can be attenuated significantly by molecular absorption. For example, after propagation over one kilometer, frequencies above a few thousand Hertz are attenuated drastically (1). Thus frequencies in the range from a few hundred to several thousand hertz are of primary interest.

The amount of power radiated by a rotor is generally extremely small compared with the aerodynamic power consumed by the rotor (by a factor of order at least one to ten thousand). Thus the acoustics do not affect the rotor performance to any extent. Noise is radiated by forces, volume displacements, or nonlinearities which are either unsteady or vary in their effects when considered in terms of retarded time (1). In general, rotor noise can be divided into three categories:

1. Discrete frequency noise (sometimes called rotational or harmonic noise) is caused by steady or harmonically varying forces, volume displacements, or nonlinear flow effects. For low to moderate blade tip Mach number these can be due to the basic blade rotation and forward flight of a helicopter or to steady inflow variations. These mechanisms have been analyzed by Gutin, Deming, Hubbard, Lowson, and Wright. The steady loading noise is generally

restricted to the first dozen or so harmonics of the blade passing frequency. Thus it is not usually of importance to helicopter main rotors or large wind turbines as these frequencies lie in the frequency range below 100 Hz where human ears are not very sensitive. These low order harmonics are, however, very important to the cases of high RPM propellers or tail rotors. Harmonically varying effects can, in principle, be important at higher frequencies for all rotors. But, in fact, the higher frequency noises tend to be caused by loads, displacements, or nonlinearities which are impulsive, due to high Mach numbers, or are randomly varying (caused by turbulence). In these cases the phenomena are better analyzed as impulsive or broadband noise as discussed below.

2. Impulsive noise (sometimes called blade slap) consists of nearly distinct repeated pulses at blade-passing frequency. After being Fourier analyzed, the repeated pulses will yield discrete or harmonic spectra, but their particular identity is due to their impulsive time histories and origins. These pulses are caused particularly by events at certain blade azimuth angles such as blade-vortex interactions or local transonic blade motion toward the observer (say Mach number greater than approximately 0.75). These noise sources have been analyzed by Widnall, Ffowcs Williams and Hawkings, Farassat, Hanson, and Schmitz et al., and George and Chang (2-9). Impulsive noise is unquestionably the most important noise source on helicopter or wind turbine rotors when it exists. However, a prime goal of aeroacoustic rotor design or operation is to avoid impulsive noise generation by control of blade-vortex interactions and by avoiding high tip Mach number. This often leaves broadband noise as the important controlling noise in many situations where relative tip speeds are not transonic and blade-vortex interactions are avoided.

3. Broadband noise, which is the subject of this study, has a continuous (although sometimes humped or peaked) spectrum and is caused by disturbances which are not precisely repeated at each blade revolution but which are basically random in nature. These random disturbances are generally due to some sort of turbulence interacting with the rotor blades. The turbulence can either be incident on the blade from the ambient atmosphere or can be generated by the blade motion itself. Recent reviews of broadband noise research may be found in references 10 and 11.

BROADBAND NOISE MECHANISMS AND ANALYSES

For this study, various analyses of broadband noise were programmed and extended. Emphasis is placed on 'first principles' analyses, which make absolute predictions of noise spectra. These analyses are not based on empirical correlation equations and do not require the determination of empirical constants for different families of rotors. Computations were made for many types of rotors in order to compare different analyses of the same mechanisms to each other and to available experiments. This enabled us to determine which mechanisms are important for different rotor parameters and for different parts of the audible spectrum. A few comparisons are also given for some of the scaling law based correlations available in the literature.

Historically, the first broadband noise prediction methods were based on empirical correlation of overall sound pressure level (OASPL) as, for example, by Widnall (12). Previously, very early investigators had erroneously identified broadband noise with some sort of turbulent 'vortex shedding' from the rear of the blades, hence the early name 'vortex noise' was used. Actually most broadband noise is due to force fluctuations on the blades due to influences of turbulent flows. Later it was found that in the atypical case of laminar flow, the laminar boundary layers on blades can indeed shed nearly regular vortices at the trailing edges and thus can radiate a narrow peaked broadband sound, sometimes called 'high frequency broadband noise'. (See e.g. Paterson et al., reference 13, Aravmudan et al., reference 14.) However, this source is not important for most full scale rotors, except perhaps for helicopter tail rotors or small fans. Even in these cases it can be eliminated easily by tripping the boundary layers, see e.g. reference 14.

According to the origin of the noise produced, the source mechanisms considered in this study can be divided into the following categories :

INFLOW TURBULENCE NOISE

The analysis of the sound generated by the unsteady loadings due to turbulence fluctuations on unducted subsonic rotors began with the quite general analysis of Homicz and George (15). They treated the general case of unsteady forces distributed in space, following the Lighthill equation of aeroacousics with specialization to rotating blades. See figure 1 for geometry. They devised an analysis for the sound radiated from arbitrarily varying forces on a rotor disk. The analysis was applied to the varying loadings on a rotating blade in the disk. The loadings were obtained from an approximate compressible aerodynamic analysis for an inflow of isotropic turbulence defined by the Dryden spectrum. Inflow turbulence was seen to be an important noise source over a range of frequencies. The analysis also explained the humped or peaked nature of the low frequency part of the spectrum as being due to the large scale components of the turbulence inflow. These large scale components give nearly periodic (i.e. modulated) disturbances as they are swept through the rotor plane; this leads to a nearly periodic but finite bandwidth radiated sound. This analysis is not well suited for high frequencies since large CPU times are required for the calculations. Thus, later high frequency analyses were developed by George and Kim (16) and by Amiet (17), and variations on them were made by Harris and co-workers (18,19).

The high frequency analysis of George and Kim (16) treated the problem in a different way. They approximated the distributed blade forces as rotating concentrated forces (dipoles) using the result of Ffowcs Williams and Hawkings (20). The analysis assumed the force components in the observer direction were statistically stationary. This assumption effectively restricted the analysis to the forces normal to the rotor plane and thus did not allow accounting for the much smaller torque forces which can be significant for observers near the plane of rotation nor for the detailed radiation directionality of the blade elements. The assumption of circular motion also does not allow accurate treatment of forward-flight helicopter cases. We will see later in this report that these are not important restrictions except for within about fifteen degrees of the rotor plane or for advance ratios greater than about 0.4 (which is beyond the range of interest for typical helicopters). The analysis gives a reasonably simple equation for the radiated sound. It gives some analytical insight into the noise generation mechanism's dependence upon rotor parameters and it can also be numerically evaluated in a quite straightforward way.

The method of Amiet (17) is based on a different concept. Initially, Amiet had analyzed the radiation of sound from a stationary, non-rotating airfoil in a uniform mean flow containing turbulence (21,22). This analysis accounted for the full range of wavelength-to-chord ratios and accurately predicted the directionality of the radiation (which becomes multi-lobed at intermediate wavelength-to-chord ratios). Later Amiet used these results to synthesize the average radiation from rotating blades by numerically summing and averaging the radiation from a series of blade straight-line motions which approximate the circular (or epicycloidal) motion of a hovering rotor (17). This approach can be shown to be accurate for high frequencies, in the same manner as the analysis of George and Kim (16). Amiet's method has the advantage of being able to treat forward flight easily and of being based on a more exact model of radiation directionality. However, as will be seen later in this report, when one sums and averages the multi-lobed radiation pattern over the range of directions to the observer, the pattern is smoothed out to a pattern which, except when observers are very near the rotor plane, is quite close to the simpler dipole pattern resulting from the approximations of George and Kim. Harris and co-workers (23,24) have carried out a range of experiments on broadband noise from model rotors and, in conjunction with their work, have developed analyses based on variations of the two methods discussed above.

The methods of George and Kim and of Amiet were used in the present study for inflow turbulence noise calculations. The inflow turbulence itself can be due to the natural turbulence in the atmosphere or to upstream disturbances, as in the case of a helicopter tail rotor ingesting the wake of the main rotor. In making the calculations for this study, the incident turbulence properties often had to be estimated based on the average measured properties of atmospheric turbulence (25) or had to be roughly estimated based on energy considerations (26). In those cases, alternative calculations were made to illustrate the sensitivity to the likely range of values. Another difficult problem in estimating the turbulent inflow properties is due to the anisotropic nature of the inflow due to the distortion of turbulent eddies as the contracting streamlines enter hovering rotors, stationary propellers, or fans (1,27,28). At present, this effect can only be estimated and alternative calculations made.

BOUNDARY LAYER TRAILING EDGE NOISE

Noise is also produced by the self-generated turbulence in a blade's boundary layer passing its trailing edge. This was recognized as far back as 1959 (29). Various investigators looked at very simplified models for this noise, but these early models were not complete and were useful only as bases for empirical correlations. Fink, for example, in reference 30, used such a correlation to predict the on-axis noise of a rotor due to boundary layer trailing edge noise. Complete first-principle analyses of rotor trailing edge noise were developed more recently by Kim and George (31) and by Schlinker and Amiet (32). Also, recently, Hubbard et al. (33) have proposed an OASPL and spectrum peak correlation for wind turbine rotors.

The analytical problem of sound radiating from the effect of turbulence being convected past a non-rotating trailing edge has been studied intensively since about 1970. A variety of model problems were studied (see the review of Howe, reference 34), but these studies primarily resulted in scaling laws which needed empirical constants to be determined. There also remained a number of questions regarding the details of the modelling and the effects of the Kutta condition. Alternatively, Amiet developed a method which is based on solving the problem of a statistically stationary pressure field being convected past a trailing edge (35,36). This result only depends upon the pressure spectrum in the boundary layers being known from experiments. Amiet's method has been compared to the experimental findings of Brooks (37) and found to be consistent.

In 1980, Kim and George constructed an analysis of boundary layer noise from rotors by using the blade forces from Amiet's flow model in the same manner as they had earlier for the inflow turbulence noise. Thus, their analysis is again restricted to angles not too close to the rotor plane and to the low advance ratios which are found in helicopter forward flight. In the calculations given in this report, an airfoil boundary layer thickness correlation was used (38, and Appendix A of this report) instead of the flat plate results used in the original publications. Later, Schlinker and Amiet (32) used the same numerical summing and averaging method that Amiet had used for the inflow turbulence noise (17) to treat the trailing edge noise problem. Again, we will see that the dipole method of Kim and George gives essentially the same results as Amiet's method except within about 15 degrees of the rotor plane, where additional source terms should be included in both methods.

TIP VORTEX NOISE

Another source of broadband noise on airfoils or rotors is that of locally-separated flow from local stall or from tip vortex formation. Kendall (39), Ahtye et al. (40), and Fink and Bailey (41) experimentally observed localized noise sources at wing and flap tips. Changes in noise from changes in rotor tip shape were experimentally observed some time ago by Lowson et al. (42), although these effects may have been due to blade loading changes. Earlier, Revell (43), for the airframe noise case, had argued on an energy basis that vortex drag and associated turbulence in the trailing vortices must lead to additional noise in some manner. George et al. (44) have identified this effect with the turbulence in the vortex formation and local separation region over the blade tip interacting with the trailing edge.

The model starts with the experimental observations of separation on the suction side of blade or rotor tips due to the boundary layer being swept around the tip by the pressure gradients at the tip. A separated vortex flow results which is very similar to the flow over the top surfaces of a sharp-edged delta wing in subsonic flow. Figures 2 and 3 are sketches of delta wing and wing/rotor tip flows. It is known that these leading edge vortices are quite turbulent. Large fluctuating pressures have been measured on the surfaces of delta wings under these vortices. George et al. (44,45) used these data, pressure fluctuation data from two dimensional flows, and data on the geometry and velocities associated with wing and rotor tip flows to estimate the separated turbulent pressure spectrum being convected past the trailing edge. This information was used to predict the resulting radiated sound in a manner similar to George and Kim's treatment of inflow turbulence and boundary layer trailing edge noise. This tip vortex noise is shown to increase with blade loading, as had been experimentally observed in many cases. The updated version of the analysis (45, and Appendix B of this report) uses turbulent pressure data measured under vortices on delta wings which are correlated with pressure on rotor tips using experimentally measured length and velocity scales. This version is used to compute spectra for the various cases in the present study.

OTHER MECHANISMS

Another local separation turbulence noise is that of the local stall associated with a high angle of attack, due to close proximity to a vortex from previous blade passage. This phenomenon was studied experimentally by Paterson et al. in reference 46 but there is presently no analytical model of either the local separation or noise radiation available. However, available detailed pressure measurements on rotor blades indicate that this phenomenon is usually not present on rotors under normal operating conditions (47).

As mentioned in the introduction, trailing edge vortex shedding noise from laminar blade boundary layers is a noise mechanism which can be eliminated in most cases by tripping the boundary layer. A similar mechanism of vortex shedding from blunt trailing edges has been identified for turbulent flows as well by Brooks and Hodgson (48). Like the laminar flow case, this noise source can be eliminated by using a sufficiently sharp trailing edge if this is structurally practical.

CORRELATION TYPE PREDICTION EQUATIONS

Due to the need for some sort of guidance in design, many empirical and semi-empirical prediction equations have been proposed over the years. We will only discuss those which predict a spectrum. Those equations dealing with overall sound pressure levels are much less useful if one is interested in a range of rotor sizes, because the basic blade passing frequency varies so widely. (Consider a full scale wind turbine versus a small fan, for example.) Some of the methods used to predict spectra are primary empirical, although based on theoretical ideas, while others are more closely related to analyses.

Perhaps the most developed of the correlation type methods for broadband noise is the method of Pegg (49) which is based on earlier methods of Lowson (50), Hubbard (51), Schlegel et al. (52) and Munch (53). It is given by :

$$SPL_{1/3} = 60 \log(M_t) + 10 \log(A/r^2)(\cos^2\theta+0.1) + S_{1/3}(f/f_p) + 10 \log(\overline{C_\ell}/0.4) + 130 \text{ dB}$$

for $\overline{C_\ell} < 0.48$ and where A = rotor blade area, $\overline{C_\ell}$ = average blade lift coefficient, f = frequency in Hz, M_t = tip Mach number, r = distance to observer, $SPL_{1/3}$ = one-third octave band sound pressure level, and θ = angle from the rotor axis. The function $S_{1/3}(f/f_p)$ is a tabulated function giving the frequency dependence of the sound spectrum. The frequency at which the spectrum peaks is given by :

$$f_p = -240\ T + 2.488\ V_t + 942$$

where T = thrust in Newtons, and V_t = tip speed in m/s. It should be noted that this correlation does not include any of the known effects of inflow turbulence on the noise prediction; presumably it would be applicable to some sort of 'typical' ambient turbulence conditions.

Another correlation equation was given by Fink (30) for the minimum broadband noise (i.e. on-axis excluding inflow turbulence) of a rotor. It is given by :

$$SPL_{1/3} = OASPL + 10 \log[0.613(f/f_m)^4 x\{(f/f_m)^{3/2}+0.5\}^{-4}]$$

$$OASPL = 50 \log(V/100\text{m/s}) + 10 \log(\delta Nb/r^2) + 10 \log(\cos(\psi)/2)^2 + 113.9 \text{ dB}$$

the peak frequency $f_p = 0.1\ V/\delta$ and a measure of the boundary layer thickness

$$\delta = 0.37\ c\ (Vc/\nu)^{-1/5}$$

where b = span, N = number of blades, r = distance to observer from rotor tip, V = tip speed, ν = kinematic viscosity, and $\psi = \sin^{-1}(b/r)$. In our application we have taken the cosine of the blade pitch angle to be approximately one.

CHOICE OF EXPERIMENTS

An extensive search of the literature was undertaken to find suitable experimental data with which to compare the various analyses. More than seventy references were examined while looking for cases in which the experimental parameters were well defined and in which 'clean' spectral data were presented, unaffected or minimally affected by extraneous influences such as reverberation, engine or drive motor noise, etc. For cases in which inflow turbulence was important, we also looked for the most complete measurements available of the inflow turbulence spectrum. We then tried to choose representative data from categories covering a range of rotors including wind turbines, helicopters, and propellers. We did not consider data where only overall sound pressure level or octave band data were given as this type of averaged data is inadequate to differentiate between source mechanisms and analyses. Appendix C is an annotated list of experimental references which we considered but which did not contain appropriate data.

Two types of full-scale helicopter rotor tests are available. Either measurements had been made for rotors tested on a whirl tower or the radiated noise had been directly recorded from an operating helicopter. First, consider the whirl tower tests; this type of experiment has several advantages over the flight tests. Since only one rotor is involved, there is no problem with aerodynamic interactions with other rotors such as main rotor/tail rotor interactions. Also, other polluting noises such as noises generated by drive motor and gear box, etc. are comparatively easy to control. Therefore, these tests are considered cleaner than the flight tests. However, the flight tests do give more information on the overall helicopter noise problem.

Two sets of whirl tower tests are available. The first set was due to Leverton (54,55). He tested a full scale S-55 rotor on a test rig in an inverted position in order to eliminate the effect of recirculation which occurs when a rotor wake is directed toward the ground. The spectra measured were taken from a tethered ballon at various angles to the test rotor plane. His tests varied both load and RPM. In the present study, only a few cases were chosen for comparison. The primary missing information in Leverton's results is any data on the inflow turbulence. Neither the turbulent intensity nor the scale were measured. As the inflow was drawn from near the ground, the turbulent integral scale could be quite reasonably estimated from the fairly well established empirical relationship that

$$\Lambda = 0.9\, h$$

where Λ is the turbulent integral scale and h is the height above the ground (56). Similarly, values for turbulent intensity for various weather conditions can also be estimated from the extensive data and correlations in Lumley and Panofsky's monograph (25). Leverton also reported a series of indoor model scale tests. Since the data did not include inflow turbulence information as did some other available model scale tests, these results are not used in this report.

Also, there was another set of experiments carried out at the Boeing Vertol test facility by Sternfeld et al. (57,58). In contrast to Leverton's test, they put the rotor in a position where the rotor wakes are blown toward the ground; therefore high turbulent intensities due to recirculation may be

expected, resulting in a higher noise level. Their tests varied both loading and rotor RPM. Still no measurement was made of the turbulence properties. Therefore, values of turbulent intensity and integral scale have to be estimated in order to make the predictions. In this report, only a few represented cases, which were chosen from the more recent of the tests, will be presented.

For a full scale helicopter, the spectra calculated by Johnson and Katz in 1971 (59) have been used for a long time. These spectra are based on the measurements of noise from a UH-1 helicopter. The spectra, of course, contain both main and tail rotor noise as well as airframe, engine, and gear noise. In this case too, no inflow turbulence information was measured, so values of integral scale and turbulent intensity were again estimated, using the helicopter altitude and assumed weather conditions (25,56).

Other sets of full scale helicopter noise measurements are also available. Pegg et al. (60) had conducted a program in 1973, where both a standard SH-3A and a modified one had been flight tested. Just as in Johnson and Katz's case, the data had also been polluted by other noises such as engine and gear box noise. They had measured the upper-air conditions, both wind speed and direction, but no turbulence measurements were made. In this study, one case of overhead flyover had been chosen to make the comparison using the estimated turbulent integral scale and intensity. A similar test program had also been conducted by Henderson et al. (61) for both standard and modified OH-6A helicopter. Just as in Pegg's experiment, weather conditions were monitored but no attention had been paid to the turbulence. Comparisons had also been made for the flyover case at overhead position using the estimated turbulence data. Sternfeld (62) also reported a series of full scale tests (involving engine noise), the test helicopters include Bell 204B, Sikorsky SH-3A, S-65 and Boeing Vertol CH-47B.

Two sets of suitable full scale wind turbine noise measurements were found in the reports of Hubbard and his co-workers (33,63). Measurements were made for the MOD-0A wind turbine at ground level and at a distance of 61 meters from the tower base in the rotor plane and at angles of 45 and 90 degrees from it. Measurements for the MOD-2 wind turbine were also made at ground level, both in the rotor plane and at several locations under the turbine axis. In both cases, the background noise was measured and shown to be well below the measured spectra. However, no information on turbulence intensity or integral scale was given. In these cases, again, the turbulence's characteristics were estimated, aided slightly by the fact that at least the wind speed was known. (It should be noted that the wind turbine noise annoyance may not be controlled by broadband noise but by low frequency impulsive noise due to the interaction with specific atmospheric inhomogeneities or vortices shed by the upwind towers.)

Several sets of indoor tests of model rotors in anechoic facilities are available for comparison with analyses. The first set that will be discussed was carried out by Paterson and Amiet in the UTRC anechoic wind tunnel facility on several model rotors (64). In these tests, both vertical ascent and forward flight were simulated and different grids were used upstream to generate controlled inflow turbulence. Measurements were made of both the turbulent intensity and integral scale so that in these cases none of the parameters needed to be estimated.

Similar sets of high quality model scale tests were carried out in the MIT anechoic wind tunnel and reported in a series of papers by Aravamudan, Harris, and Humbad (23,24). A number of the tests results contained large amounts of laminar vortex shedding noise (high frequency broadband noise) which partially covered the more interesting sources. However, in most cases, if this peaked part of the spectrum is ignored, a significant part of the measured spectra is still useful for comparisons. In these experiments, as in those of Paterson and Amiet, different grids were used upstream and the turbulence's intensity and integral scale were measured.

Another set of indoor experiments for a low speed fan is due to Lowson et al. (42). Tests were run in an anechoic room, for both a ducted and an unducted fan, both before and after recirculation built up in the room. The non-recirculation cases were used for our comparisons since conditions are better defined. RPM, tip angle, and tip shape were varied as well. The turbulence was measured by a limited frequency range hot wire anenometer giving reasonable estimates for the turbulent intensity in the room before the recirculation set in. We estimated the turbulent integral scale as 0.1 meter. The boundary layer was not tripped in these tests. Thus, some laminar vortex shedding humps appeared in the high frequency part of the spectrum which we again ignored. (It is interesting to note that when the tip was cut back in the tests, the laminar boundary layer hump was greatly reduced.)

Full scale propeller tests are also available. Magliozzi (65) made a series of tests for a twin-engine, high wing, light STOL transport aircraft. Noises were recorded for flyover, taxi operations and the static tests as well. Measurements were taken by microphones located at the wing tip and on the ground. Turbulence data were sensed by a hot wire anemometer mounted on the aircraft nose boom. Also Brown and Ollerhead (66) reported a whirl tower test of several full scale propellers. A number of one-third octave band spectra containing broadband noises are available.

COMPARISONS OF ANALYSES TO EXPERIMENTS

In the comparisons, the data estimated as input to the analyses and to the correlations are given in the figure captions. Other input parameters were taken from the experimental papers. Inflow velocities were estimated using simple momentum theory with thrusts determined by simple blade element theory. As mentioned above, the inflow turbulence values were often estimated. In cases where separate calculations are shown for separate mechanisms, the results should be summed in order to compare to the experiments. However, in order not to clutter the figures, this was not done in most cases. It is comparatively easy to envision the sum on the decibel scale as the resulting curve essentially has only a 3 dB increase if two additive curves have the same level and a 4.8 dB increase if three additive curves have the same level.

The first results to be presented are those for the full scale rotor whirl tower test by Leverton (55). Data were taken at an angle of -75 degrees from the rotor plane where all of the analyses would be expected to be within the range of their assumptions. Figure 4 shows the comparison of a range of predictions. It is first clear that the correlation of Pegg (49) is too high for this case. It is also clear that at the lower frequencies, say below 1000 Hz, the boundary layer trailing edge noise and the tip vortex noise mechanisms are not important. However, at frequencies above 1000 Hz they become quite important, with boundary layer trailing edge noise being the more important one in this case. Fink's boundary layer noise correlation is seen to be a reasonable approximation to the more exact boundary layer trailing edge noise calculations. Most of the noise below 1000 Hz is shown to be inflow turbulence noise based on the estimated turbulent properties. Both the analyses of George and Kim (16) and of Amiet (17) agree within 5 dB with each other and with Leverton's data.

In figure 5, a comparison is shown among calculations based on the three mechanisms of George and co-workers, the two of Amiet, and some data of Leverton at an angle of -11.5 degrees from the rotor plane. As all of these analyses ignore in-plane force components and as George and co-workers use a blade dipole directivity, the agreement would not be expected to be quite as good, although it is not clear how many of the differences are due to which of these effects. The inflow turbulence noise calculations made by using the Karman spectrum did however seem to be in better agreement with the experiments in this case.

Figures 6 and 7 show the comparisons to some whirl tower data of Sternfeld (private communication, 1982), where figure 6 is for the 5130 lb rotor loading and figure 7 for the 15150 lb loading case. The measurements were taken from an angle of about -14 degrees from the rotor plane. Just as in Leverton's -11.5 degrees case, the analyses are expected to be lower than the experimental measurements. Since the rotor was operating to blow the rotor wake toward the ground, significant recirculations are expected. By using estimated turbulence properties, calculations were made and shown in the figures. Note that the inflow turbulence noise calculations shown in these two figures use the Karman spectrum. The calculations using the Dryden spectrum appear to be much lower.

Figure 8 shows the comparison of some main rotor noise calculations with the full scale helicopter experiment data of Johnson and Katz (59). As

mentioned previously, other sources in addition to the main rotor are present in this case. However, the results are still reasonable, being within about 10 dB, and show the importance of all three mechanisms in various parts of the spectrum. In figure 8, the inflow turbulence noise calculations used the Karman spectrum. Calculations using the Dryden spectrum were also made and appear to be about 5 to 10 dB lower.

Also, comparisons were made for experiments with a full scale SH-3A helicopter by Pegg (60). The case we chose corresponds to the measurements from a flyover of a SH-3A at an altitude of 61 m overhead. Using estimated turbulent integral scale and intensity, figure 9 shows the comparison between calculations and the data. Again the inflow turbulence noise prediction shown was the result of using the Karman spectrum; the level predicted using the Dryden spectrum is lower. It should be noted that Pegg reported that there was no blade slap observed during the experiment.

Figure 10 shows a similar comparison for full scale OH-6A helicopter flight tests by Henderson et al. (61). The case presented here corresponds to the measurements for flyover at an altitute of 31 m and at the overhead position. Using estimated turbulence properties, similar agreement with experiments, as in the previous case, was obtained. Note that there are two sets of data shown in the figure, which correspond to the highest and the lowest level observed during the tests.

Figures 11 and 12 show comparisons to full scale wind turbine data presented by Hubbard and co-workers (33,63). Here again some extraneous sources may have been present and turbulence properties had to be estimated. Nevertheless, the agreement with the predicted absolute spectra is good and it is seen that the primary source for frequencies above a few hundred Hertz is boundary layer trailing noise as was also suggested by Hubbard and co-workers. There is no question that the predictions using the Karman spectrum are in better agreements with the experiments than those using the Dryden spectrum.

Figure 13 compares some data of Lowson et al. (42) for a fan to some correlations and calculations. Again, the correlation of Pegg (49) seems to be too high. Here the inflow turbulence noise is predicted to be important over the full range of frequencies and the calculations agree very well with the measured spectrum. Figures 14, 15 and 16 show comparisons for different RPM's and figures 17 through 20 show comparisons for different blade pitch angles. Just as in figure 13, excellent agreements were obtained. Note that the inflow turbulence noise predictions were made using the Dryden spectrum which seems to be better suited to indoor turbulence. However in figures 13, 14 and 20, calculations using the Karman spectrum are also shown for comparison.

Figures 21 through 23 show comparisons of calculations to data presented by Paterson and Amiet (64). In the no grid case (low inflow turbulence), it is clear that both tip vortex and boundary layer noise are important at the higher frequencies. In all the cases, the calculations and experiments agree to within about 5 dB. Unlike the full scale rotor cases, inflow turbulence noise calculations using the Dryden spectrum agree better with the experiments than those using the Karman spectrum. In Paterson and Amiet's original report, they had also shown good agreement with Amiet's inflow turbulence noise analysis whenever the primary noise source was inflow turbulence.

Figures 24 and 25 show similar satisfactory agreements to Aravamudan and Harris' model test data with varying inflow turbulence due to upstream grid changes (23). Note that the predictions of inflow turbulence noise use the Dryden spectrum only. Figures 26 through 33 show comparisons with Humbad and Harris' similar data as tunnel speed (advance ratio), upstream grid, and rotor RPM's are varied (24). The analyses in Harris and co-workers' original papers also showed good agreements with the data. The inflow turbulence noise predictions shown in figure 26 to 33 use the Dryden spectrum; however in figure 26, 27 and 29, predictions using the Karman spectrum are also shown.

COMPARISONS OF ANALYSES TO EACH OTHER

In this section the results calculated by the methods of Amiet and of George and co-workers are compared to show the effects of different assumptions in the analyses. The computational approach of Amiet allows treatment of forward flight (non-zero advance ratios) and more accurate basic blade noise directionality. The George and Kim approach has been implemented for both the Von Karman model and the Dryden model of the inflow turbulence spectrum. We will examine each of these effects by comparing the results of the calculations made by different methods.

Figure 34 shows the plots of the Dryden spectrum, which is available in the George and Kim inflow turbulence model, and of the Karman spectrum, which is available in both the George and Kim and the Amiet models. It is clear that the Karman spectrum contains more energy at high frequencies. Although the Doppler shifts make it more complicated, one can roughly identify a given frequency radiation with the inverse time for a blade to pass through a turbulence component of length 1/k, where k is the wavenumber. Thus, for frequencies on the order of 10 kHz at a tip speed of 100 m/s, one is interested in turbulence component wavenumbers of order 100 m^{-1}. If, as for a full scale helicopter, the integral scale is of order 100 m, then the peak of the spectrum is at wavenumber k of order 0.01 m^{-1}, implying that the high frequencies come from wave numbers 10^4 higher than the inverse integral scale. Referring to figure 20 we see that the difference between the two atmospheric turbulence models can be of order 10 dB at these wavenumbers. For another way of looking at it, figure 35 shows comparisons between inflow turbulence noise calculations for a full scale rotor for both 0.1 m and 67.0 m integral scales. It is apparent that for a small integral scale and low frequencies the results for different assumed turbulence spectra are in close agreement, although even so, the differences become more marked at high frequencies. One concludes that the Von Karman spectra should be used particularly for cases in which the integral scale is large. However, some comparisons in the previous section did indicate that for indoor tests (which small scale turbulence involves), the Dryden spectrum gives better results.

Figure 36 shows the effect of forward flight on inflow turbulence noise as calculated by Amiet's analysis and compared to hover calculations based on George and Kim's analysis. It is notable that the advance ratio effect is not very important for any case of interest to helicopters (i.e. advance ratio below 0.4). Similarly, figure 37 compares changing advance ratio for boundary layer trailing edge noise. Here the basic inputs vary since the calculation of Kim and George uses an airfoil boundary layer thickness correlation (38) rather than the flat plate results incorporated in their earlier publications and in those of Amiet. In this boundary layer trailing edge noise case, the results again show that the effects of advance ratio are not important for values less than 0.4.

As discussed in a previous section, Amiet's computational model incorporates an accurate basic blade noise radiation directionality for the pressures normal to the blade mean line. The methods of George and co-workers approximate the basic directionality by a dipole normal to the rotor plane, which would be expected to lead to underestimates for angles near the rotor plane. Both Amiet's and George and coworkers' analyses ignore in-plane forces and other in-plane mechanisms. Figures 38 through 40 compare the

directionalities for both inflow turbulence and boundary layer noises. It is clear that, aside from overall differences, the directionalities are quite close except within about ten to fifteen degrees of the rotor plane.

COMPARISONS OF DIFFERENT MECHANISMS IN DIFFERENT SITUATIONS

It is already apparent from the results presented thus far that the various mechanisms can each be important in different situations. We have seen that inflow turbulence noise can dominate the noise radiation when the inflow turbulence is strong. On the other hand, at high frequencies, either boundary layer trailing noise or tip vortex noise can be important, as seen in figures 4-5, 8-12 and 21. Both of these sources increase with blade angle of attack, while tip vortex noise depends strongly upon blade chord and is more severe for square tip shapes. Some of these dependencies are shown in figure 41. Calculated spectra are shown for pitch angles of 10 and 15 degrees for boundary layer noise and for tip vortex noise based on both square and round tip shapes for a rotor similar to that of a UH-1 (compare with figure 8). Clearly, tip vortex noise is favored by high angles of attack and wide tip chords (low aspect ratio, untapered blades). On the other hand, wind turbines generally have tapered blades and we have seen that their primary noise source in the frequency range of interest is boundary layer trailing edge noise (see figures 11 and 12).

The relative importance of various mechanisms on a full scale helicopter configuration is an interesting yet complex question as various noise mechanisms exist on both the main and tail rotors. Some calculations showing the effects of varying the inflow turbulence scale are shown in figure 28 for a UH-1 helicopter main rotor. The varying turbulent intensities give some idea of the variations expected between quiet nighttime conditions and typical daytime conditions. They could be considerably higher in windy conditions. Also, as first demonstrated experimentally by Hanson (67) and later by Pegg et al. (28), the contraction of the streamtubes into a hovering rotor or a stationary propeller or fan leads to an anisotropic and intensified inflow turbulence. This dynamic effect on the inflow turbulence has not yet been treated analytically or experimentally in any detail.

Next we question the relative importance of the tail rotor as compared to the main rotor. The primary added difficulty in dealing with tail rotor noise is that the tail rotor operates in the main rotor's wake, which is itself not very well understood. The main rotor's wake consists of a number of components : the overall downwash field, the tip trailing vortices and other vortices shed from the main rotor blades, the wakes of the fuselage, engines, and rotor hub, and the turbulence present in these flows as well as that already existing in the atmosphere. The main rotor's mean wake can be approximately calculated by several methods, but has a fairly minor influence on the tail rotor noise. This is because it leads primarily to only low order loading harmonics and noises. On the other hand, the tip vortices in the wake are quite localized and lead to more annoying, higher frequency noise. The tip vortices' positions and structures are difficult to predict. In forward flight, they follow initially epicycloidal paths which are perturbed by : 1) the roll-up of the main rotor wake into a horseshoe vortex system; 2) the self-induced instabilities of the vortex trajectories; and 3) the action of pre-existing atmospheric turbulence. In addition, the actual structure of the vortices is not well known. They can contain axial velocities in their cores which are of the order of their maximum circumferential velocities. For the interaction geometry associated with forward flight, where the vortex core will be approximately perpendicular to the plane of the tail rotor, these axial velocities will be strong contributors to the loading fluctuations on

the tail rotor blades. Also, the tip vortices are found to diffuse or 'burst' under some conditions (the 'vortex breakdown' phenomenon). After they breakdown, the vortices become more spread out and turbulent. This will strongly affect both the mean and the turbulent inflow seen by the tail rotor. The importance of wake ingestion on noise was pointed out in some experiments of Levine (68). He reported some experiments where increases of 5 to 10 dB were found in both narrowband and broadband noise of a Sikorsky S-58T operated with the main rotor wake being blown into the tail rotor. Significant reductions in tail rotor noise were also reported by Barlow et al. for a redesigned OH-6A tail rotor (69). Another experimental study of tail/main rotor wake interaction noise involved wind tunnel tests of a model with variable tail rotor position and direction (70,71). Balcerak (70) made a parametric study varying tail rotor location, fin blockage area, tail rotor rotation direction, rotor speeds and thrusts, and tail rotor pusher/tractor configuration. Later Pegg and Shidler (71) tested the same model, extending the work and emphasizing identifying the aeroacoustic mechanisms producing the noise. They found about a 12 dB increase in broadband noise when the main rotor flow was added to the tail rotor and significant increases in harmonics under a variety of conditions. These experiments are very important and point out the complexity and the need for more analytical understanding of tail rotor broadband noise sources and how to reduce these sources.

In the present study all we can do is present a few simple calculations to show the importance of the various mechanisms to tail rotors. Figure 43 presents UH-1 tail rotor noise for conditions corresponding to the main rotor calculations shown in figure 42 (i.e. with no main rotor wake effects). Under those conditions, tail rotor noise is clearly less important than main rotor noise. In contrast, figure 44 presents calculations for inflow turbulence noise due to ingestion of assumed main rotor wake turbulence. (The tail rotor tip and boundary layer noise sources are unchanged from figure 43.) The turbulence intensity estimates range from those found in the atmosphere to large values, and the length scales are alternatively taken as the main rotor chord or radius. Although these estimates range widely, it is clear by comparing figure 44 to 42 that the tail rotor ingestion of the main rotor wake is very important and deserves much more attention in the future.

The final comparisons of mechanisms are for a typical light aircraft propeller. Figure 45 compares calculations for a static propeller on the ground. A number of different inflow turbulence intensity values are used, ranging from representative of quiet nighttime conditions to typical daytime conditions. It is evident that under high atmospheric turbulence conditions, inflow turbulence is dominant over nearly all of the spectrum. On the other hand, for low turbulence intensities, or for a flyover case as shown in figure 46, we find that tip or trailing edge noise can be important, depending on blade angle of attack. Figure 46 shows calculations somewhat arbitrarily based on 4.0 and 8.5 degree angles of attack. The higher sensitivity of tip vortex noise to blade thrust (angle of attack) is quite evident.

CONCLUSIONS

The understanding of and the ability to predict broadband rotor noise are approching a satisfactory state in many respects. Until about ten years ago, understanding was essentially qualitative, sometimes erroneous, and several mechanisms were not even recognized. As shown in this report, the important broadband noise mechanisms are now understood well enough to be able to make predictions to within about five dB of the experimental data. This understanding should enable designers to minimize broadband noise in the cases where it is a controlling factor in a design.

The calculations and comparisons shown indicate that inflow turbulence induced lift fluctuations are the most important broadband noise sources at low frequencies. This radiation can be predicted down to the lowest blade passing frequency, including the smooth peaked spectral structure, by the method of Homicz and George (15). For the higher frequencies, which are of more practical interest, the methods of George and Kim (16) and of Amiet (17) are just as satisfactory and are much easier to compute. When the same inflow turbulence spectrum is used, both of the methods seem to agree well with each other and with measurements over a full range of parameters, except at angles within about ten to fifteen degrees of the rotor plane. The Karman spectrum, which had been implemented in both George and Kim's and Amiet's methods, is suitable for use in predicting the inflow turbulence noise radiating from full-size rotors. However, the Dryden spectrum, which is only available in George and Kim's method, is more suitable to predict the indoor model rotor inflow turbulence noise where small scale turbulence are involved. Further research is needed on broadband rotor noise near the rotor plane.

Most experiments do not include enough inflow turbulence data to define the inputs to the analyses. In particular, the effect of streamtube contraction on generating anisotropic and large scale inflow turbulence needs more theoretical and experimental attention.

Boundary layer trailing edge noise is now well understood. The analyses of Kim and George (31) and of Schlinker and Amiet (32) and the correlation of Fink (30) all appear to give results which agree reasonably well with experiments. This source was seen to be the primary broadband noise source for full scale wind turbines. This source often is the important noise source at high frequencies on large rotors when inflow turbulence is weak. It increases significantly with angle of attack due to the increase of boundary layer thickness.

Tip vortex formation noise seems to be satisfactorily predicted, although it is not sufficiently dominant in any of the experiments to definitively establish the precise accuracy of the model of George et al. (44,45), which uses delta wing leading edge vortex data to model the tip vortex. Much more experimental data is needed on flows and fluctuating pressure on different shapes of rotors and wing tips. Tip vortex noise is most important for square tips and for wide chords. This noise probably can be reduced significantly by detailed tip shape changes, but this is presently unexplored.

The noises radiated from helicopter tail rotors remain poorly understood. The main rotor wake is very complex and itself poorly understood, although it is the primary input needed for tail rotor noise predictions.

Finally, further comparisons of the mechanisms to better defined experimental measurements are still needed to establish the analyses' accuracies and enable further improvements of the broadband noise analyses and noise minimization techniques.

APPENDIX A

EFFECT OF ANGLE OF ATTACK ON ROTOR TRAILING EDGE NOISE

Previous analyses of the boundary layer trailing edge noise mechanism used zero blade angle of attack for boundary layer input data. In practice, to produce desired loadings, rotor blades are operated at various angles of attack. This appendix sets forth the important effect of the change of a blade's angle of attack on rotor trailing edge noise. It is based on the paper of Kim and George (31) which gives the underlying analysis.

Using the same model and assumptions, the general result for the far-field sound pressure level radiated by the turbulent boundary layer passing the rotor blades' trailing edges can be directly adapted from reference 31 as

$$\langle S_1(x,f)\rangle = \frac{Bf^2b^2U_c^2\sin^2\phi}{2\pi\rho c_0^3 r^2} \sum_{n=-\infty}^{n=\infty} \frac{F_g(|f-n\Omega|)S_{pp}(|f-n\Omega|)}{(f-n\Omega)^2\left(1+\frac{b}{\ell_2(|f-n\Omega|)}\right)} J_n^2\left(\frac{f}{\Omega} M_0 \cos\phi\right) \qquad (A\text{-}1)$$

where B = number of blades
f = acoustic frequency in Hertz
b = blade span
U_c = turbulence convection velocity
ϕ = elevation angle of observer from the rotor plane
ρ = density of the acoustic media
c_0 = the undisturbed sound speed
r = distance from rotor hub to observer

$$F_g = F^2 + G^2$$

$$F = \left(\frac{\mu+M\mu+K_1}{\mu+M\mu}\right)^{1/2} \{(c_1+s_1)\cos 2K_1 + (c_1-s_1)\sin 2K_1\} + 1 - (c_2+s_2)$$

$$G = \left(\frac{\mu+M\mu+K_1}{\mu+M\mu}\right)^{1/2} \{(c_1-s_1)\cos 2K_1 - (c_1+s_1)\sin 2K_1\} - (c_2-s_2)$$

$$c_1 - is_1 = E^*[2\mu(1+M)]$$

$$c_2 - is_2 = E^*[2(\mu+\mu M+K_1)]$$

$$K_1 = \frac{\omega c}{2U_c}, \quad \mu = \frac{Mk}{\beta^2}$$

$$S_{pp}(|f-n\Omega|) = \left(\frac{1}{2}\rho U^2\right)^2 \left(\frac{\delta^*}{U}\right) S_0(\tilde{\omega}) , \quad \tilde{\omega} \equiv \frac{2\pi|f-n\Omega|\delta^*}{U}$$

$$\ell_2(|f-n\Omega|) \simeq 2.1\frac{U_c}{2\pi|f-n\Omega|}$$

As the blade's angle of attack and Mach number are changed, the characteristics of the turbulent boundary layer over the rotor change, resulting in a change of δ^*, the displacement thickness. Previous studies used flat plate boundary layer theory to calculate δ^* and used it as an input to the analysis. However, as pointed out by Schlinker and Amiet (32), the flat plate boundary layer theory cannot predict δ^* except approximately for the zero lift case. Schlinker and Amiet measured the boundary layer thickness for a NACA 0012 airfoil section of 0.41m chord, as the Mach number ranged from 0.15 to 0.5 and the angle of attack changed from -0.4^0 to 12^0. Theoretically, both Reynolds number and Mach number affect δ^*. With increasing Reynolds number, δ^* decreased slowly with $Re^{-1/5}$; with increasing Mach number , the compressibility effect tended to increase δ^*. Thus, in fact, these two effects essentially cancelled each other, thus explaining the fact that their data showed a very weak variation with Mach number or Reynolds number. This result suggested a simple correlation of δ^* with α, th angle of attack alone. Note that the data were measured for boundary layer thickness, δ, while in equation (A-1), the surface pressure spectrum S_{pp} was characterized by the displacement thickness δ^*. Thus, by using the well known one-seventh power law, δ was transformed to δ^*. Then a curve fitting technique led to the following empirical expression

$$\delta^*/c = (24.3+0.6625\alpha)\times10^{-4} \qquad \text{(A-2a)}$$

for $\alpha < 4^0$, and

$$\delta^*/c = (26.95+0.6625\beta+0.3044\beta^2+0.0104\beta^3)\times10^{-4} \qquad \text{(A-2b)}$$

for $\alpha > 4^0$, where $\alpha = \beta - 4^0$, and α and β are in degrees. This curve and the data are shown in figure A-1. Due to the very limited number of data available, no correlations are made to Reynolds number and Mach number. This limits the application of the above equations to Reynolds number between 9.5×10^5 and 5.2×10^6.

Next we examine S_{pp}, the incident surface pressure spectral density. As can be seen in equation (A-1), the term that is still left undetermined is $S_0(\tilde{\omega})$. An empirical expression for $S_0(\tilde{\omega})$ can be obtained from experiments. In this study, two set of experiments were used: by Yu and Joshi (72) and by Brooks and Hodgson (48). Their data seem to agree well, and again, curve fitting leads to the following expression

$$S_0(\tilde{\omega})=1.732\times10^{-3}\tilde{\omega}/(1-5.489\tilde{\omega}+36.74\tilde{\omega}^2+0.1505\tilde{\omega}^5) \qquad \text{(A-3a)}$$

for $\tilde{\omega} < 0.06$, where $\tilde{\omega} = 2\pi f\delta^* / U$, and

$$S_0(\tilde{\omega})=1.4216\times10^{-3}\tilde{\omega}/(0.3261+4.1837\tilde{\omega}+22.818\tilde{\omega}^2+0.0013\tilde{\omega}^3+0.0028\tilde{\omega}^5) \qquad \text{(A-3b)}$$

for $0.06 < \tilde{\omega} < 20.$, figure A-2 shows the plot of $S_0(\tilde{\omega})$ vs. $\tilde{\omega}$ along with the experimental data and the flat plate result. It is clear that one will expect about a 10 dB difference due to the spectrum alone as well as the additional δ^* effect of high angle of attack. Figure A-3 shows the effect of changing angle of attack on trailing edge noise for an UH-1 helicopter. The result leads to a conclusion that the primary difference due to the change of angle of attack is in the low to mid frequency range, where the noise increases with angle of attack. However, in the high frequency range, the change of noise

level due to change of angle of attack is not as significant. The comparison with predictions made using only flat plate data (31) shows the importance of the angle of attack.

Boundary layer trailing edge noise is not the only source of rotor broadband noise; other mechanisms such as inflow turbulence and tip vortex separation also contribute significantly to the noise radiation. Thus to evaluate the present analysis by comparison with existing experiments, one must also include other possible sources. As discussed in the main body of this report, trailing edge noise can be important for low inflow turbulence levels or when considering a large rotor. Figures 11, 12 and 21 in the main body of this report show good agreement with experiments in such cases.

APPENDIX B

TIP VORTEX SEPARATION MODELS

The original analysis of noise radiated by the turbulence-trailing edge interaction in the tip vortex separation area used a simplified cross-flow analogy to estimate the turbulence level and surface pressure spectrum in the tip separation region (44). Under the present grant the tip vortex noise analysis was extended to also include the use of turbulent intensity and pressure spectrum information measured for the three dimensional separated flow associated with leading edge vortices on delta wings.

We start from the analysis of George, Najjar, and Kim (44) where, in a manner similar to the work of Kim and George on attached boundary layer-trailing edge noise, the far field sound pressure level radiated by the statistically stationary converted surface pressure spectrum S_{pp} is shown to be given by

$$\langle S_1(x,f)\rangle = \frac{Bf^2L^2U_c^2\sin^2\phi}{8\pi\rho c_0^3 r^2} \sum_{n=-\infty}^{n=\infty} \frac{F_g(|f-n\Omega|)S_{pp}(|f-n\Omega|)}{(f-n\Omega)^2(1+\frac{L}{\ell_2(\omega)})} \quad J_n^2(\frac{f}{\Omega}M_o\cos\phi) \tag{B-1}$$

where the notation is the same as in Appendix A except that L is the spanwise extent at the trailing edge of the separation due to the tip vortex.

In this tip vortex case the model of statistically stationary turbulence being convected past the trailing edge may be less accurate than for the attached boundary layer case. However, it should certainly be reasonable enough to calculate an approximate spectrum of the radiation and determine the importance of this mechanism for rotors.

The models we use for the tip flow are based on the fact that in the cross-flow plane the tip flow separates and then reattaches as shown in the simplified sketch of figure 3. Data from two different flows are used: first, two-dimensional separated flow; and second, three-dimensional delta wing leading edge vortex flow.

Mabey (73) has analyzed a large number of two-dimensional separated flow geometries and shown that the nondimensional pressure fluctuation spectra can be reasonably well correlated between a wide variety of geometries, when the separation bubble length is used as the nondimensionalizing length for the data. The pressure fluctuations scale with dynamic pressure to within a factor of less than three. Thus the spectra are put in the nondimensional form $\hat{S} = S_{pp} V_m q^{-2} L^{-1}$ where $q = 0.5\rho V_m^2$ and V_m is the maximum velocity along the separation steamline. Similarly the frequency is nondimensionalized; $\hat{f} = fLV_m^{-1}$. Similar correlations were also established by Fricke (74). We scaled our two-dimensional spectrum from the experiments of Fricke and Stevenson (75). They measured pressure spectra for a two dimensional fence followed by a separated flow and reattachment. This geometry is similar to

our cross flow view shown in Figure B-1. Figure B-2 shows the spectrum of Fricke and Stevenson and the curve fit to it which can be expressed as

$$\hat{S} = \begin{cases} 0 ; & \hat{f} < 0.1375 \\ 5.9703 \times 10^{-3}\,\hat{f} - 3.5673 \times 10^{-4} ; & 0.1375 < \hat{f} < 0.3872 \\ 3.144 \times 10^{-3} \sin (3.2388\,\hat{f} - 0.5506) ; & 0.3872 < \hat{f} < 0.7935 \\ (93.035 + 557.09\,\hat{f})^{-1}; & 0.7935 < \hat{f} < 1.0605 \\ (-258.896 + 1964.19\,\hat{f} - 2416.78\,\hat{f}^2 + 1288.94\,\hat{f}^3 - 100.862\,\hat{f}^4)^{-1}; & \\ & 1.0605 < \hat{f} \end{cases} \quad \text{(B-2)}$$

For the second model we based our pressure spectra on those measured under the similar edge separation vortices on delta wings. As sketched in figure 2, the delta flow geometry is very similar to tip flow, including the primary and secondary separation from the edge and the axial outer flow. The separation geometry is influenced by rounded or sharp edges as in the tip case. Our goal was to construct a suitable correlation for the pressure spectra in the delta case and to relate it to the tip flow case of interest.

Richard and Fahy (76) have analyzed the turbulent flow beneath the leading edge vortices of several delta wings of different planforms and various angles of attack. They presented spectra from a number of investigators, nondimensionalized in several ways, none of which were satisfactory for our case. In order to find a normalization suitable for application to our tip case we first studied the delta wing flow geometry and pressure data measured in the comprehensive experiments of Peckham (77). Based on flow visualization results, the locations of peak negative pressures, and on pressure distributions, the value of the transverse separation scale L was found relative to the local chord and plotted as L/C versus angle of attack α as shown in figure B-3. The edge shape is definitely important as noted also by Bartlett and Vidal (78). Next the maximum negative pressure coefficients under the vortices relative to those on the nearby surface were used with the Bernouilli equation to derive the maximum velocity ratio V_m/U. Assuming that the velocity in the vicinity of the vortex is approximately the same as that on nearby surfaces one obtains:

$$V_m/U = (1 - C_{p_{min}})^{1/2} \quad \text{(B-3)}$$

The resulting values are plotted as a function of angle of attack α of the delta wing in figure B-4.

Thus, using figures B-3 and B-4 the values of L and V_m can be estimated for each of the spectra given by Richards and Fahy (76) and the data normalized by these two physically important parameters. The results, as shown in figure B-5, give a somewhat better correlation of the spectra than either of the two other normalizations given in Richards and Fahy's paper.

These spectra can be approximated by the curve defined by

$$\log_{10} \hat{S} = \begin{cases} -3.475 - 1.654\,(\log_{10} \hat{f} + 0.82)^2 ; & \log_{10} \hat{f} < -0.82 \\ -3.475 - 0.984\,(\log_{10} \hat{f} + 0.82)^2 ; & \log_{10} \hat{f} > -0.82 \end{cases} \qquad \text{(B-4)}$$

but $\hat{S} = 0$ if $\hat{f} < 0$.

This curve is comparable to the identically normalized two-dimensional data, showing that the method of normalizing satisfactorily relates pressure spectra in different types of flows. The primary difference between the two spectra is the slower fall-off with frequency of the delta wing spectrum compared to the two-dimensional spectrum.

In order to be able to find an appropriate spectrum for a rotor tip case we need estimates of L and V_m for rotor tips at different angles of attack. The flow visualization, pressure measurements, and velocity measurements of Gray et al. (79) and of Chigier and Corsiglia (80) were used in a similar manner as for the delta wing cases to estimate L/C and V_m/U versus α as shown in figures B-6 and B-7 respectively. V_m/U can be expressed as

$$V_m/U = 1.0 + 0.0359\,\alpha \qquad \text{(B-5)}$$

where α is the local tip angle of attack in degrees. The spanwise extent of the spectrum can be expressed as

$$L/c = 0.023 + 0.0089\,\alpha \qquad \text{(B-6a)}$$

for a square tip cross section or

$$L/c = 0.0074\,(\alpha - 2.0) \qquad \text{(B-6b)}$$

for a round edged tip. Gray et al. tested both a rounded and a square tip and thus the values of L/C are more accurately related to edge shape than in the available delta data given above. On the other hand, the values V_m/U were estimated from Gray et al.'s C_p data and from the hot wire measurements of reference 80 and are only approximate. Further work is needed to definitively establish the turbulence properties on wing and rotor tips.

In summary, given a tip shape and angle of attack the values of L and V_m are obtained from equations B-5 and B-6 and then these values are used to obtain a pressure spectrum from either the two-dimensional or delta results given by equations B-2 or B-4. This spectrum is actually applicable near the reattachment line. The spectrum is somewhat lower in the separated region before reattachment and it drops off past reattachment. At this state of approximation, rather than integrating this spanwise variation we used the reattachment spectrum and assumed it to be constant over the distance L. By not including any of the blade outside of the separation region of length L we should roughly compensate for the actual changes in spectrum shape and amplitude in the tip region.

The value of U_c is taken as $U_c = 0.8\ U$ and $\ell_2(\omega) \approx 2.1(U_c/\omega)$ based on results for boundary layer turbulence (81). Thus the final calculations are made by substituting one of the analytical curve fits, equation B-2 or B-4, into equation B-1 and evaluating it numerically as outlined in reference 44. In the results presented in this report the delta wing data (equation B-4) were used for the predictions given.

APPENDIX C

ANNOTATED LIST OF EXPERIMENTAL REFERENCES WHICH WERE NOT USED IN COMPARISONS

Baade, P. K.: Effects of Acoustic Loading on Axial Flow Fan Noise Generation. Noise Control Engineering, vol. 8, Jan.-Feb. 1977, pp. 5-15.
- duct acoustics effects involved

Balcerak, J. C.: Parametric Study of the Noise Produced by the Interaction of the Main Rotor Wake with the Tail Rotor. NASA CR-145001, 1976.
- tail rotor noise
- strong rotor/wake interaction effects

Balombin, J. R.: An Exploratory Survey of Noise Levels Associated with a 100kW Wind Turbine. NASA TM-81486, 1980.
- similar data given in references 33, 63

Barger, R. L: Theoretical Prediction of Nonlinear Propagation Effects on Noise Signatures Generated by Subsonic or Supersonic Propeller or Rotor-Blade Tips. NASA-TP-1660, 1980.
- no data

Bausch, W. E., Schlegel, R. G.: Helicoptor Main Rotor Noise Prediction and Control. Journal of the American Helicoptor Society, vol. 14, NO. 3, pp. 38-47, 1969
- octave band data only

Brooks, B. M.: Acoustic Measurements of Three Prop-Fan Models, AIAA-80-0995, AIAA 6th Aeroacoustics Conference, Hartford, Conn., June 4-6, 1980, p. 13.
- high speed noise dominates

Cicci, F., Toplis, A. F.: Noise Level Measurements on a Quiet Short Haul Turboprop Transport --- de Havilland Dash 7 STOL Propulsion. Society of Automotive Engineers, Business Aircraft Meeting, Wichita, Kan. April 6-9, 1976.
- high speed noise dominates

Damongeot, A.: Helicopter Tail Rotor Noise Generated by Aerodynamic Interactions. Paper No. 57, 4th European Rotorcraft and Powered Lift Aircraft Forum, Stresa, Italy, Sept. 13-15, 1978.
- tail rotor noise (wake effects)

Dittmar, J, H., Jeracki, R. J.: Noise of the SR-3 Propeller Model at 2 Deg and 4 Deg Angle of Attack. NASA TM-82738, 1982.
- high speed noise generated by supersonic tip speed propeller

Dittmar, J. H., Jeracki, R. J.: Additional Data on the SR-3 Propeller. NASA TM-81736, 1981.
- high speed noise generated by supersonic tip speed propeller

Fink, M. R., Schlinker, R. H., Amiet, R. K.: Prediction of Rotating-Blade Vortex Noise from Noise of Non-Rotating Blades. NASA CR-2611, 1976.
- rotational noise dominates
- low frequency spectrum (~ 1200 Hz)

Ford, D. W., Rickley, E. J.: Noise Levels and Data Correction Analysis for Seven General Aviation Propeller Aircraft. FAA-EE-80-26, 1980.
• EPNL data only

Fujii, S.: Acoustics and Performance of High-Speed, Unequally Spaced Fan Rotors. ASME Paper 79-GT-4, ASME, Gas Turbine Conference and Exhibit and Solar Energy Conference, San Diego, CA., March 12-15, 1979.
• high speed noise dominates

Gliebe, P. R., Kerschen, E. J.: Analytical Study of the Effects of Wind Tunnel Turbulence on Turbofan Rotor Noise --- NASA Ames 40 by 80 Foot Wind Tunnel. NASA CR-152359, 1980.
• tone noise dominates

Grosche, F. R., Stiewitt, H.: Investigation of Rotor Noise Source Mechanisms with Forward Speed Simulation. AIAA-77-1361, AIAA 4th Aeroacoustics Conference, Atlanta, GA., Oct. 3-5, 1977.
• in-plane noise measurements

Hanson, D. B.: Spectrum of Rotor Noise Caused by Atmospheric Turbulence. Journal of Acoustic Society of American, vol. 56, July 1974, pp. 110-126.
• rotational noise dominates

Hilton, D. A., Henderson, H. R., Pegg, R. J.: Ground Noise Measurements During Flyover, Hover, Landing and Take-Off Operations of a Standard and a Modified HH-43B Helicopter. NASA TM-X-2226, 1972.
•coaxial rotors - strong wake effects

Hilton, D. A., Scheiman, J., Shivers, J. P.: Acoustical Measurements of the Vortex Noise for a Rotating Blade Operating With and Without Shed Wake Blown Downstream. NASA TN-D-6364 1971.
• strong wake effects

Hodder, B. K.: An Investigation of Possible Causes for the Reduction of Fan Noise in Flight. AIAA-76-585, AIAA 3rd Aeroacoustics Conference, Palo Alto, CA, July 20-23, 1976.
• tone noise dominates

Hodder, B. K.: Further Studies of Static to Flight Effects on Fan Tone Noise Using Inlet Distortion Control for Source Identification. NASA TM-X-73183, 1973.
• tone noise dominates

Hodder, B. K.: Investigation of the Effect of Inlet Turbulence length Scale on Fan Discrete Tone Noise. NASA TM-X-62300, 1973.
• discrete tone noise dominates

Hubbard, H. H., Shepard, K. P.: Noise Measurements for Single and Multiple Operation of 50 KW Wind Turbine Generators. NASA CR-166052, 1982.
• wind turbine arrays noise

Hubbard, J. E., Harris, W. L.: Model Helicopter Rotor Impulsive Noise. Journal of Sound and Vibration, vol. 78, 1981, pp.425-437.
• impulsive noise

JanakiRam, D. S., Scruggs, B. W.: Investigation of Performance, Noise and Detectability Characteristics of Small-Scale Remotely Piloted Vehicle (RPV) Propellers. AIAA-81-2005, AIAA 7th Aeroacoustics Conference, Oct. 5-7, Palo Alto, CA, 1981.
• harmonic noise dominates
• in-plane noise measurements

Kantola, R. A., Warren, R. E.: Reduction of Rotor-Turbulence Interaction Noise in Static Fan Noise Testing. AIAA-79-0656, AIAA 5th Aeroacoustics Conference, Seattle, WA, March 12-14, 1979.
• tone noise dominates

Keast, D. N., Potter, R. C.: A Preliminary Analysis of the Audible Noise of Constant Speed, Horizontal Axis Wind Turbine Generators. DOE/EV-0089, 1980.
. similar data given in references 33, 63

Kobayashi, H.: Three-Dimensional Effects on Pure Tone Fan Noise Due to Inflow Distortion --- Rotor Blade Noise Prediction. NASA TM-78885, 1978.
• tone noise dominates

Kobayashi, H., Groeneweg, J. F.: Effects of Inflow Distortion Profiles on Fan Tone Noise Calculated Using a 3-D Theory. NASA TM-79082, 1979.
• tone noise dominates

Lane, F.: Broadband Noise Generated by Turbulent Inflow to Rotor or Stator Blades in an Annular Duct. NASA CR-2503, 1975.
• no data

Laudien, E.: Main and Tail Rotor Interaction Noise During Hover and Low-Speed Conditions. 2nd European Rotorcraft and Powered Lift Aircraft Forum, Bueckenburg, West Germany, Sept. 20-22, 1976.
• tail rotor harmonic noise/main rotor impulsive noise dominate

Lee, A, Harris, W. L., Widnall, S. E.: An Experimental Study of Helicopter Rotor Rotational Noise in a Wind Tunnel. AIAA-76-564, AIAA 3rd Aeroacoustics Conference, Palo Alto, CA, July 20-23, 1976.
• rotational noise dominates
• OASPL data only

Leverton, J. W.: Reduction of Helicopter Noise by Use of a Quiet Tail Rotor. 6th European Rotorcraft and Powered Lift Aircraft Forum, Bristol, England, Sept. 16-19, 1980, Conference Papers, Part 1.
• tail rotor noise

Lewy. S., Lambourion, J., Malarmey, C., Rafine, B., Perulli, M.: Direct Experimental Verification of the Theoretical Model Predicting Rotor Noise Generation. AIAA-79-0658, 1979.
• fan rotor/stator tone noise dominates

Lucas, J. G., Woodward, R. P., MacKinnon, M. J.: Forward Acoustic Performance of a Shock-Swallowing High-Tip-Speed Fan (QF-13). NASA TP-1668, 1980.
• high speed noise dominates

Mani, R., Berkofske, K.: Experimental and Theoretical Studies of Subsonic Fan Noise. NASA CR-2660, 1976.
• high RPM fan noise
• harmonic noise dominates

Munch, C. L., Paterson, R. W., Bay, H.: Rotor Brandband Noise Resulting from Tip Vortex/Blade Interaction. Sikorsky Aircraft SER-50909, 1975.
• strong tip vortex/blade interaction effects

Neise, W, Koopmann, G. H.: Reduction of Centrifugal Fan Noises by Use of Resonators. Journal of Sound and Vibration, vol. 73, Nov. 22, 1980, pp. 297-308.
• high RPM turbofan noise with resonator effects

Nelson, W. L., Alaia, C. M.: Aerodynamic Noise and Drag Measurements on a High-Speed Magnetically Suspended Rotor. WADC-TR-57-339.
• high speed noise dominates

Newman, J. S.: Helicopter Noise Exposure Level Data: Variations with Test Target, Indicated Airspeed, Distance, Main Rotor RPM and Take-Off Power. FAA-AEE-80-34, 1980.
• noise exposure level data only

Pegg, R. J., Mariliozzi, B., Farassat, F.: Some Measured and Calculated Effects of Forward Velocity on Propeller Noise. American Society of Mechanical Engineers, Paper No. 77-GT-70, 1977.
• harmonic noise dominates
• similar tests in reference 65

Pegg, R. J., Shidler, P. A.: Exploratory Wind-Tunnel Investigation of the Effect of the Main Rotor Wake on Tail Rotor Noise --- Langley Anechoic Noise Facility. In Helicopter Acoustics, pp. 205-219.
• tail rotor noise

Piersol, A. G., Wilby, E. G., Wilby, J. F.: Evaluation of Aero Commander Propeller Acoustic Data: Taxi Operations. NASA CR-159124, 1979.
• harmonic noise dominates
• octave band spectrum only

Rathgeber, R., Sipes, D. E.: The Influence of De sing Parameters on Light Propeller Aircraft Noise. SAE-770444 Society of Automotive Engineers, Business Aircraft Meeting, Century II, Wichita, KA, March 29-April 1, 1977.
• OASPL in most cases
• high speed noise dominates

Rijgrok, G. J. J.: Experiments on the Validity of Ground Effect Predictions for Static Noise Testing of Propeller Aircraft. Journal of Sound and Vibration, vol. 72, 1980, pp. 469-479.
• propeller noise with strong ground effects on inflow
• harmonic noise dominate

Scheiman, J.: Further Analysis of Broadband Noise Measurements for a Rotating Blade Operating With and Without Its Shed Wake Blown Downstream. NASA TN D-7623, 1974.
• strong rotor/wake interaction effects

Schlegel, R., King, R., Mull, H.: Helicopter Rotor Noise Generation and Propagation. USAAVLABS-TR-66-4, 1966.
• full scale S-58 data, similar data given in reference 61

Shaw, L. M., Woodward, R. P., Glaser, F. W., Dastoli, B. J.: Inlet Turbulence and Fan Noise Measured in an Anechoic Wind Tunnel and Statically with an Inlet Flow Control Device. AIAA-77-1345, AIAA, 4th Aeroacoustics Conference, Atlanta, GA., Oct. 3-5, 1977.
• tone noise dominates

Shreve, J. C.: Propeller Aircraft Flyover Noise Testing. SAE-770443 Society of Automotive Engineers, Business Aircraft Meeting, Century II, Wichita, KA, March 29-April 1, 1977.
• no data

Tadghighi, H., Cheeseman, I. C.: A Study of Helicopter Rotor Noise, with Special Reference to Tail Rotors, Using Acoustic Wind Tunnel. Vertica, Vol. 7, No. 1, 1983.
• rotational noise dominates

Trebble, W. J. G., Williams, J., Donnelly, R. P.: Comparative Acoustic Wind-Tunnel Measurements and Theoretical Correlations on Subsonic Aircraft Propellers at Full-Scale and Model-Scale. AIAA-81-2004, AIAA 7th Aerocoustics Conference, Palo Alto, CA., Oct. 5-7, 1981.
• in-plane noise measurements
• harmonic noise dominates in most cases

REFERENCES

1. George, A. R.: Helicopter Noise: State-of-the-Art. Journal of Aircraft, Vol. 15, No. 11, November 1978, pp. 707-715.

2. Widnall, S. E.: Helicopter Noise Due to Blade-Vortex Interaction. Journal of the Acoustical Society of America, Vol. 50, No. 1, 1971, pp. 354-365.

3. Widnall, S. E. and Wolf, T. L.: Effect of Tip Vortex Structure on Helicopter Noise Due to Blade-Vortex Interaction. Journal of Aircraft, Vol. 17, No. 10, 1980, pp. 705-711.

4. Ffowcs Williams, J. E. and Hawkings, D. L.: Sound Generated by Turbulence and Surfaces in Arbitrary Motion. Philosophical Transactions of the Royal Society of London, Vol. A264, 1969, pp. 321-342.

5. Farassat, F.: Theory of Noise Generation from Moving Bodies with an Application to Helicopter Rotors. NASA TR R-541, 1975.

6. Farassat, F. and Succi, G. P.: A Review of Propeller Discrete Frequency Noise Prediction Technology with Emphasis on Two Current Methods for Time Domain Calculations. Journal of Sound and Vibration, Vol. 71, No. 3, 1980, pp. 399-419.

7. Hanson, D. B. and Fink, M. R.: The Importance of Quadrupole Sources in Prediction of Transonic Tip Speed Propeller Noise. Journal of Sound and Vibration, Vol. 62, No. 1, 1979, pp. 19-38.

8. Yu, Y. H. and Schmitz, F. H.: High-Speed Rotor Noise and Transonic Aerodynamics. AIAA Paper 80-1009, AIAA 6th Aeroacoustic Conference, June 4-6, 1980.

9. George, A. R. and Chang, S. B.: Noise Due to Transonic Blade-Vortex Interactions. American Helicopter Society, Paper A-83-39-50-0000, May 1983.

10. Schlinker, R. H. and Brooks, T. F.: Progress in Rotor Broadband Noise Research. Presented at the 38th Annual Forum of the American Helicopter Society, Anaheim, CA, May 4-7 1982.

11. George, A. R. and Chou, S. T.: Comparison of Broadband Noise Mechanisms, Analyses, and Experiments on Helicopter Rotors, Propellers, and Wind Turbines. AIAA Paper 83-0690, April 1983; also Presented at the NASA-Stanford International Symposium on Recent Advances in Aerodynamics and Aeroacoustics, August 22-26, 1983.

12. Widnall, S. E.: A Correlation of Vortex Noise Data from Helicopter Main Rotors. Journal of Aircraft, Vol. 6, 1969, pp. 279-281.

13. Paterson, R. W., Vogt, P. G., Fink, M. R. and Munch, C. L.: Vortex Noise of Isolated Airfoils. Journal of Aircraft, Vol. 10, 1973, pp. 296-302.

14. Aravamudan, K. S., Lee, A. and Harris, W. L.: An Experimental Study of

High Frequency Noise from Model Rotors: Prediction and Reduction. Vertica, Vol. 3, 1979, pp. 47-63.

15. Homicz, G. F. and George, A. R.: Broadband and Discrete Frequency Radiation from Subsonic Rotors. Journal of Sound and Vibration, Vol. 36, No. 2, 1974, pp. 151-177.

16. George, A. R. and Kim, Y. N.: High Frequency Broadband Rotor Noise. AIAA Journal, Vol. 15, April 1977, pp. 538-545; also AIAA Paper No. 76-561, July 1976.

17. Amiet, R. K.: Noise Produced by Turbulent Flow into a Propeller or Helicopter Rotor. AIAA Journal, Vol. 15, March 1977, pp. 307-308; Also AIAA Paper 76-560, July 1976.

18. Aravmudan, K. S. and Harris, W. L.: Low Frequency Broadband Noise Generated by a Model Rotor. Journal of the Acoustical Society of America, Vol. 66, August 1979, pp. 522-533.

19. Humbad, N. G. and Harris, W. L.: Model Rotor Low Frequency Broadband Noise at Moderate Tip Speed. AIAA Paper 80-1013, June 1980.

20. Ffowcs Williams, J. E. and Hawkings, D. L.: Theory Relating to the Noise of Rotating Machinery. Journal of Sound and Vibration, Vol. 10, 1969, pp. 10-21.

21. Amiet, R. K.: Acoustic Radiation from an Airfoil in a Turbulent Stream. Journal of Sound and Vibration, Vol. 41, April 1975, pp. 407-420.

22. Paterson, R. W. and Amiet, R. K.: Noise and Surface Pressure Response of an Airfoil to Incident Turbulence. Journal of Aircraft, Vol. 14, pp. 729-736, August 1977.

23. Aravamudan, K. S. and Harris, W. L.: Experimental and Theoretical Studies on Model Helicopter Rotor Noise. MIT FDRL Report 78-1, January 1978.

24. Humbad, N. G. and Harris, W. L.: Effects of Tip Geometry on Model Helicopter Rotor Low Frequency Broadband Noise. MIT FDRL Report 81-2, May 1981. (Also available as AIAA Paper 81-2003, October 1981.)

25. Lumley, J. L. and Panofsky, H. A.: The Structure of Atmospheric Turbulence. Wiley, New York, 1964, Chapters 4 and 5.

26. Tennekes, H. and Lumley, J. L.: A First Course in Turbulence. MIT Press, Cambridge, MA, Chapter 8.

27. Hanson, D. B.: Spectrum of Rotor Noise Caused by Atmospheric Turbulence. Journal of the Acoustical Society of America, Vol. 56, 1974, pp. 110-126.

28. Pegg, R. J., Magliozzi, B. and Farassat, F.: Some Measured and Calculated Effects on Forward Velocity on Propeller Noise. ASME Paper 77-GT-70, 1977.

29. Powell, A. O.: On the Aerodynamic Noise of a Rigid Flat Plate Moving at

Zero Incidence. Journal of the Acoustical Society of America, Vol. 31, December 1959, pp. 1649-1653.

30. Fink, M. R.: Minimum On-Axis Noise for a Propeller or Helicopter Rotor. Journal of Aircraft, Vol. 15, October 1978, pp. 700-702.

31. Kim, Y. N. and George, A. R.: Trailing-Edge Noise from Hovering Rotors. AIAA Journal, Vol. 20, September 1982, pp. 1167-1174; also American Helicopter Society Peprint 80-60, 36th Annual Forum Proceedings, 1980.

32. Schlinker, R. H. and Amiet, R. K.: Helicopter Rotor Trailing Edge Noise. AIAA Paper 81-2001, October 1981; also NASA CR-3470.

33. Hubbard, H. H., Shepherd, K. P. and Grosveld, F. W.: Sound Measurements of the MOD-2 Wind Turbine Generator. NASA CR-165752, July 1981.

34. Howe, M. S.: A Review of the Theory of Trailing Edge Noise. Journal of Sound and Vibration, Vol. 61, 1978, pp. 437-465.

35. Amiet, R. K.: Noise Due to Turbulent Flow Past a Trailing Edge. Journal of Sound and Vibration, Vol. 47, 1976, pp. 387-393.

36. Amiet, R. K.: Effect of Incident Surface Pressure Field on Noise Due to Turbulent Flow Past a Trailing Edge. Journal of Sound and Vibration, Vol. 57, 1978, pp. 305-306.

37. Brooks, T. F.: Trailing Edge Noise Prediction Using Amiet's Method. Journal of Sound and Vibration, Vol. 77, March 1981, pp. 437-439.

38. Chou, S. T. and George, A. R.: Effect of Angle of Attack on Rotor Trailing Edge Noise. Cornell University Fluid Dynamics and Aerodynamics Program Report FDA-83-03, 1983.

39. Kendall, J. M.: Measurements of Noise Produced by Flow Past Lifting Surfaces. AIAA Paper 78-239, 1978.

40. Ahtye, W. F., Miller, W. R. and Meecham, W. C.: Wing and Tip Noise Measured by Near- and Far-Field Cross-Correlation Techniques. AIAA Paper 79-0667, Seattle, 1979.

41. Fink, M. R. and Bailey, D. A.: Airframe Noise Reduction Studies and Clean Airframe Noise Investigation. NASA CR-159311, April 1980.

42. Lowson, M. V., Whatmore, A. and Whitfield, C. E.: Source Mechanisms for Rotor Noise Radiation. Loughborough University of Technology, Department of Transport Technology Report TT-7202, February 1972.

43. Revell, J. D.: Induced Drag Effect on Airframe Noise. In Progress in Astronautics and Aeronautics, Vol. 45, Aeroacoustics, I. R. Schwartz (ed.), MIT Press, 1976, pp. 221-235; also AIAA Paper 75-487, March 1975.

44. George, A. R., Najjar, F. E. and Kim, Y. N.: Noise Due to Tip Vortex Formation on Lifting Rotors. AIAA Paper 80-1010, June 1980.

45. George, A. R., Najjar, F. E. and Kim, Y. N.: Noise Due to Tip Vortex Formation on Lifting Rotors. Cornell University Fluid Dynamics and Aerodynamics Program Report FDA-83-02, April 1983.

46. Paterson, R. W., Amiet, R. K. and Munch, C. L.: Isolated Airfoil Tip Vortex Interaction Noise. Journal of Aircraft, Vol. 12, January 1975, pp. 34-40.

47. Shockey, G. A., Williamson, J. W. and Cox, C. R.: Helicopter Aerodynamics and Structure Loads Survey. 32nd Annual National V/STOL Forum of the American Helicopter Society, Washington, D. C., May 1976.

48. Brooks, T. F. and Hodgson, T. H.: Trailing Edge Noise Prediction from Measured Surface Pressures. Journal of Sound and Vibration, Vol. 78, March 1981, pp. 69-117.

49. Pegg, R. J.: A Summary and Evaluation of Semi-Empirical Methods for the Prediction of Helicopter Rotor Noise. NASA TM-80200, December 1979.

50. Lowson, M. V.: Thoughts on Broadband Noise Radiation by a Helicopter. Wyle Lab Report WR 68-20, 1968.

51. Hubbard, H. H.: Propeller- Noise Charts for Transport Airplanes. NACA TN 2968, 1953.

52. Schlegel, R. G., King, R. J. and Mull, H.: Helicopter Rotor Noise Generation and Propagation. USAAVLABS TR 66-4, U. S. Army, October 1966.

53. Munch, C. L.: Prediction of V/STOL Noise for Application to Community Noise Exposure. DOT-TSC-OST-73-19, U. S. Department of Transportation, May 1973.

54. Leverton, J. W. and Pollard, J. S.: A Comparison on the Overall and Broadband Noise Characteristics of Full-Scale and Model Helicopter Rotors. Journal of Sound and Vibration, Vol. 30, 1976, pp. 135-152.

55. Leverton, J. W.: The Noise Characteristics of a Large 'Clean' Rotor. Journal of Sound and Vibration, Vol. 27, 1973, pp. 357-376.

56. Etkin, B.: Theory of the Flight of Airplanes in Isotropic Turbulence - Review and Extension. AGARD Report 372, 1961.

57. Sternfeld, H., Spencer, R. H. and Schairer, J. O.: An Investigation of Noise Generation on a Hovering Rotor. Boeing Vertol Report D210-10229-1, (Contract DAHC04-69-C-0087), January, 1971.

58. Sternfeld, H., Bobo, C., Carmichael, D., Fukushima, T. and Spencer, R. H.: An Investigation of Noise Generation on a Hovering Rotor, Part II. Boeing Vertol Report D210-10550-1, (Contract DAHC04-69-C-0087), November 1972.

59. Johnson, H. K. and Katz, W. M.: Investigation of the Vortex Noise Produced by a Helicopter Rotor. USAAMRDL Report TR-72-2, February 1972.

60. Pegg, R. J., Henderson, H. R. and Hilton, D. A.: Results of the Flight

Noise Measurement Program Using a Standard and Modified SH-3A Helicopter. NASA TN D-7330, December 1973.

61. Henderson, H. R., Pegg, R. J. and Hilton, D. A.: Results of the Noise Measurement Program on a Standard and Modified OH-6A Helicopter, NASA TN D-7216, 1973.

62. Sternfeld, H. and Doyle, L. B.: The Effects of Engine Noise and Rotor Broadband Noise on Civil Helicopter Operations. NASA CR-145085, 1976.

63. Shepherd, K. P. and Hubbard, H. H.: Sound Measurements and Observations of the MOD-0A Wind Turbine Generator. NASA CR-165856, February 1982.

64. Paterson, R. W. and Amiet, R. K.: Noise of a Model Helicopter Rotor Due to Ingestion of Turbulence. NASA CR-3213, November 1979.

65. Magliozzi, B.: The Influence of Forward Flight on Propeller Noise. NASA CR-145105, 1977.

66. Brown, D. and Ollerhead, J. B.: Propeller Noise at Low Tip Speed. Wyle Lab Report 71-55; also AFAPL-TR-71-55, 1971.

67. Hanson, D. B.: Measurements of Static Inlet Turbulence. AIAA Paper 75-467, March 1975.

68. Levine, L. S.: An Analytical Investigation of Techniques to Reduce Tail Rotor Noise. NASA CR-145014, July 1976.

69. Barlow, W. H., McClusky, W. C. and Ferris, H. W.: OH-6A Phase-II Quiet Helicopter Program. USAAMRDL TR-72-29, September 1972.

70. Balcerak, J. C.: Parametric Study of the Noise Produced by the Interaction of the Main Rotor Wake with the Tail Rotor. NASA CR-145001, 1976.

71. Pegg, R. J. and Shidler, P. A.: Exploratory Wind-Tunnel Investigation of the Effect of the Main Rotor Wake on Tail Rotor Noise. Helicopter Acoustics, NASA CP-2052, Part I, 1978, pp. 205-219.

72. Yu, J. C. and Joshi, M. C.: On Sound Radiation from the Trailing Edge of an Isolated Airfoil in an Uniform Flow. AIAA Paper AIAA-79-0603, March, 1979.

73. Mabey, D. G.: Analysis and Correlation of Data on Pressure Fluctuations in Separated Flow. Journal of Aircraft, Vol. 9, 1972, pp. 642-645.

74. Fricke, F. R.: Pressure Fluctuations in Separated Flows. Journal of Sound and Vibration, Vol. 17, 1971, pp. 113-123.

75. Fricke, F. R. and Stevenson, D. C.: Pressure Fluctuations in a Separated Flow Region. Journal of the Acoustical Society of America, Vol. 44, 1968, pp. 1198-1201.

76. Richards, E. J. and Fahy, F. J.: Turbulent Boundary Layer Pressure

Fluctuations over Two-Dimensional Surfaces and Narrow Delta Wings. Acoustic Fatigue in Aerospace Structures, Syracuse University Press, Syracuse, 1965, pp. 39-62.

77. Peckham, D. H.: Low-Speed Wind-Tunnel Tests on a Series of Uncambered Slender Pointed Wings with Sharp Edges. British A. R. C., R.& M.No. 3186, 1961.

78. Bartlett, G. E. and Vidal, R. J.: Experimental Investigation of Influence of Edge Shape on the Aerodynamic Characteristics of Low Aspect Ratio Wings at Low Speeds. Journal of Aeronautical Sciences, Vol. 22, 1955, pp. 517-533.

79. Gray, R. B., McMahon, H. M., Shenoy, K. R. and Hammer, M. L.: Surface Pressure Measurements at Two Tips of a Model Helicopter Rotor in Hover. NASA CR-3281, May 1980.

80. Chigier, N. A. and Corsiglia, V. R.: Tip Vortices - Velocity Distributions. NASA TM X-62087, 1971; also Preprint No. 522, 27th Annual National V/STOL Forum of the American Helicopter Society, May 1971.

81. Corcos, G. M.: The Structure of the Turbulent Pressure Field in Boundary-Layer Flows. Journal of Fluid Mechanics, Vol. 18, 1964, pp. 353-378.

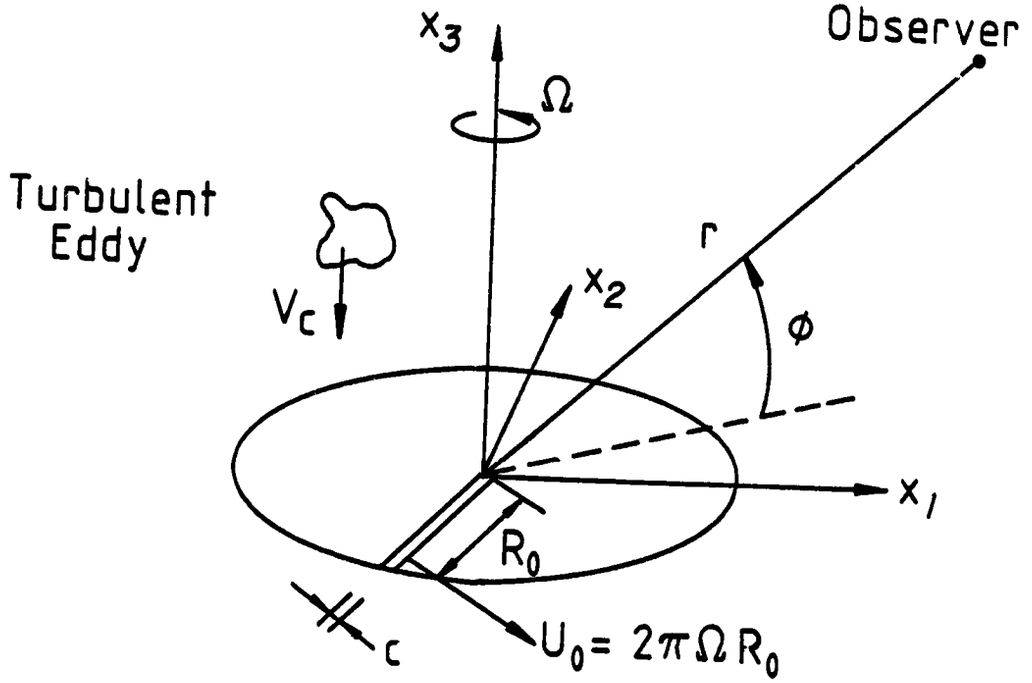

Figure 1 Rotor Geometry Showing Definitions of Symbols

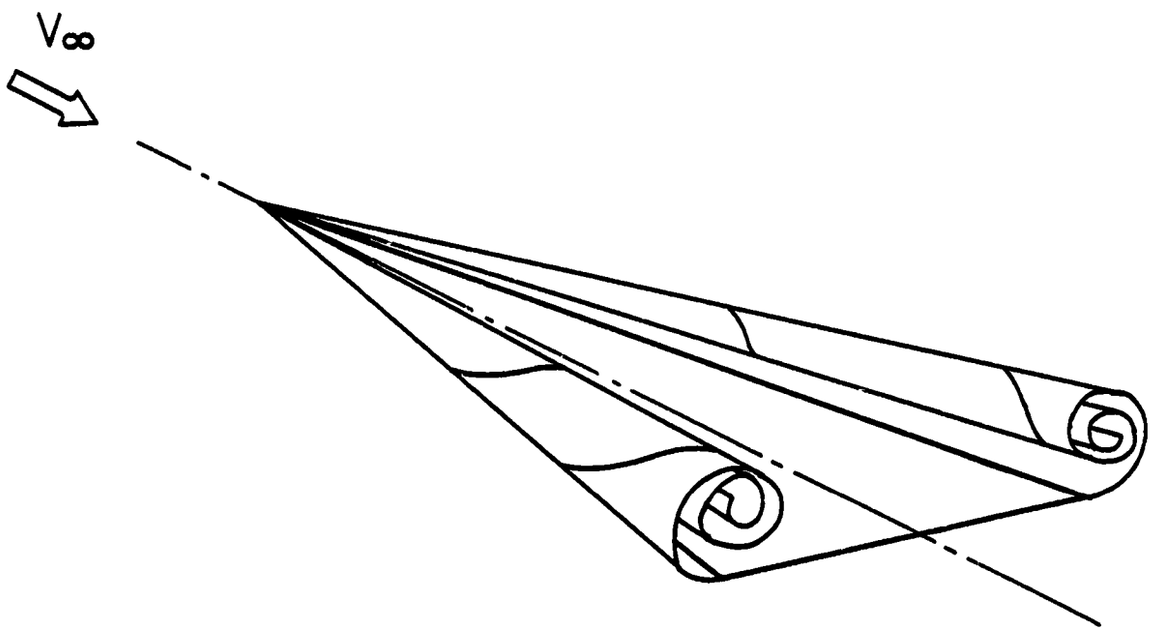

Figure 2 Vortex Formation on a Lifting Delta Wing

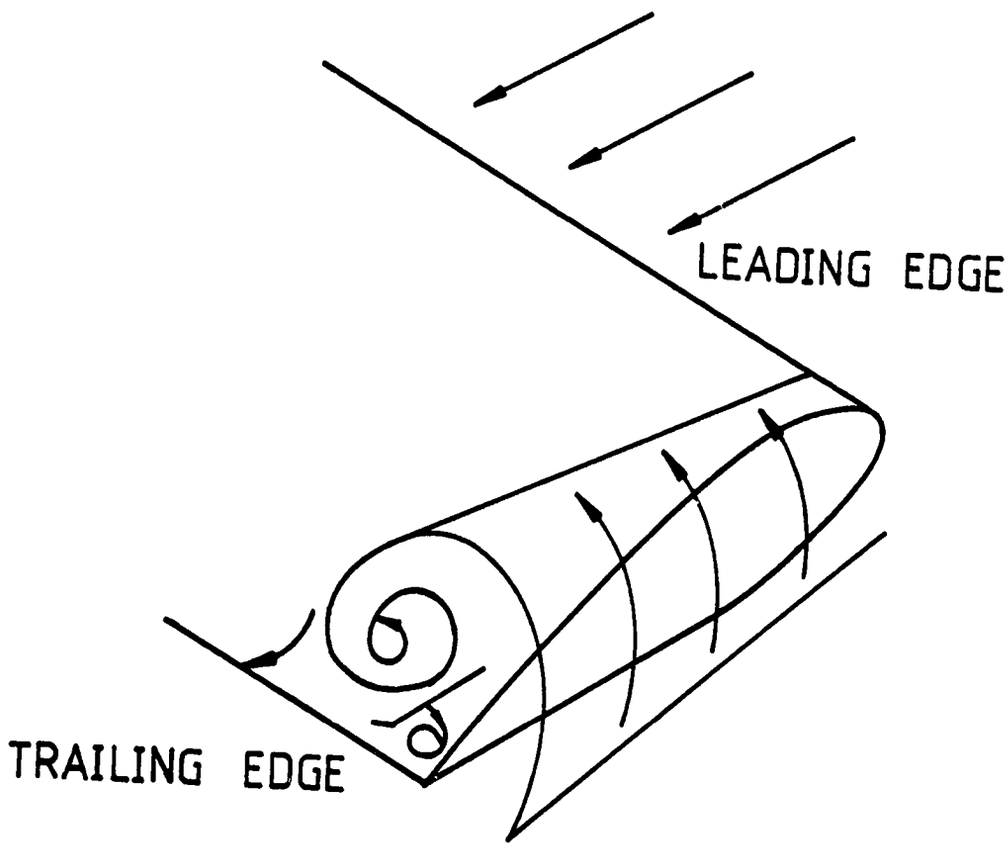

Figure 3 Vortex Formation on the Tip of a Lifting Wing or Rotor Blade

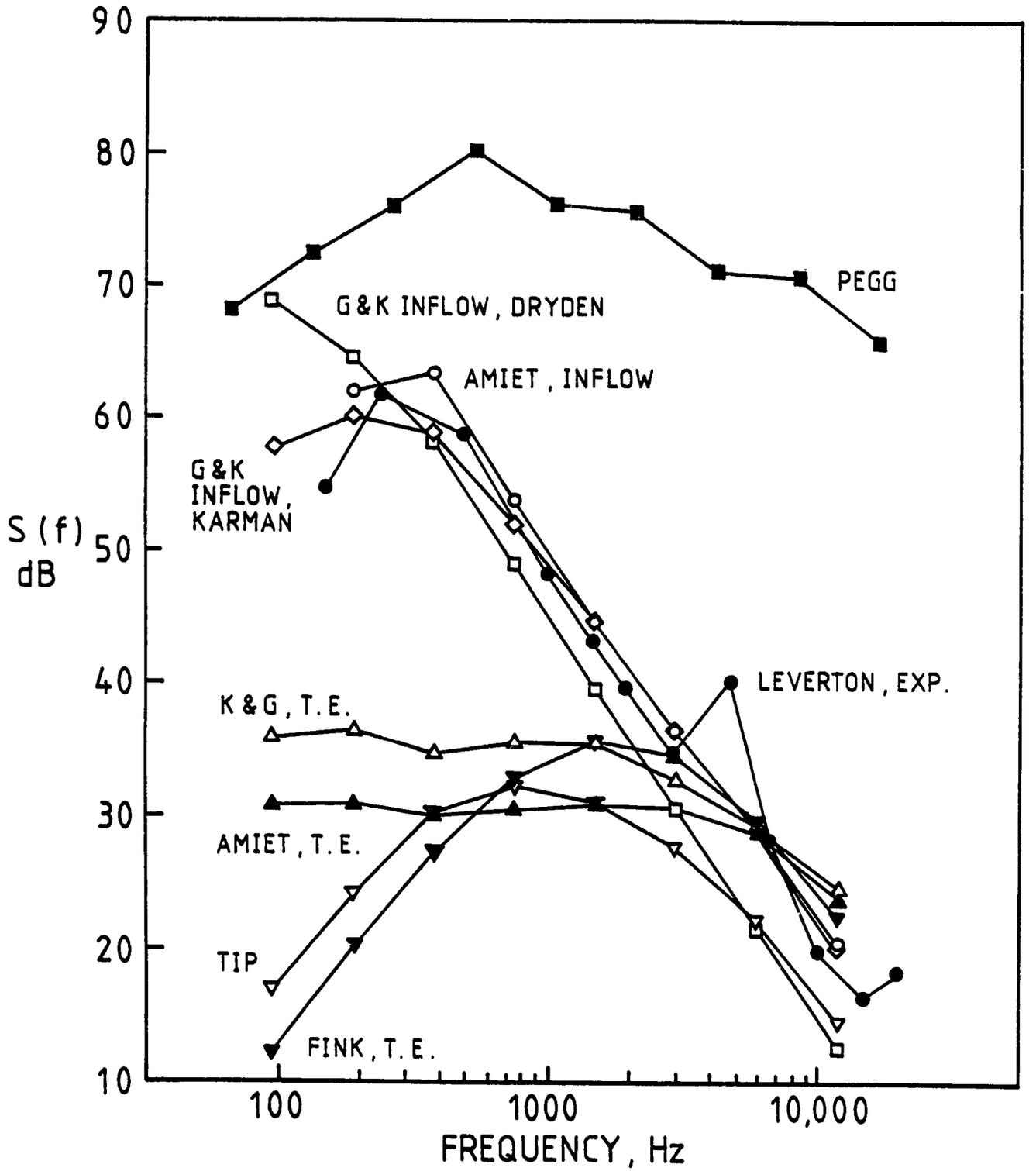

Figure 4 Comparison of the Range of Predictions for a Full Sized Helicopter Rotor with Experiment of Leverton (55), ϕ = -75°, Λ = 0.57 m, $\sqrt{w^2}$ = 1 m/s

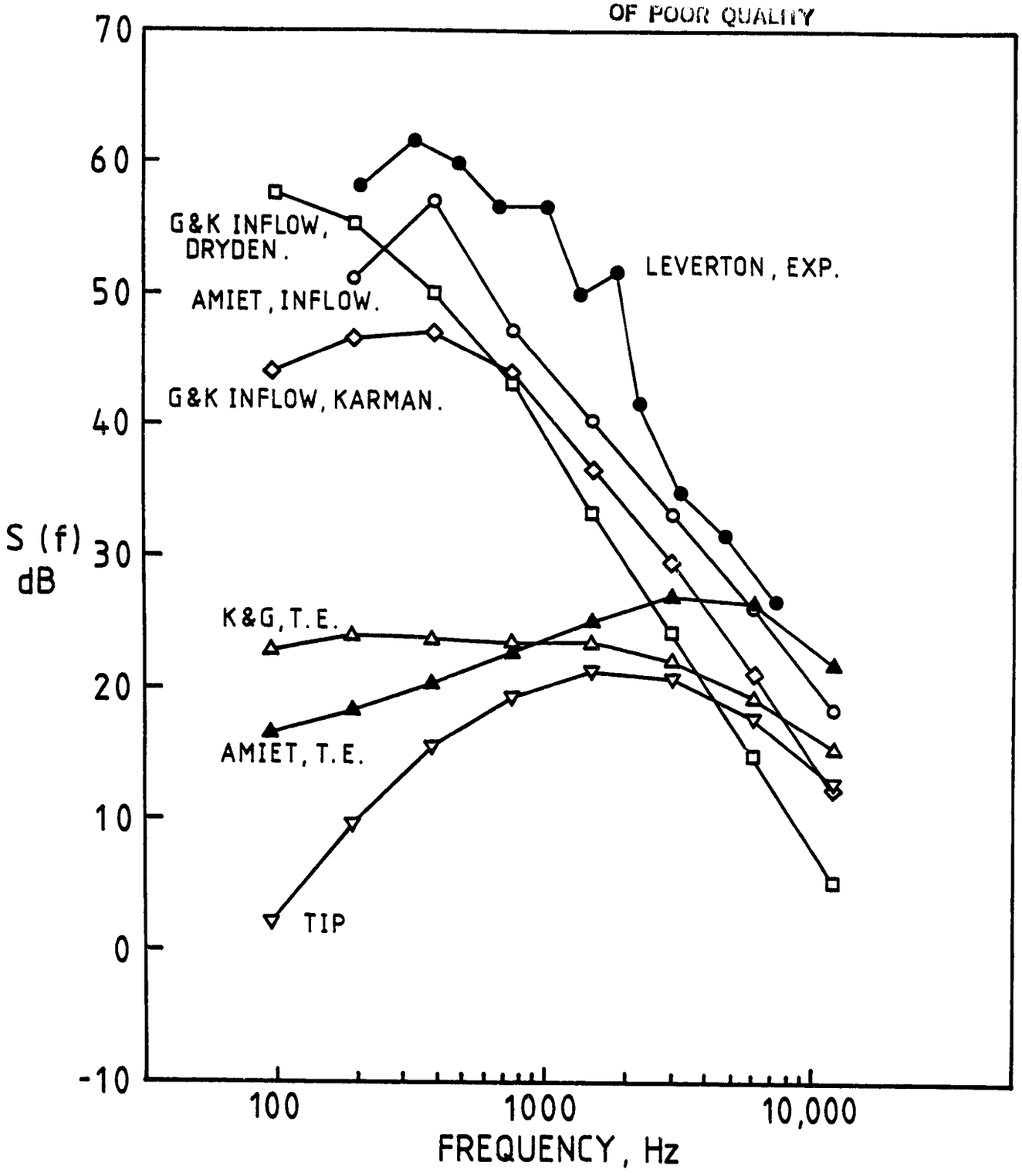

Figure 5 Comparison of Predictions with the Experiment of Leverton (55), ϕ = -11.5°, Same Turbulent Properties as in Figure 4

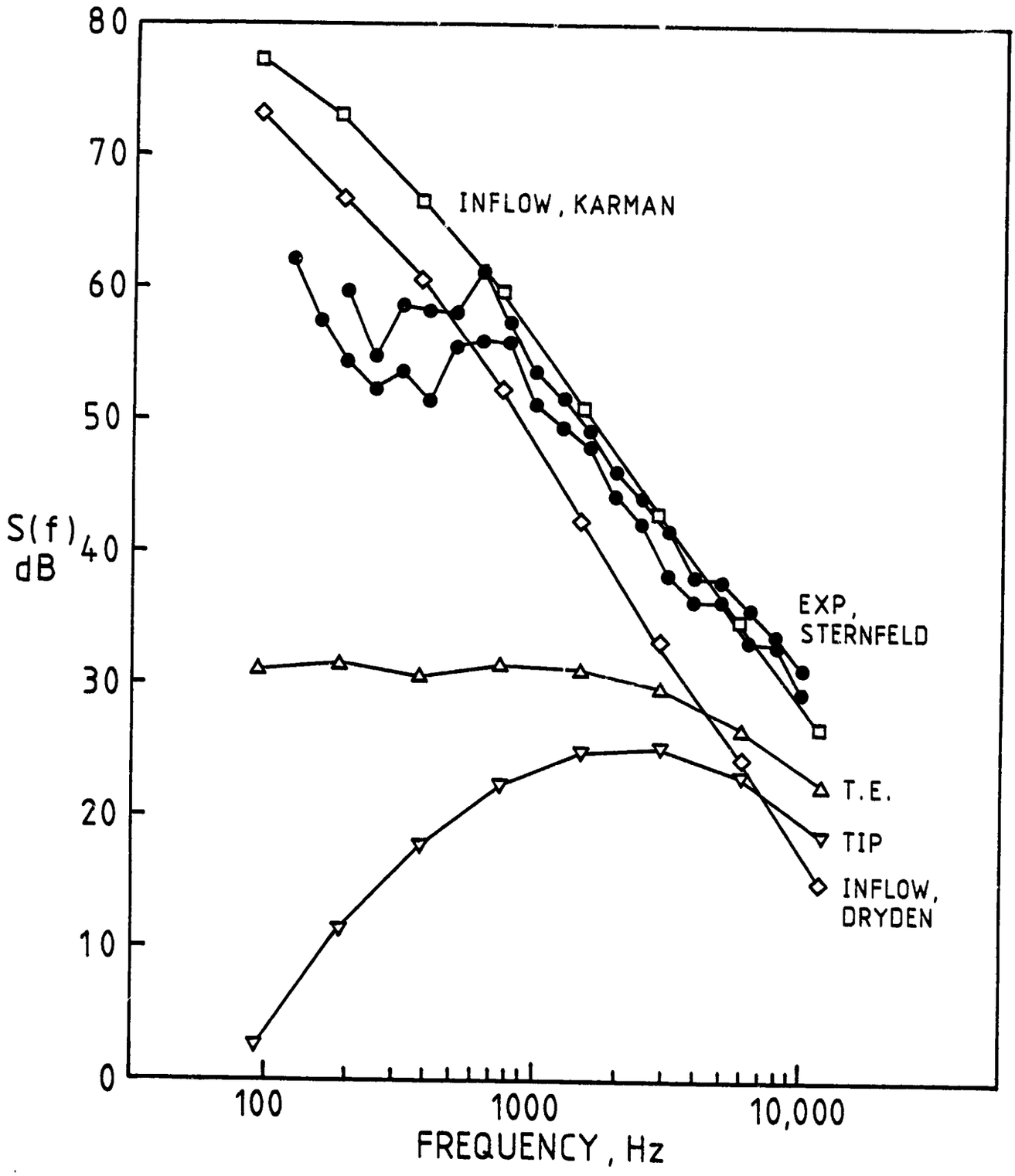

Figure 6 Comparison of Predictions with the Experiment of Sternfeld (59), ϕ = -14°, Λ = 13.7 m, $\sqrt{w^2}$ = 7 m/s, Thrust = 5130 lb

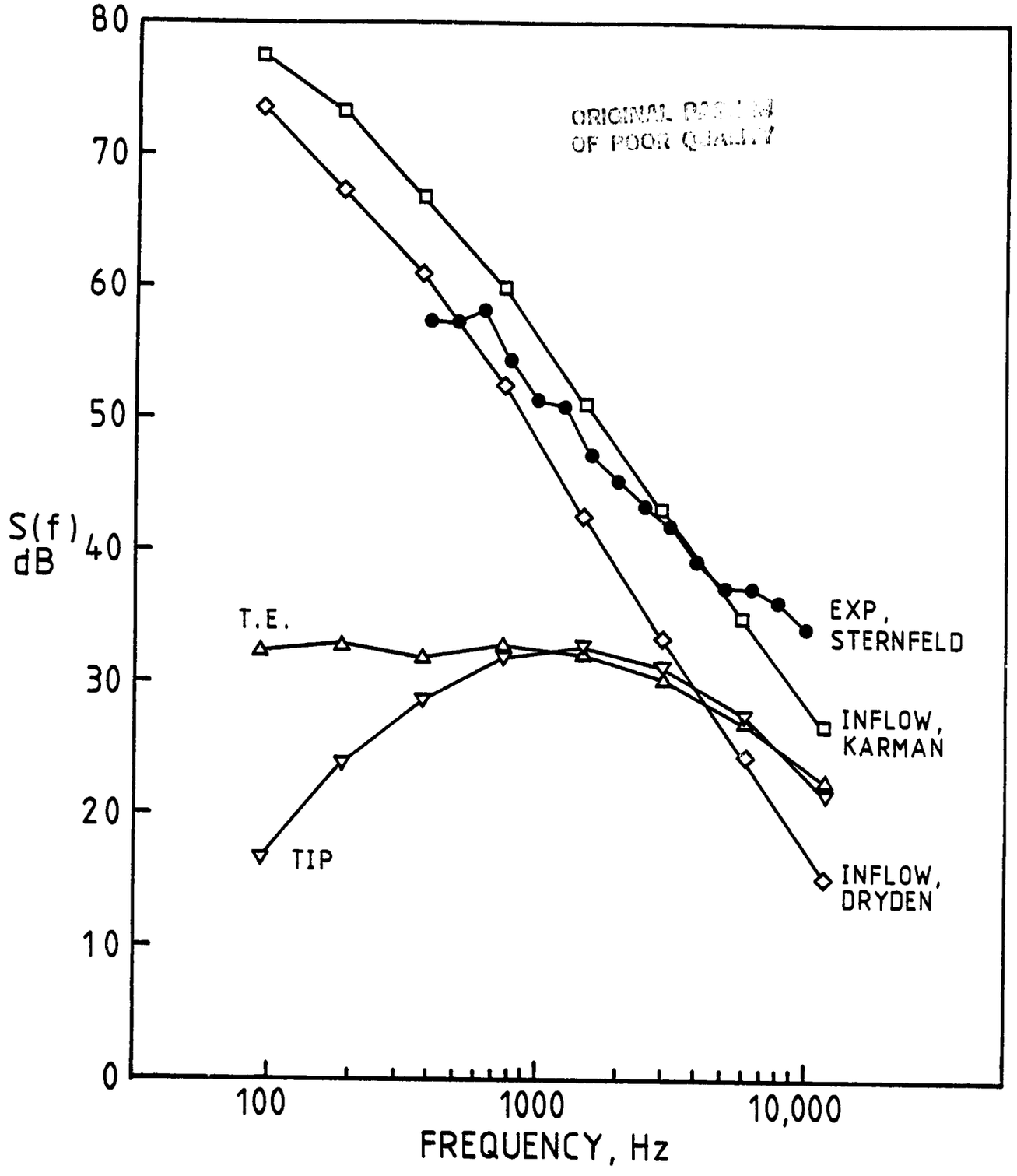

Figure 7 Comparison of Predictions with the Experiment of Sternfeld (59), ϕ = -14°, Λ = 13.7 m, $\sqrt{w^2}$ = 7 m/s, Thrust = 15150 lb

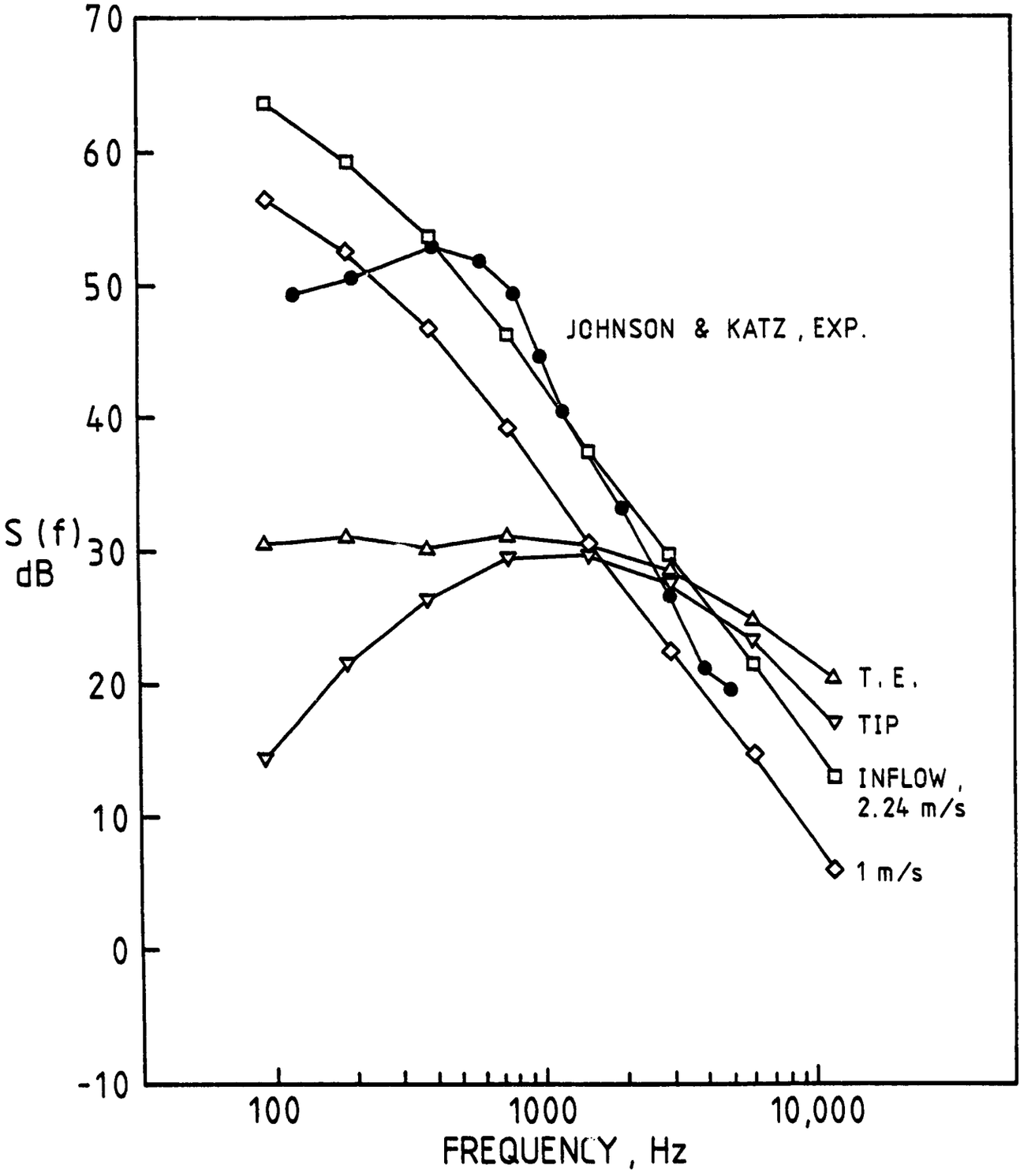

Figure 8 Comparison of Main Rotor Noise Calculations with Experiment of Johnson and Katz (60), for Full Scale UH-1 helicopter, $\varphi = -27°$, $\Lambda = 27$ m

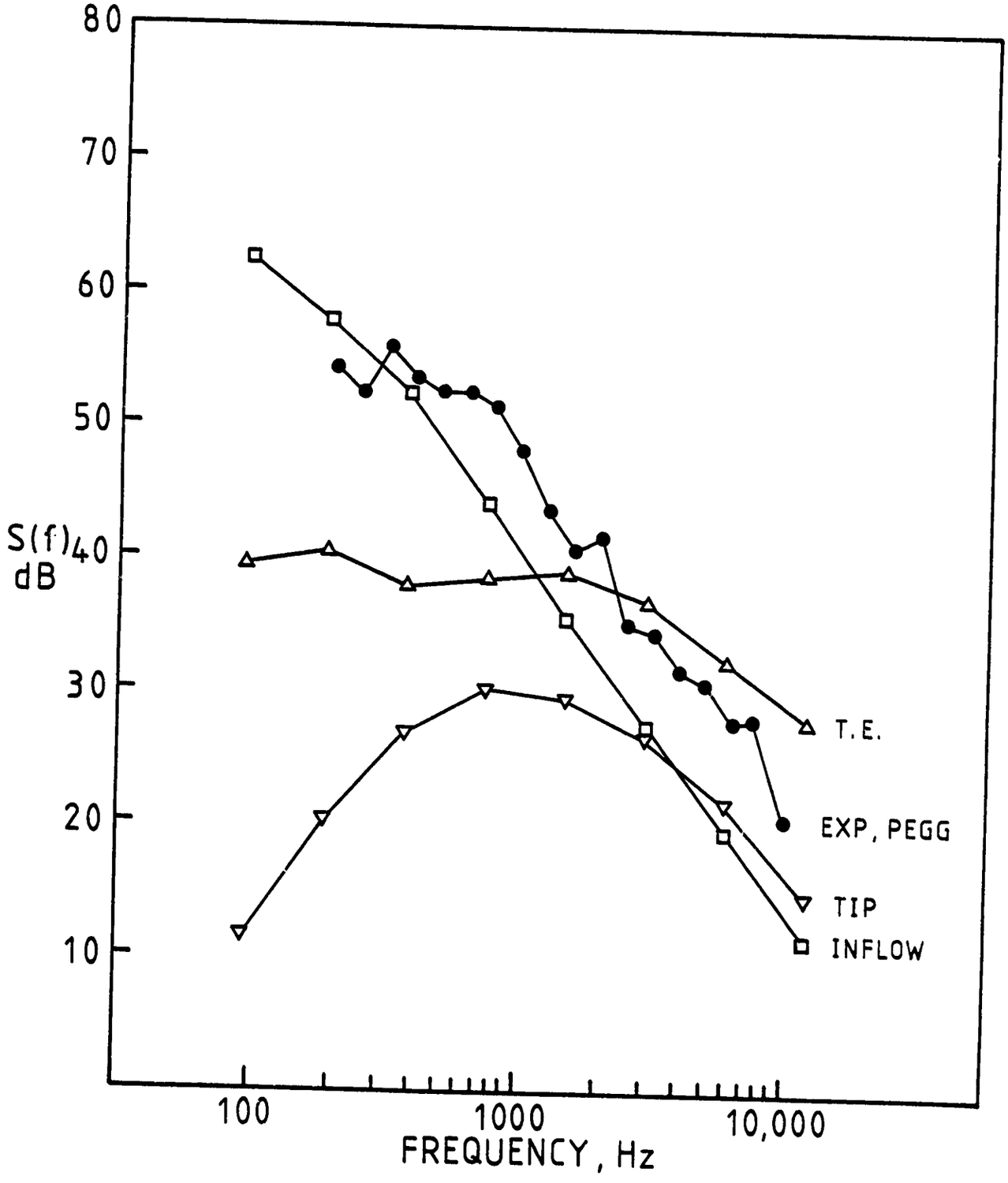

Figure 9 Comparison of Main Rotor Noise Calculations with Experiment of Pegg et al.[61], for Full Scale SH-3A helicopter, $\phi = -90°$, $\Lambda = 55$ m, $\sqrt{\overline{w^2}} =$ 1 m/s

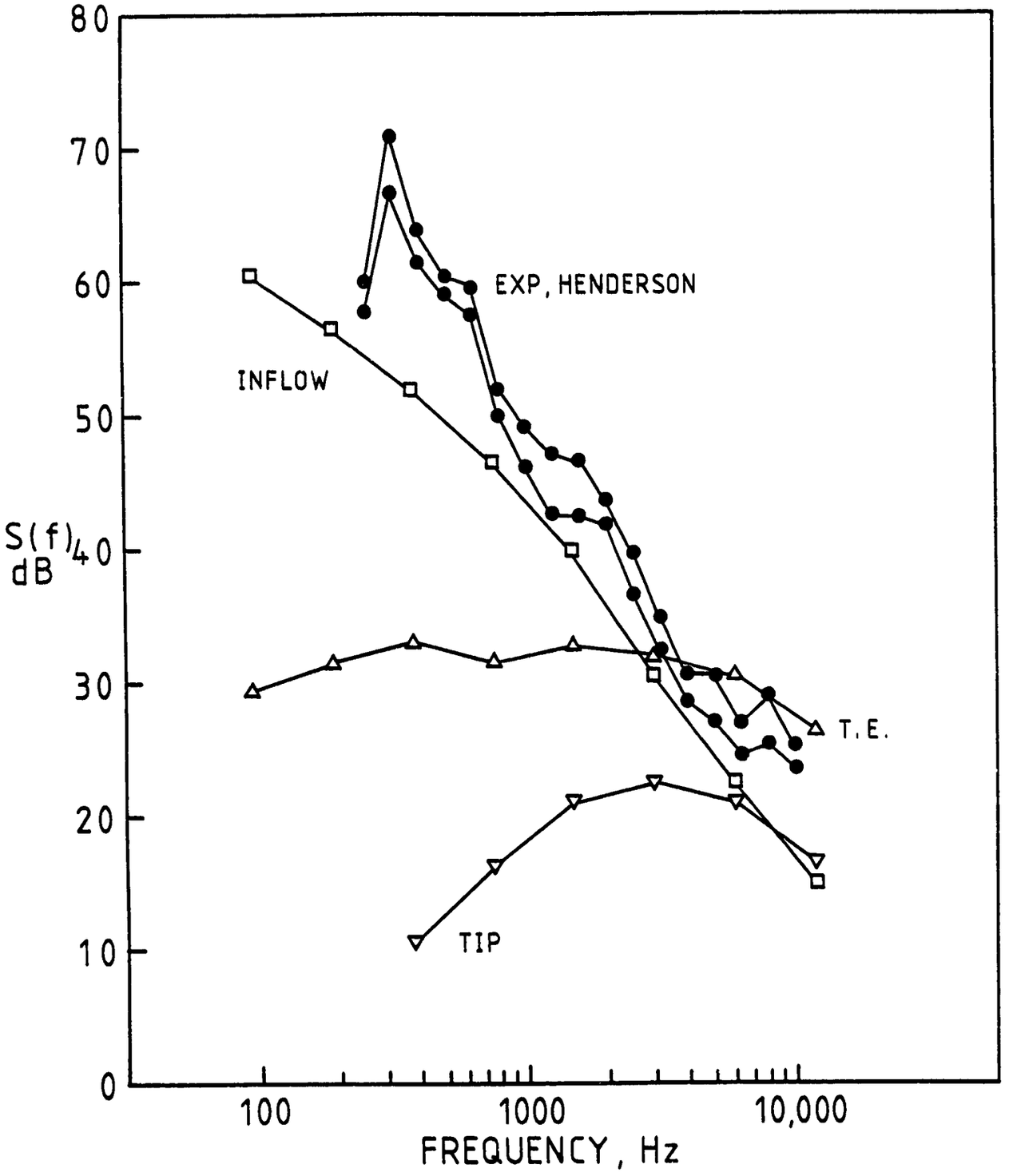

Figure 10 Comparison of Main Rotor Noise Calculations with Experiment of Henderson et al. (62), for Full Scale OH-6A Helicopter, ϕ = -90°, Λ = 27m, $\sqrt{w^2}$ = 1 m/s

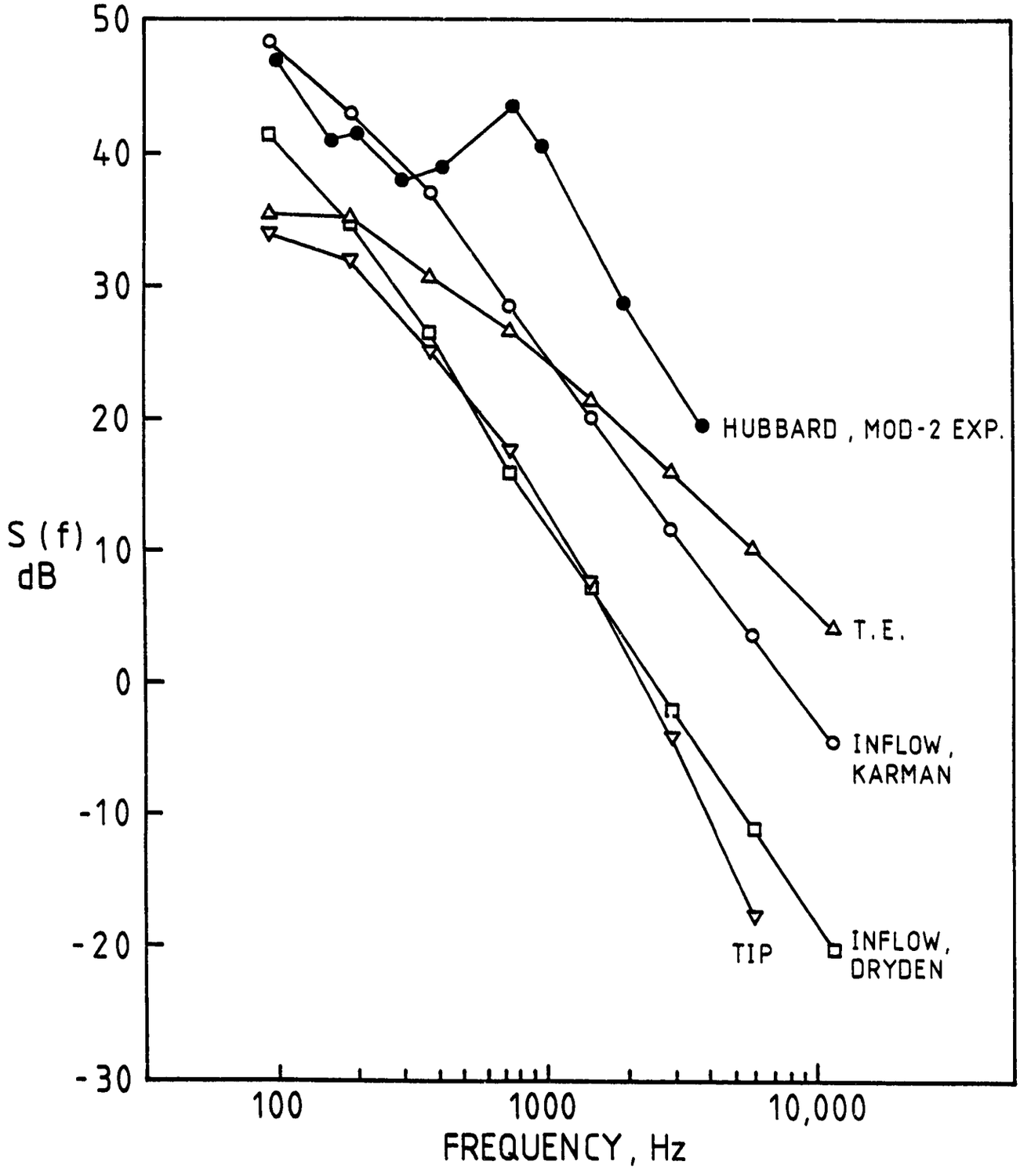

Figure 11 Comparison of Predictions with Hubbard et al.'s Experiment (33) for MOD-2 Wind Turbine, Λ = 55 m, $\sqrt{\overline{w^2}}$ = 1 m/s, Ground Distance = 69 m

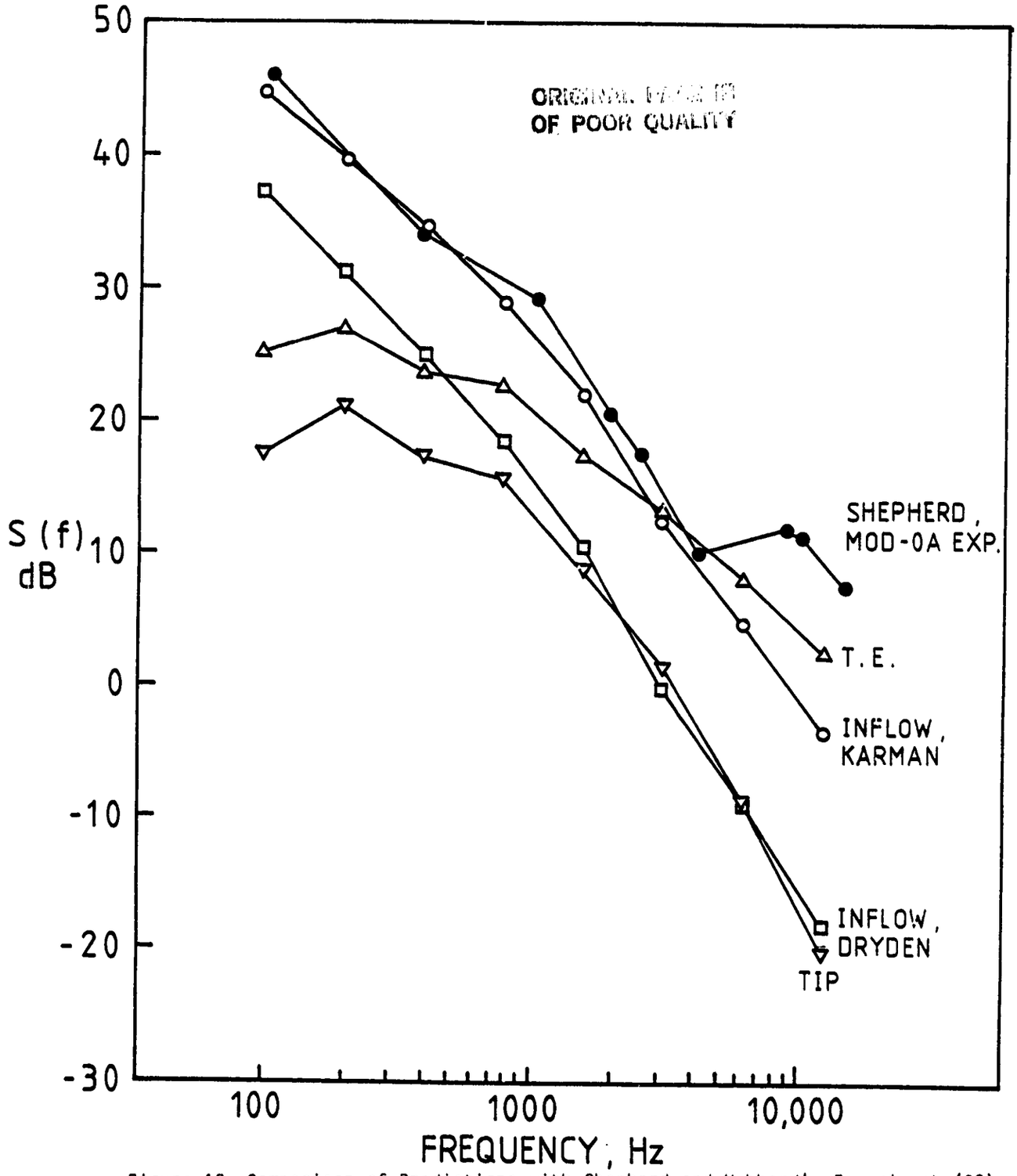

Figure 12 Comparison of Predictions with Shepherd and Hubbard's Experiment (63) for MOD-0A Wind Turbine, Λ = 27.5 m, $\sqrt{w^2}$ = 1 m/s, Ground Distance = 61 m

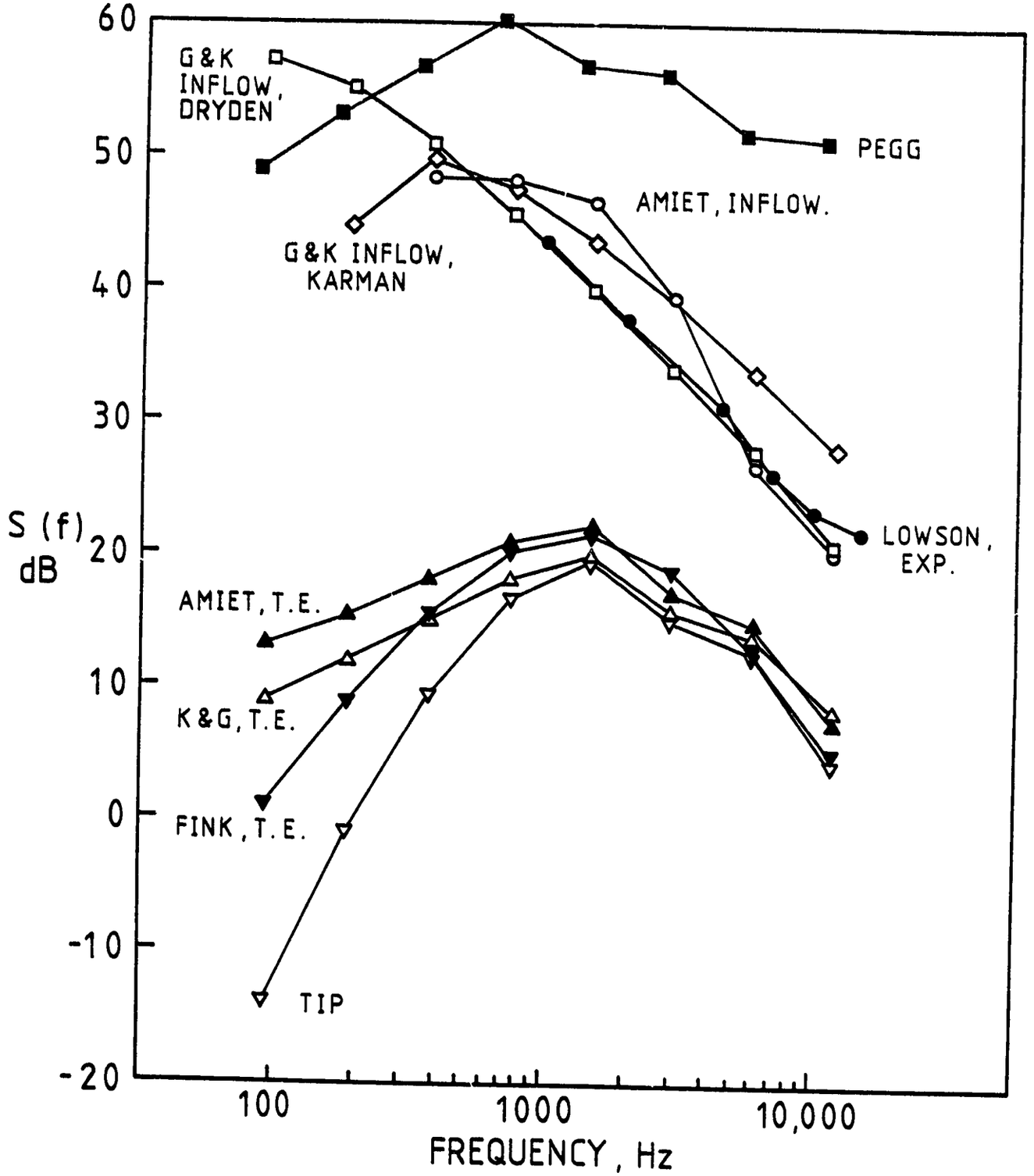

Figure 13 Comparison of Predictions for Low Speed Fan Noise, Experiment of Lowson (42), 1500 RPM, Tip Pitch = 15°

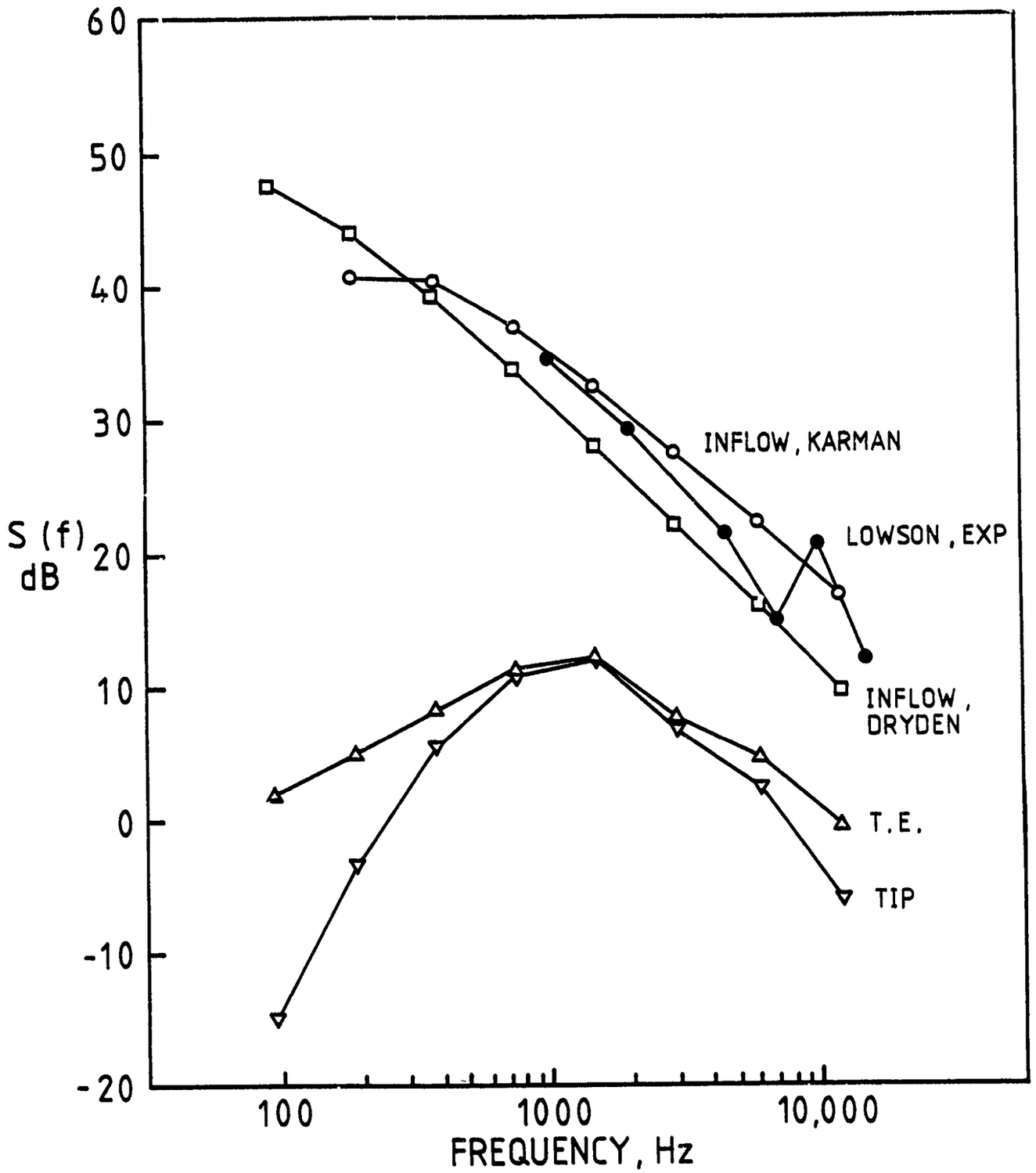

Figure 14 Comparison of Predictions for Low Speed Fan Noise, Experiment of Lowson (42), 1000 RPM, Tip Pitch = 15°

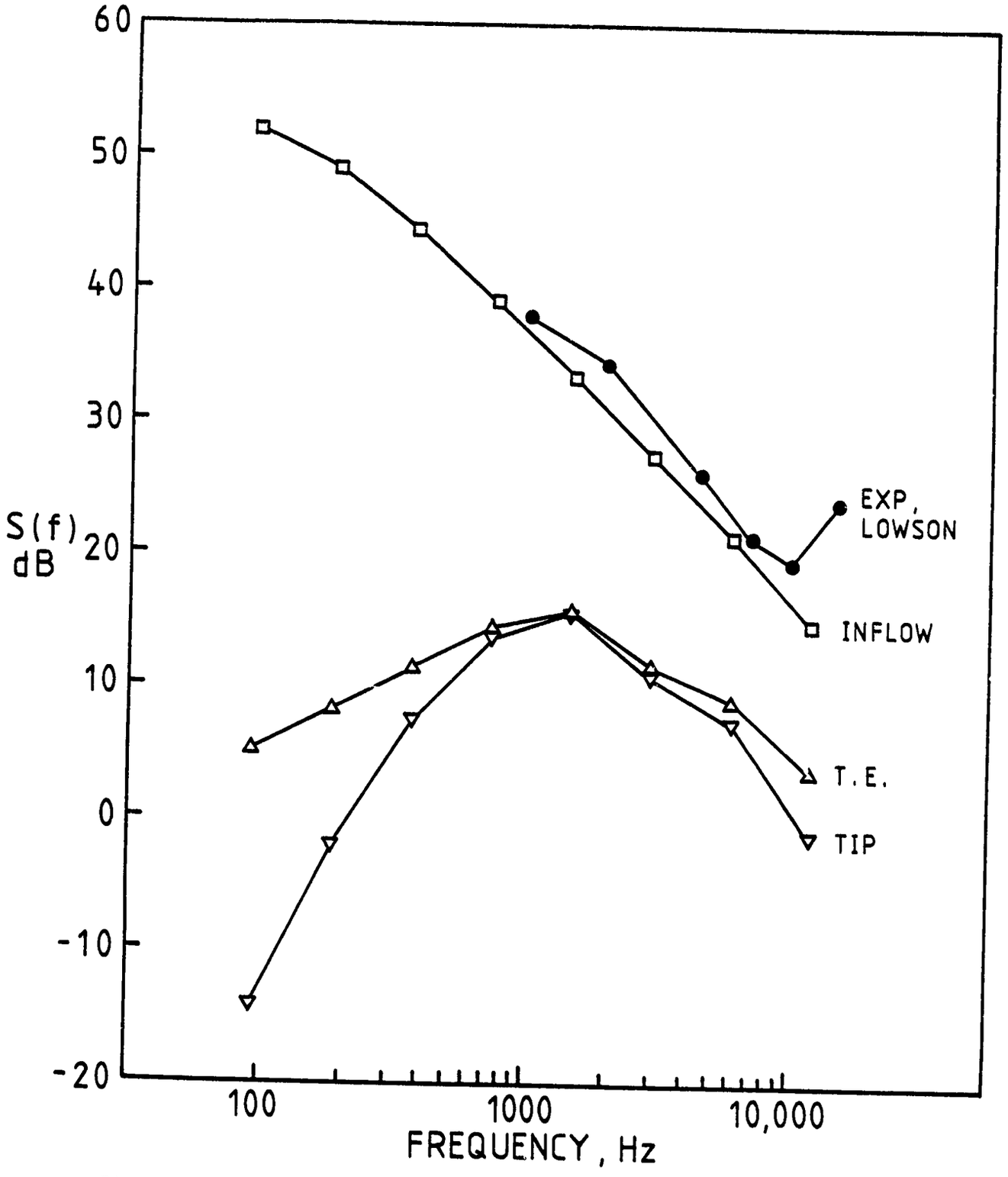

Figure 15 Comparison of Predictions for Low Speed Fan Noise, Experiment of Lowson (42), 1200 RPM, Tip Pitch = 15°

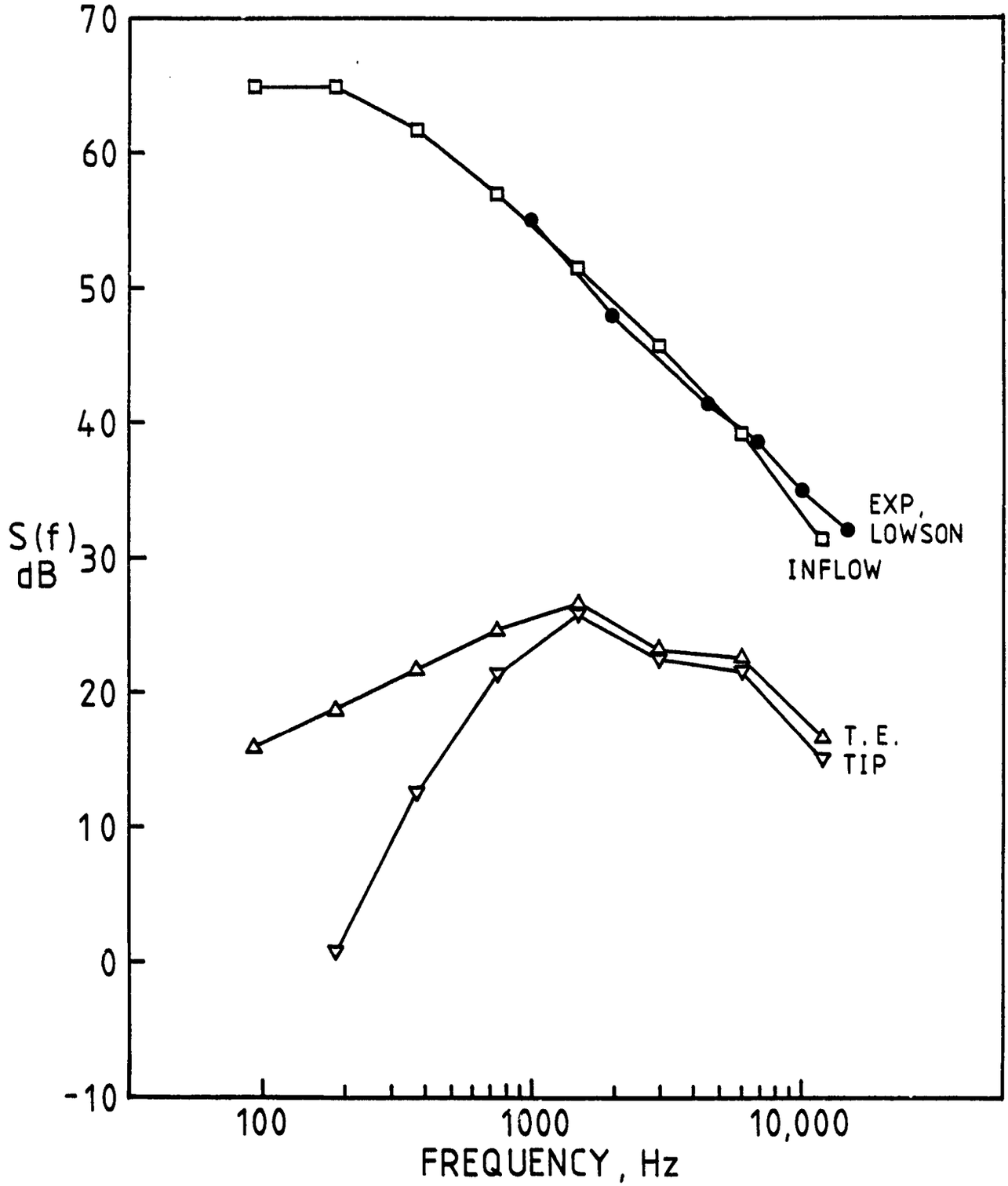

Figure 16 Comparison of Predictions for Low Speed Fan Noise, Experiment of Lowson (42), 2200 RPM, Tip Pitch = 15°

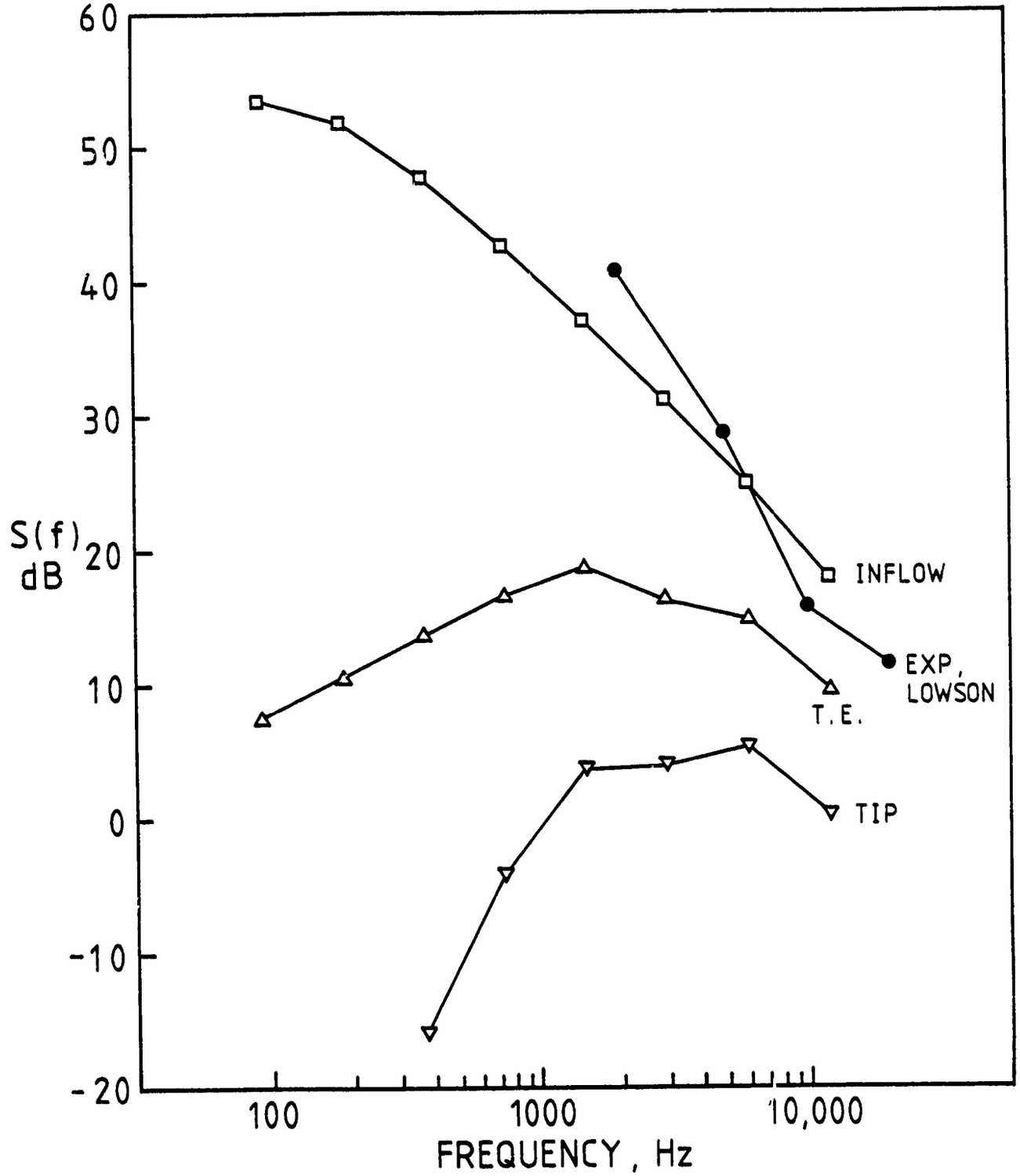

Figure 17 Comparison of Predictions for Low Speed Fan Noise, Experiment of Lowson (42), 1600 RPM, Tip Pitch = 5°

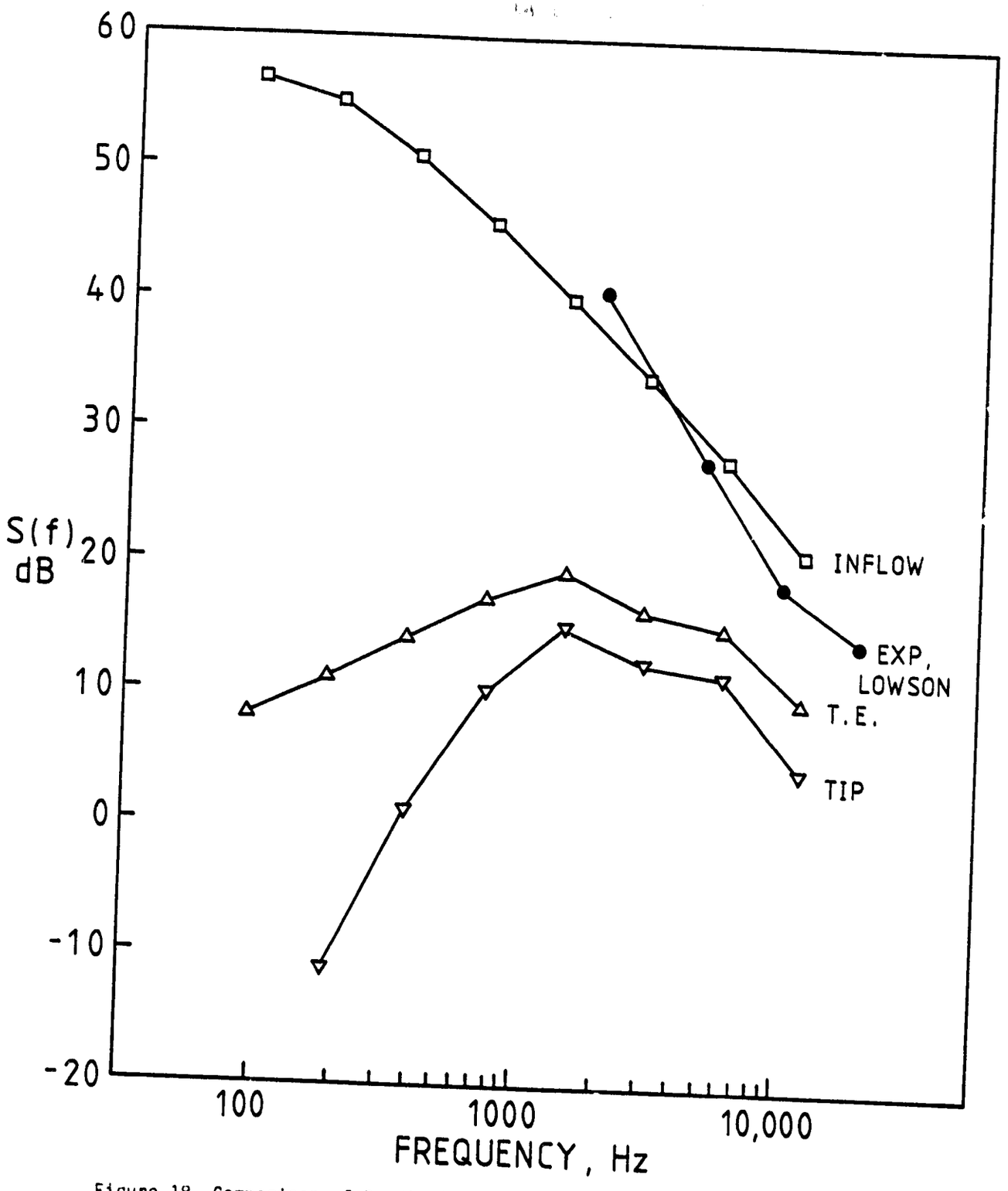

Figure 18 Comparison of Predictions for Low Speed Fan Noise, Experiment of (42), 1600 RPM, Tip Pitch = 10°

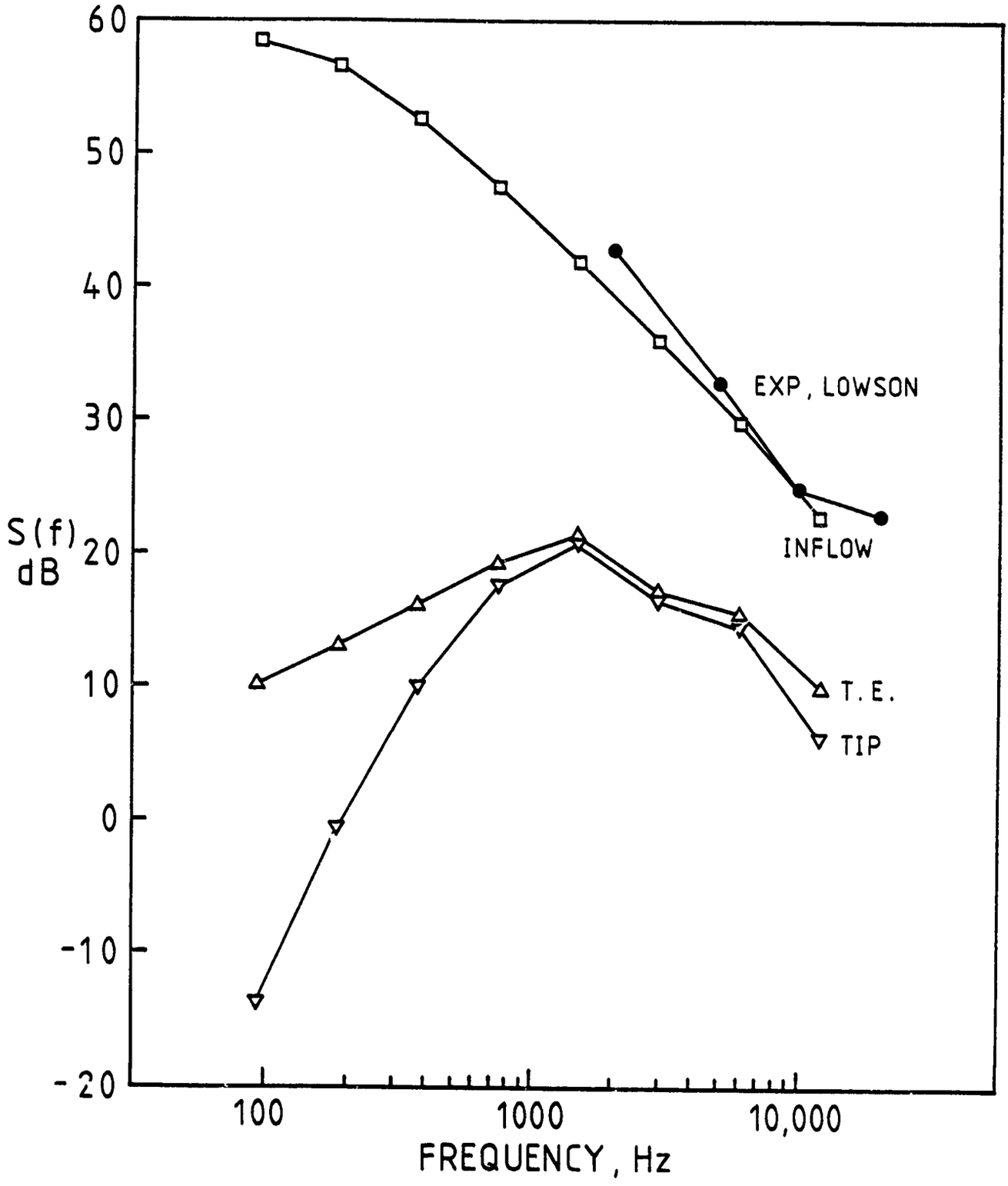

Figure 19 Comparison of Predictions for Low Speed Fan Noise, Experiment of Lowson (42), 1600 RPM, Tip Pitch = 15°

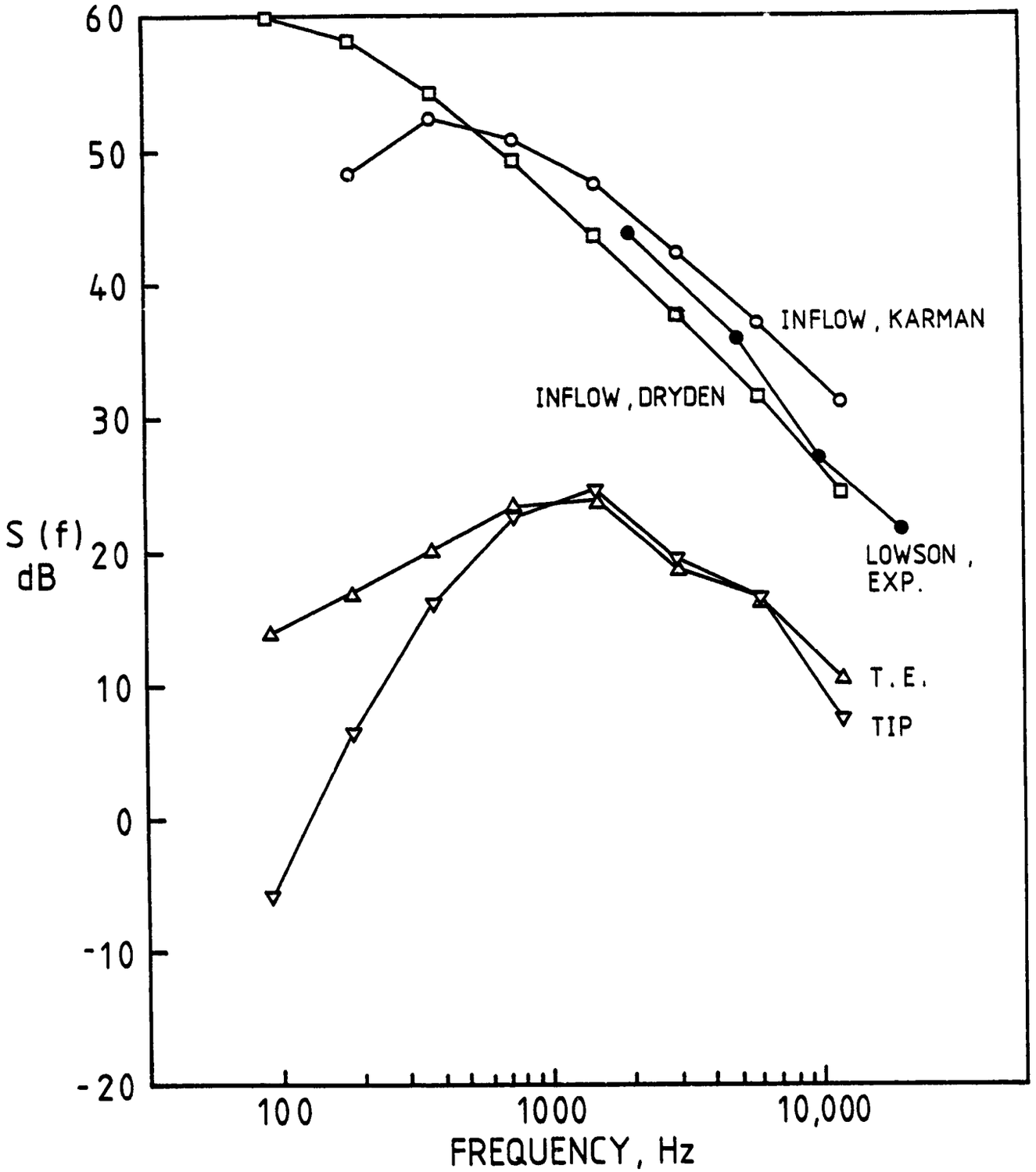

Figure 20 Comparison of Predictions for Low Speed Fan Noise, Experiment of Lowson (42), 1600 RPM, Tip Pitch = 20°

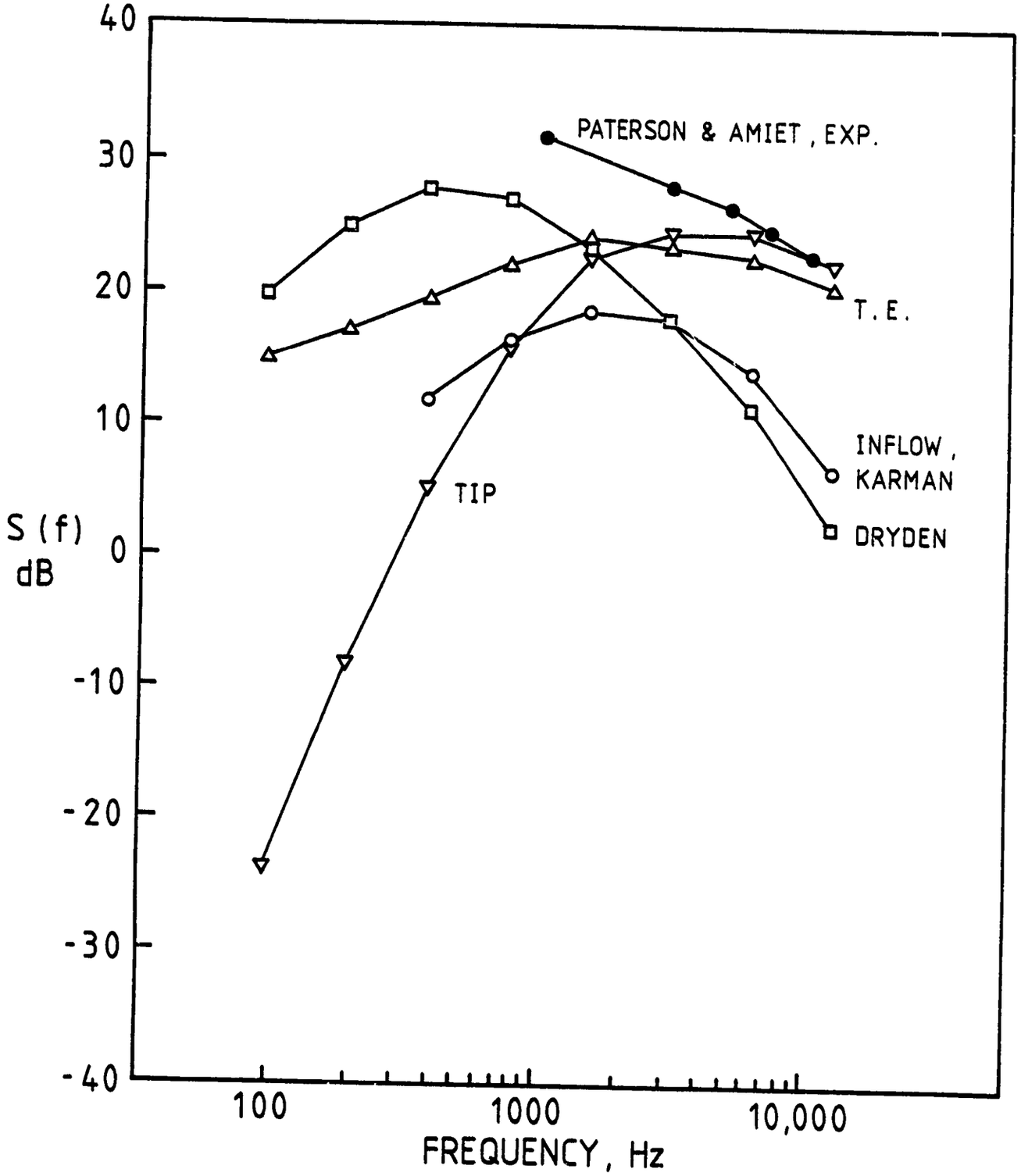

Figure 21 Comparison of Predictions for Model Rotor, Experiment of Paterson and Amiet (64), No Grid, TEST VA-C-1

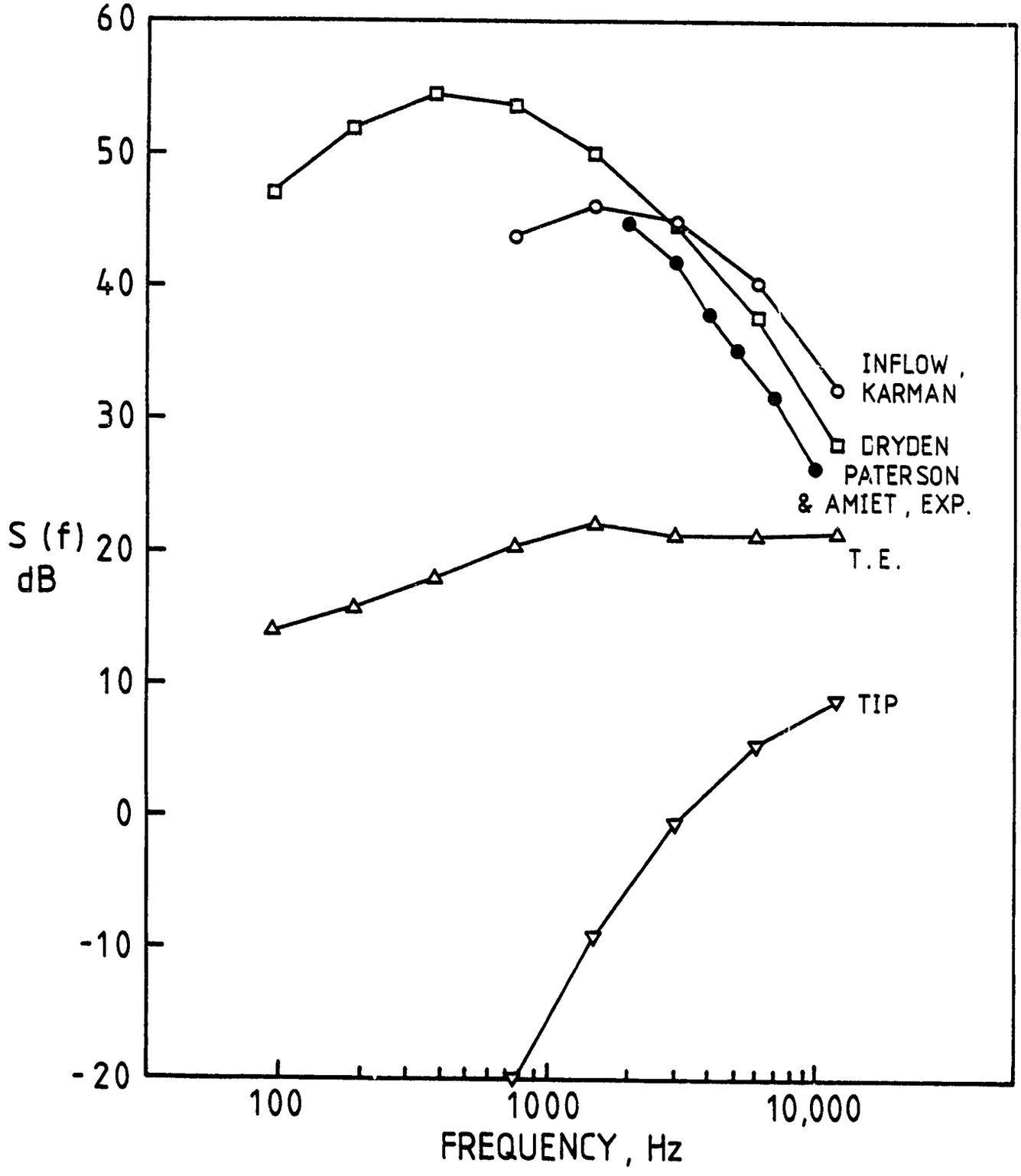

Figure 22 Comparison of Predictions for Model Rotor, Experiment of Paterson and Amiet (64), Medium Grid, TEST VA-M-4

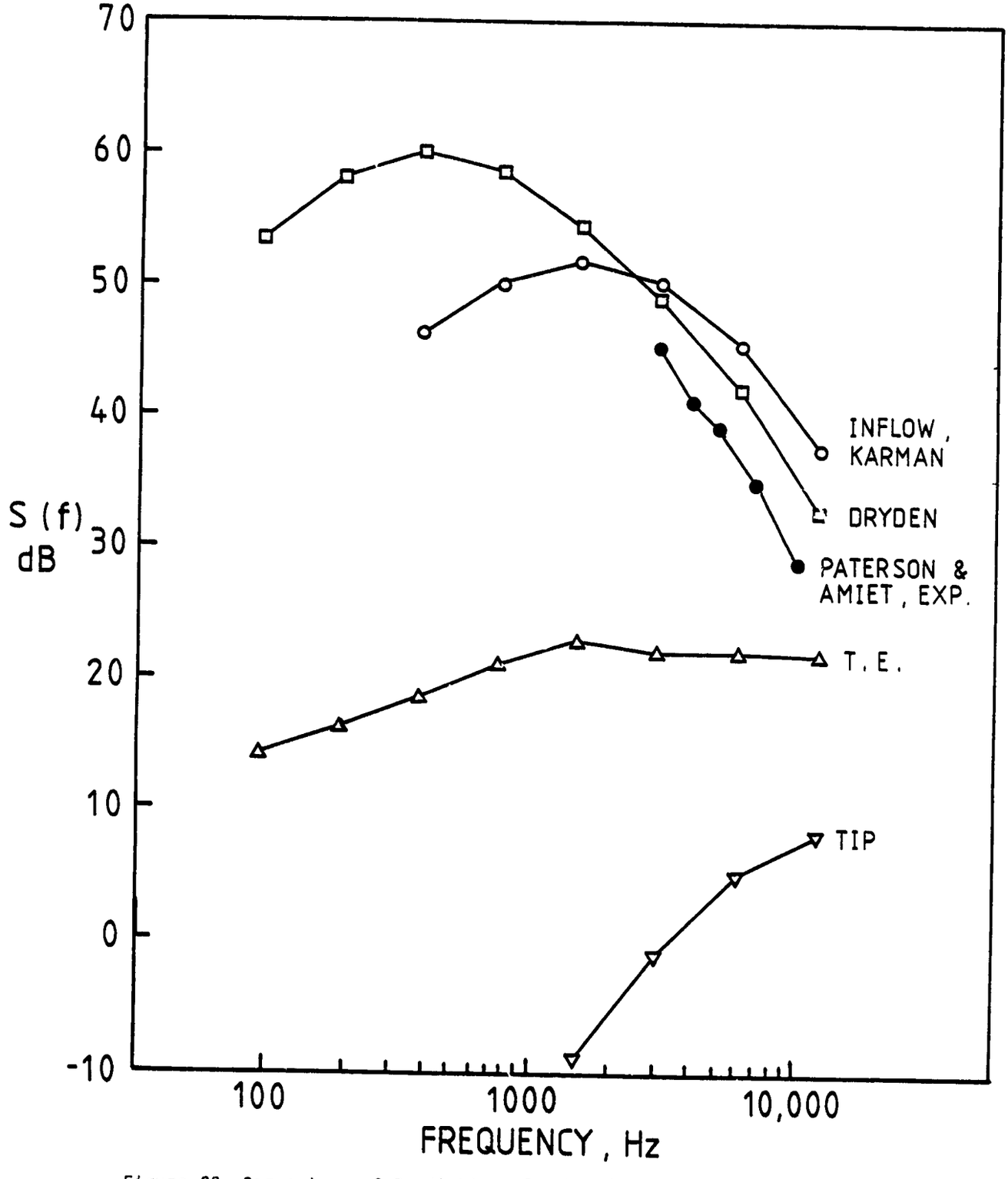

Figure 23 Comparison of Predictions for Model Rotor, Experiment of Paterson and Amiet (64), Large Grid, TEST VA-L-3

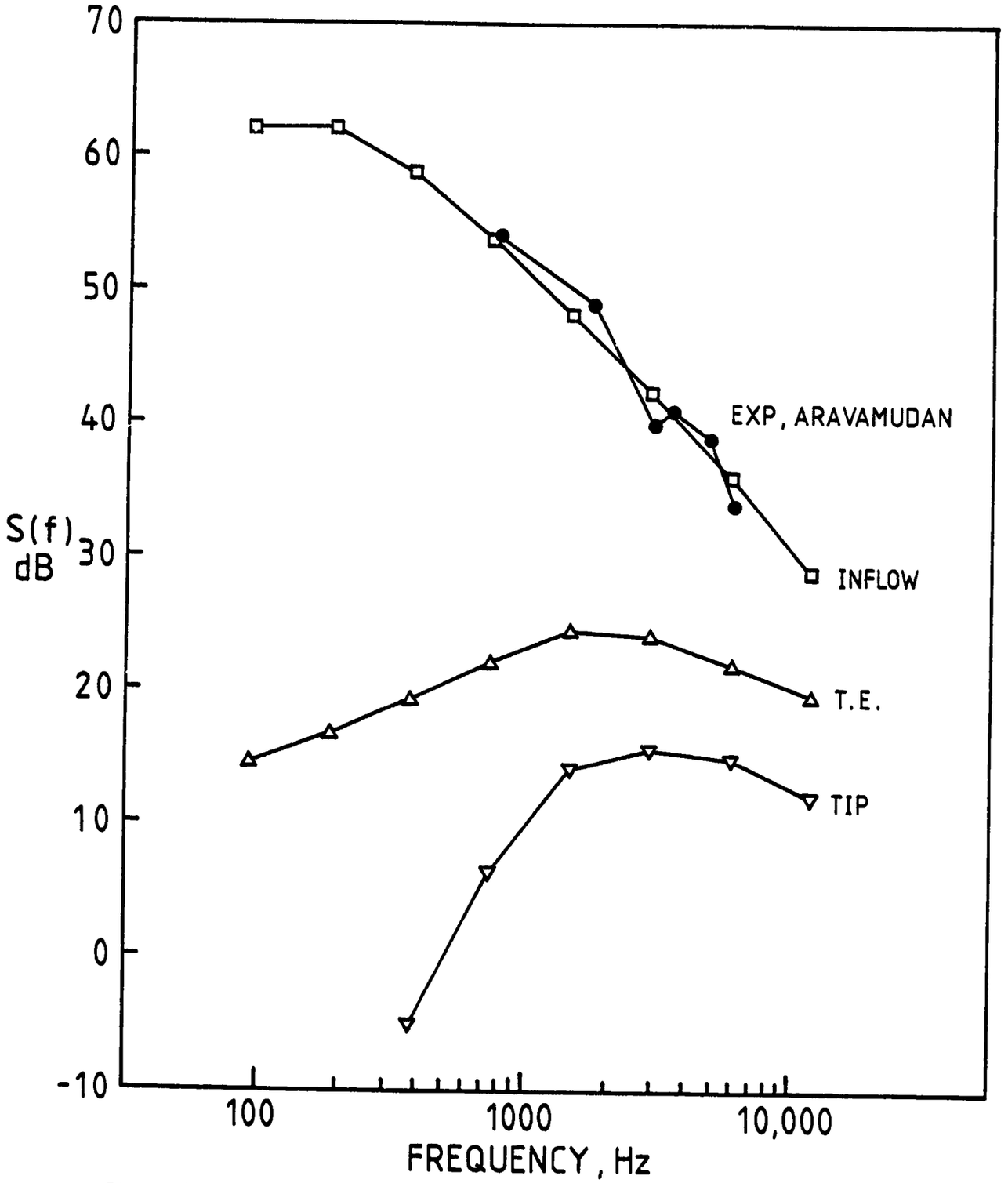

Figure 24 Comparison of Predictions for Model Rotor, Experiment of Aravamudan and Harris (18), 0.75" x 6" Grid, Tunnel Speed = 51 fps

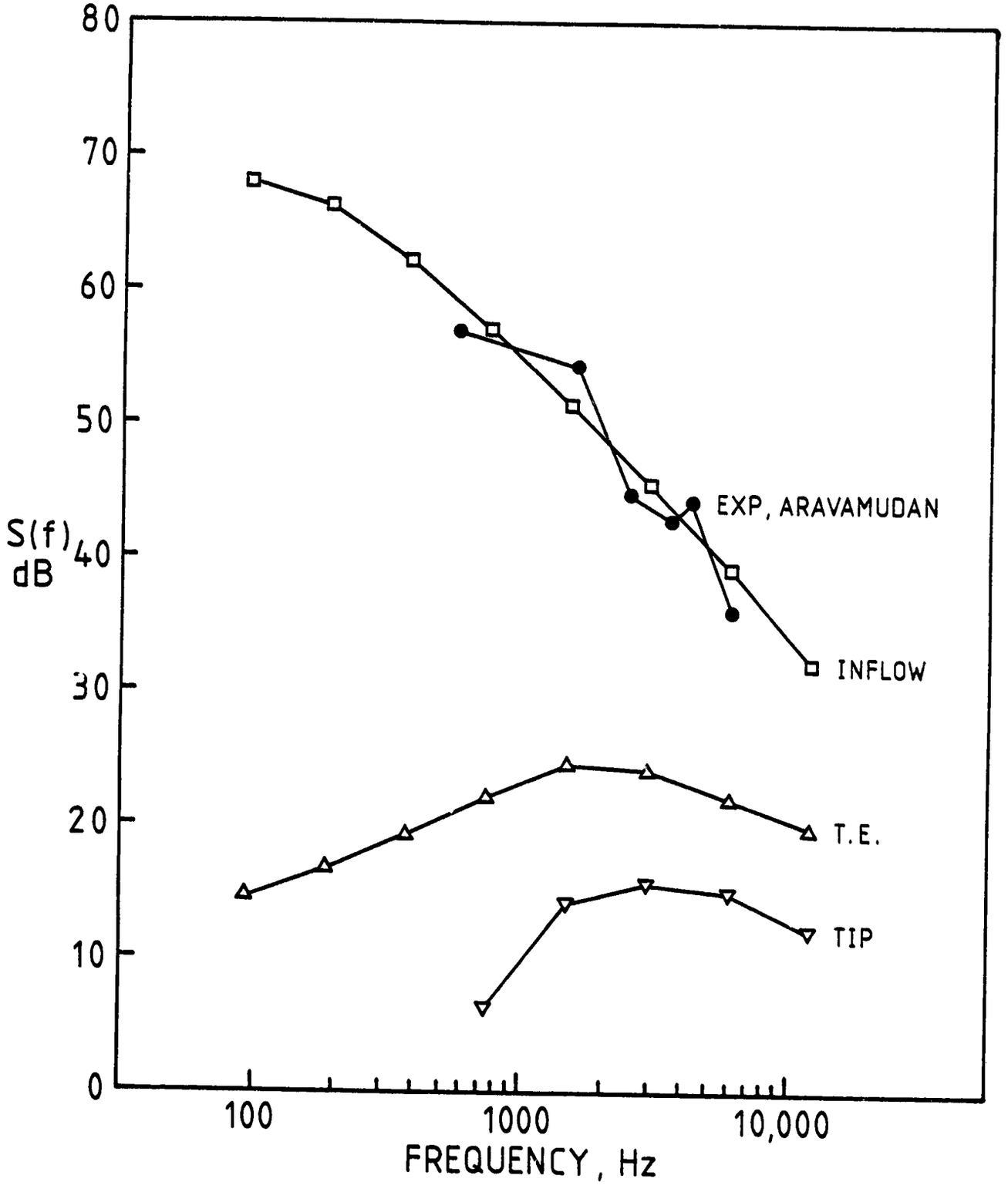

Figure 25 Comparison of Predictions for Model Rotor, Experiment of Aravamudan and Harris (18), 13.5" x 20" Grid, Tunnel Speed = 51 fps

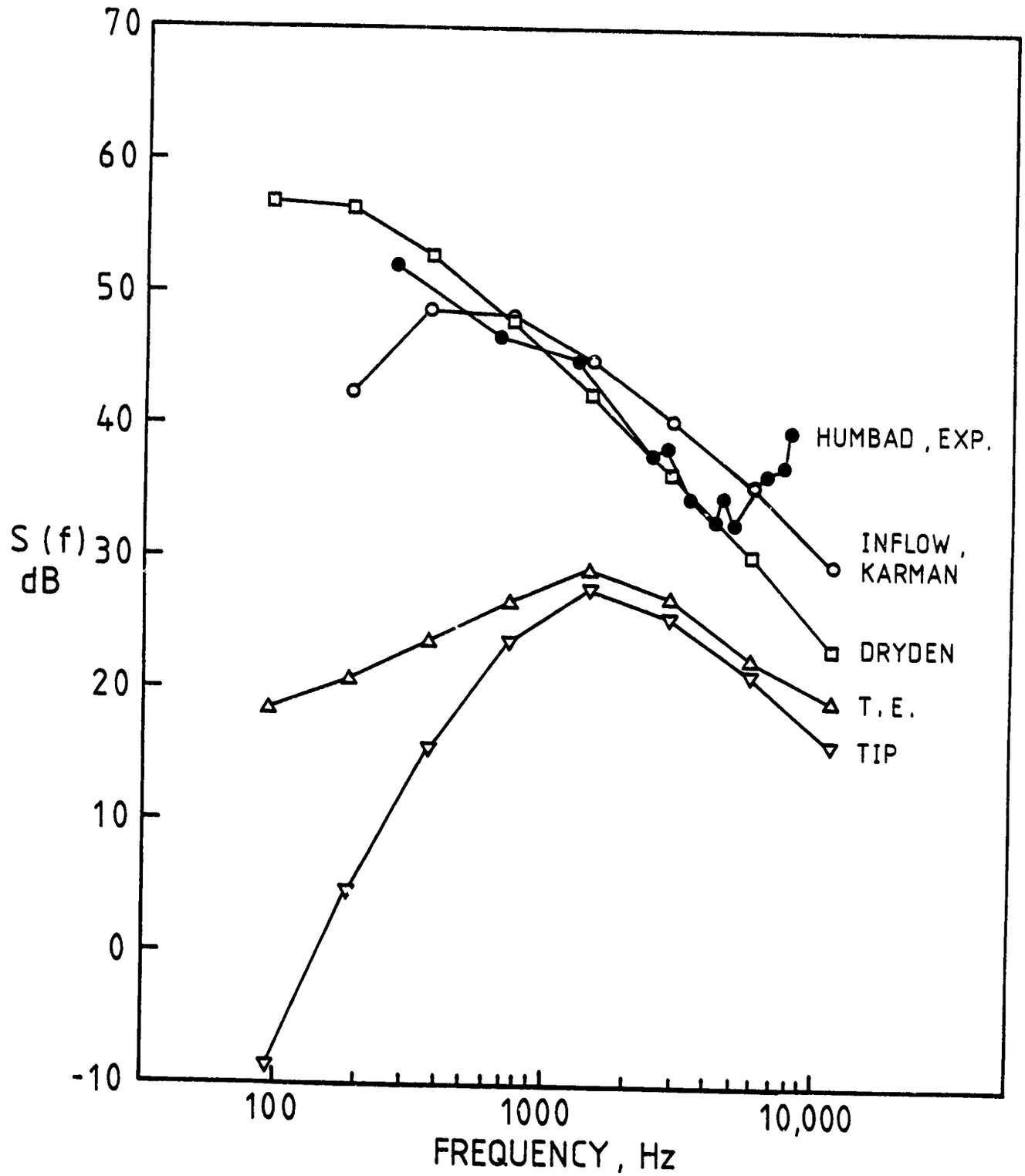

Figure 26 Comparison of Predictions for Model Rotor, Experiment of Humbad and and (19), Small Grid, $\mu = 0.125$

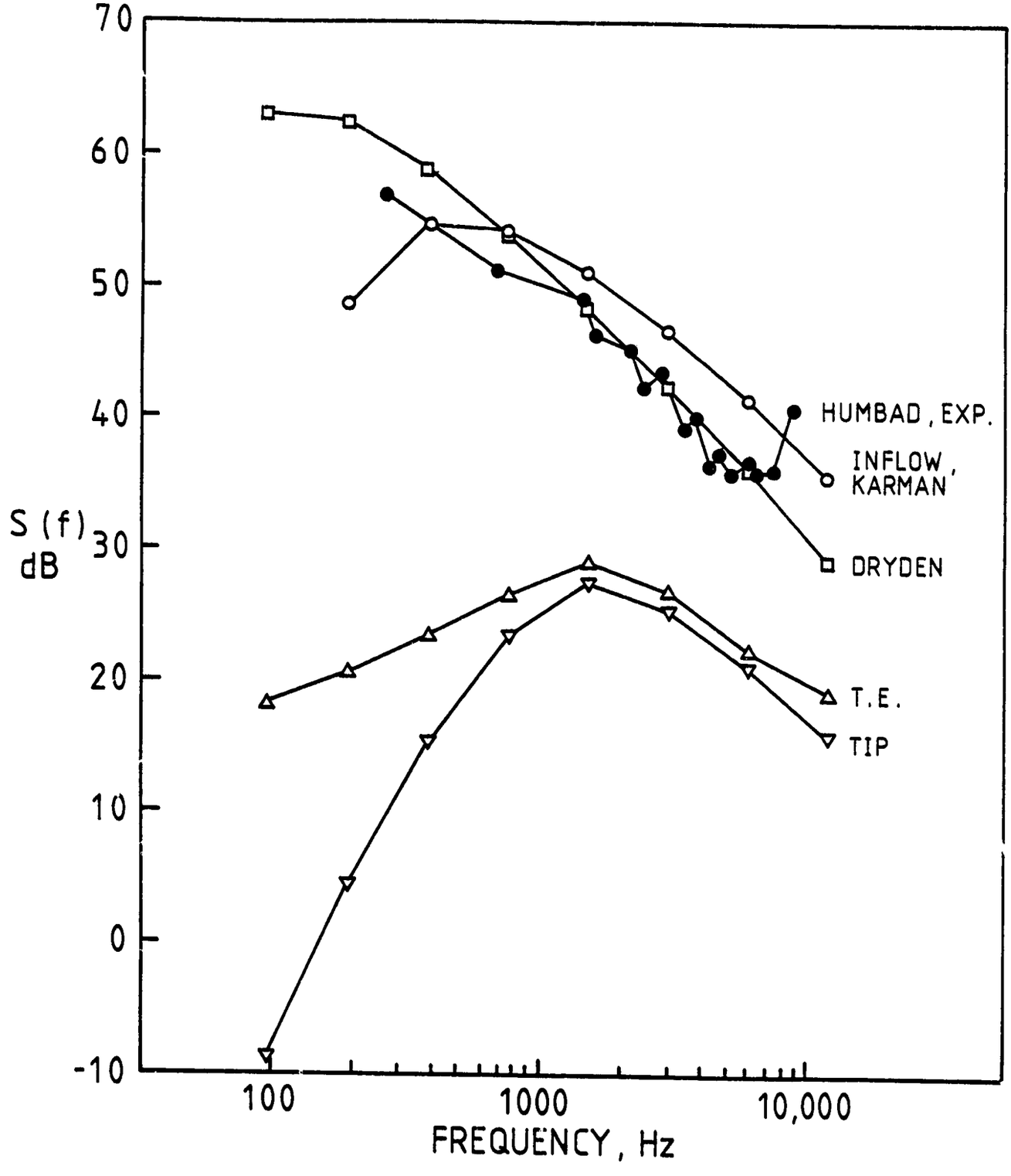

Figure 27 Comparison of Predictions for Model Rotor, Experiment of Humbad and Harris (19), Small Grid, $\mu = 0.25$

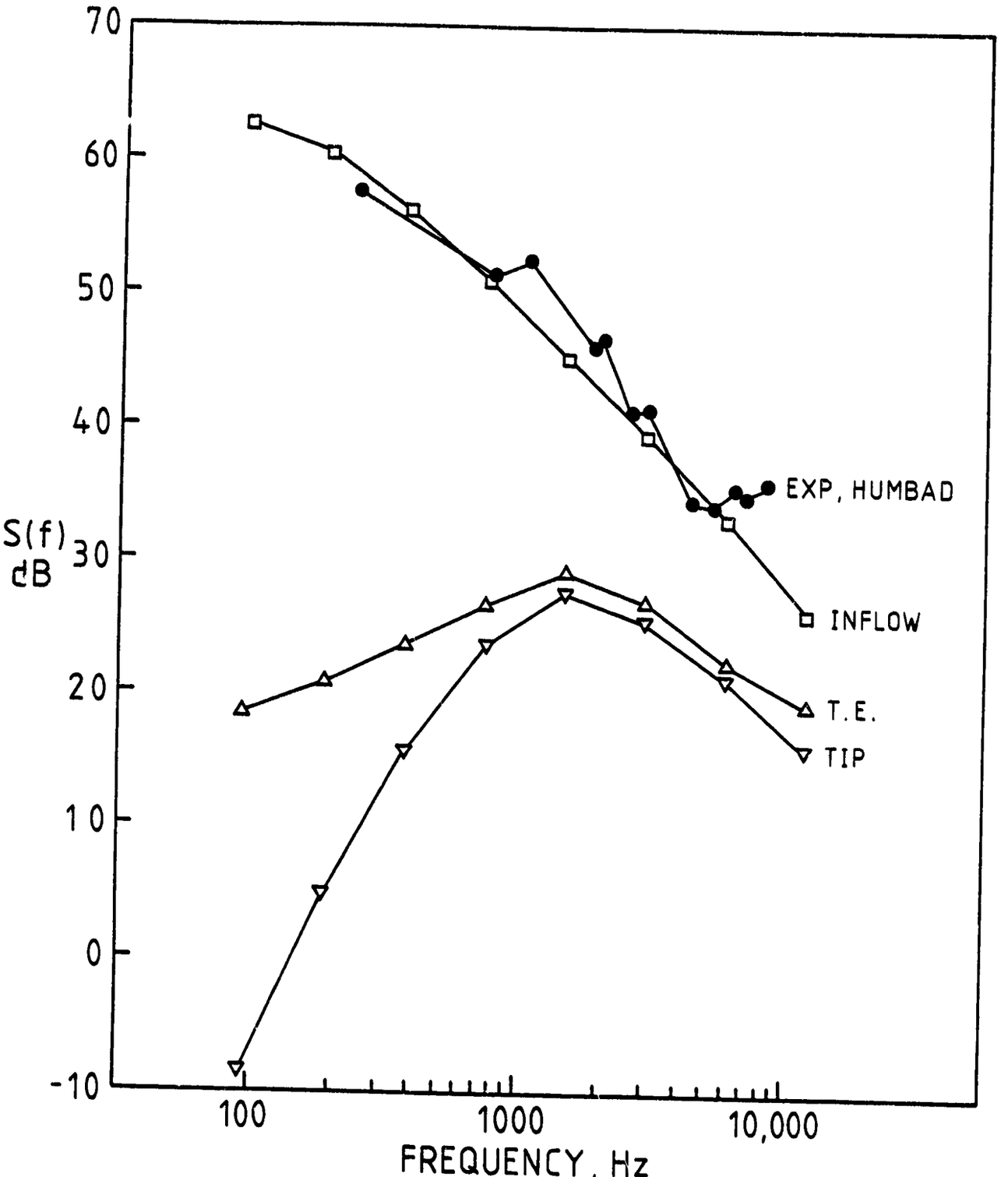

Figure 28 Comparison of Predictions for Model Rotor, Experiment of Humbad and Harris (19), Large Grid, $\mu = 0.125$

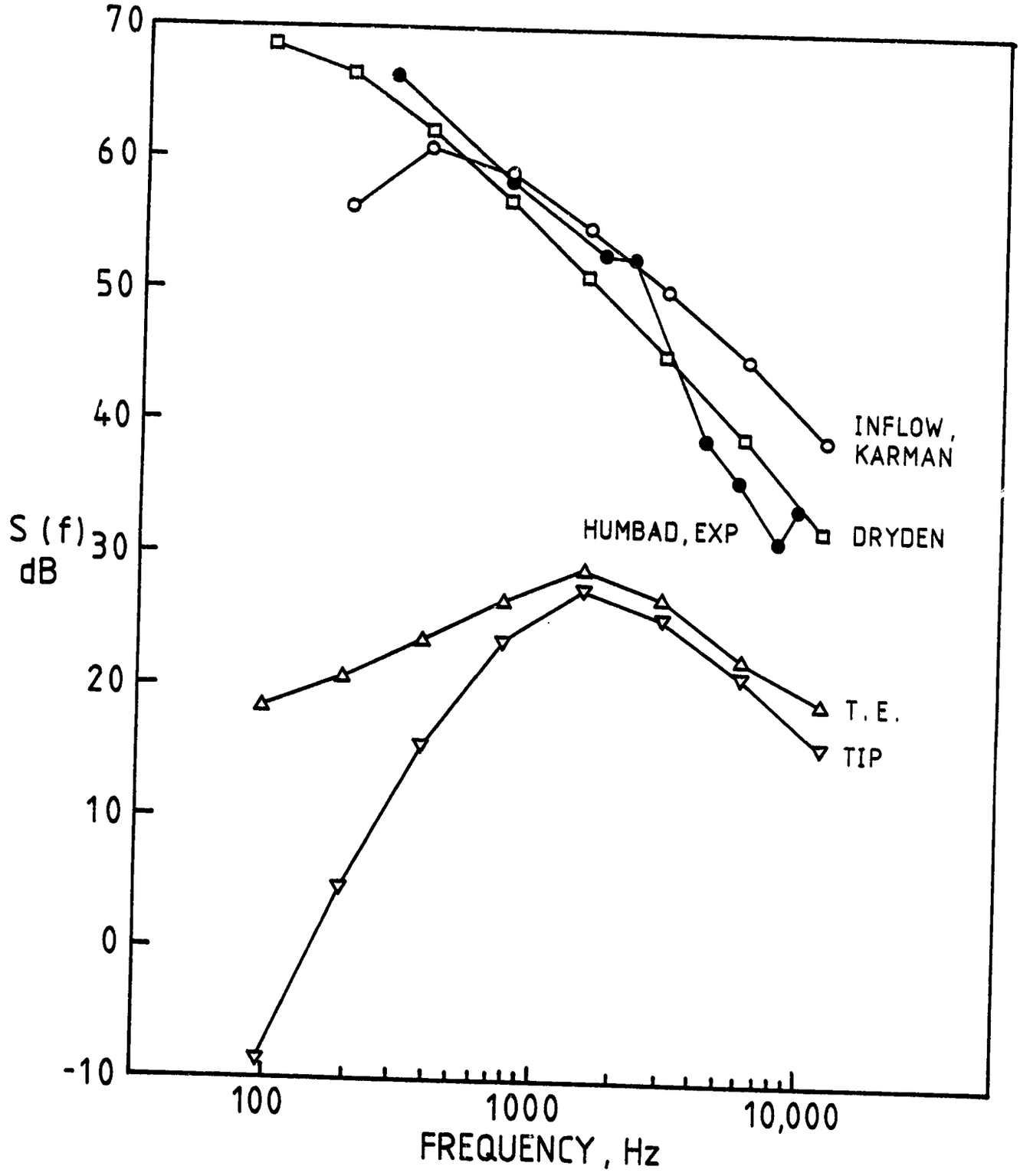

Figure 29 Comparison of Predictions for Model Rotor, Experiment of Humbad and Harris (19), Large Grid, $\mu = 0.25$

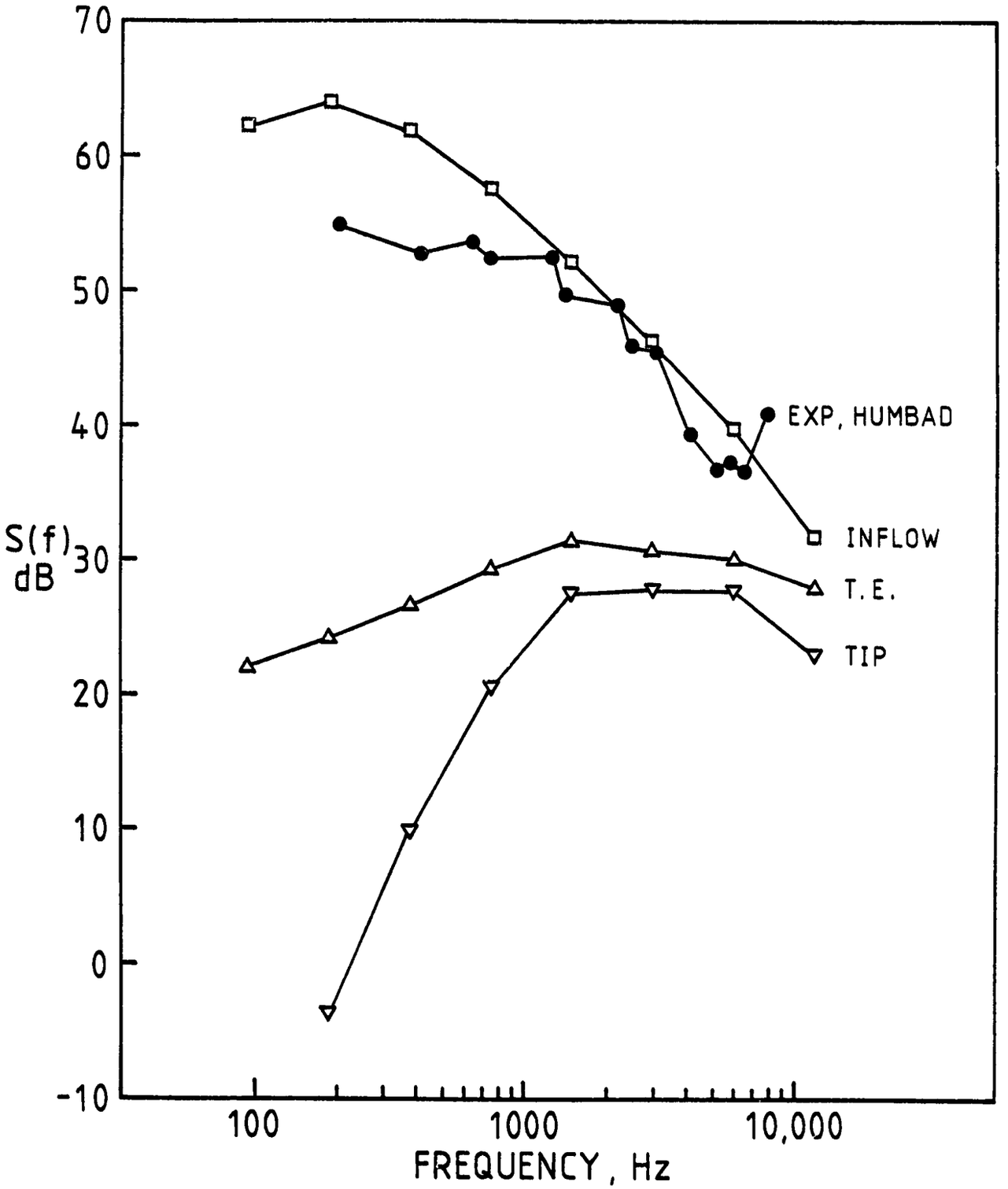

Figure 30 Comparison of Predictions for Model Rotor, Experiment of Humbad and Harris (19), Small Grid, 1500 RPM

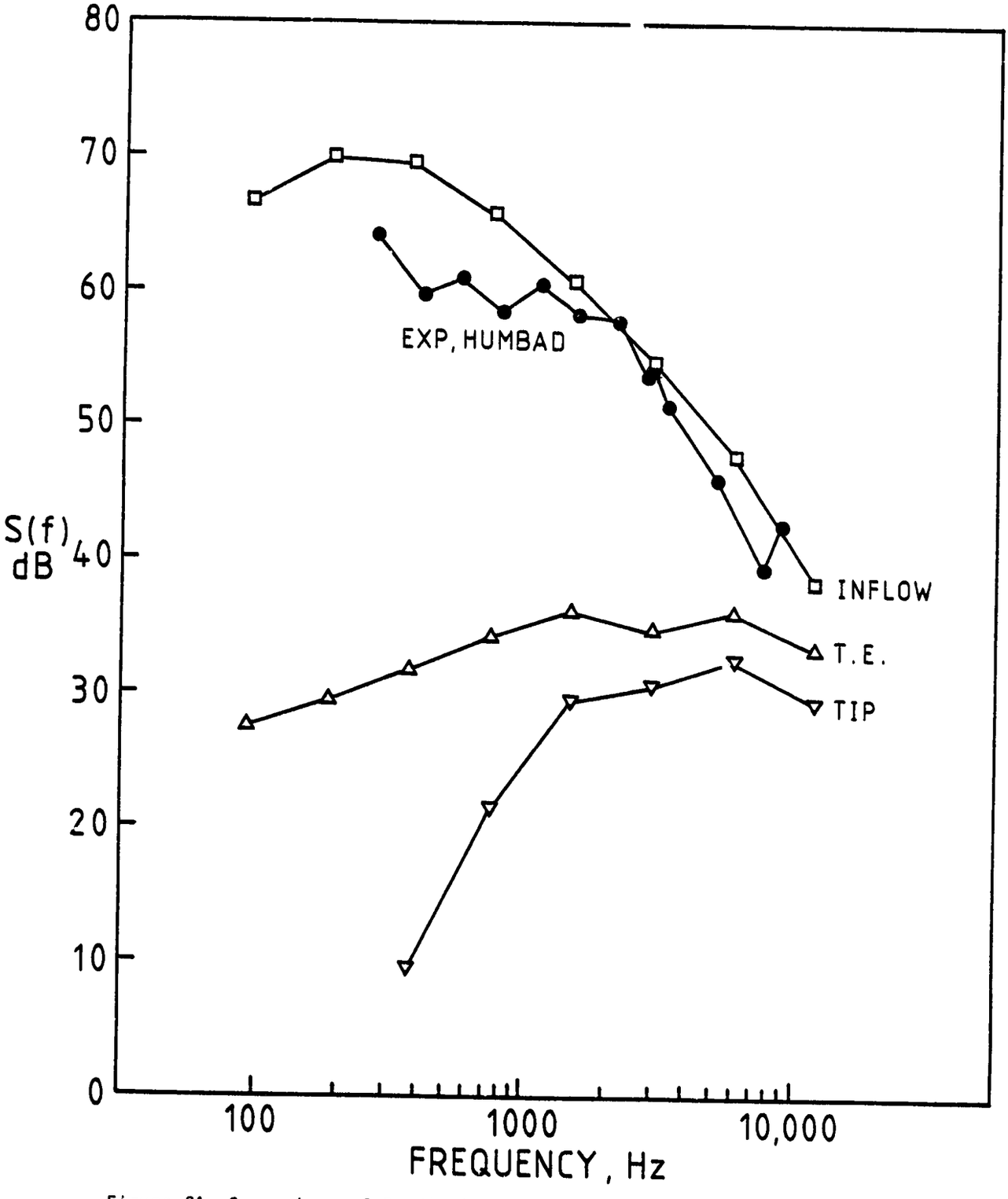

Figure 31 Comparison of Predictions for Model Rotor, Experiment of Humbad and Harris (19), Small Grid, 2000 RPM

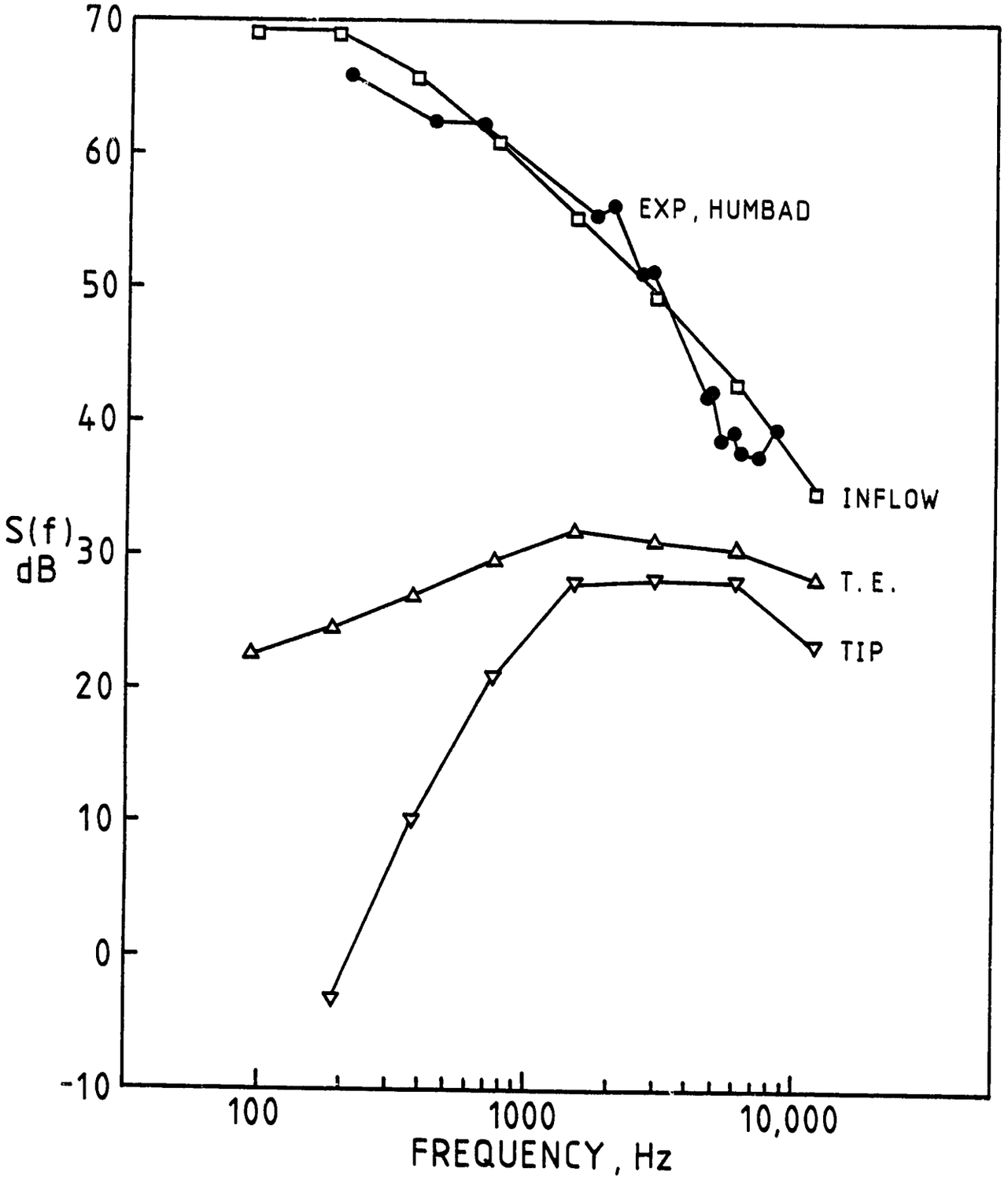

Figure 32 Comparison of Predictions for Model Rotor, Experiment of Humbad and Harris (19), Large Grid, 1500 RPM

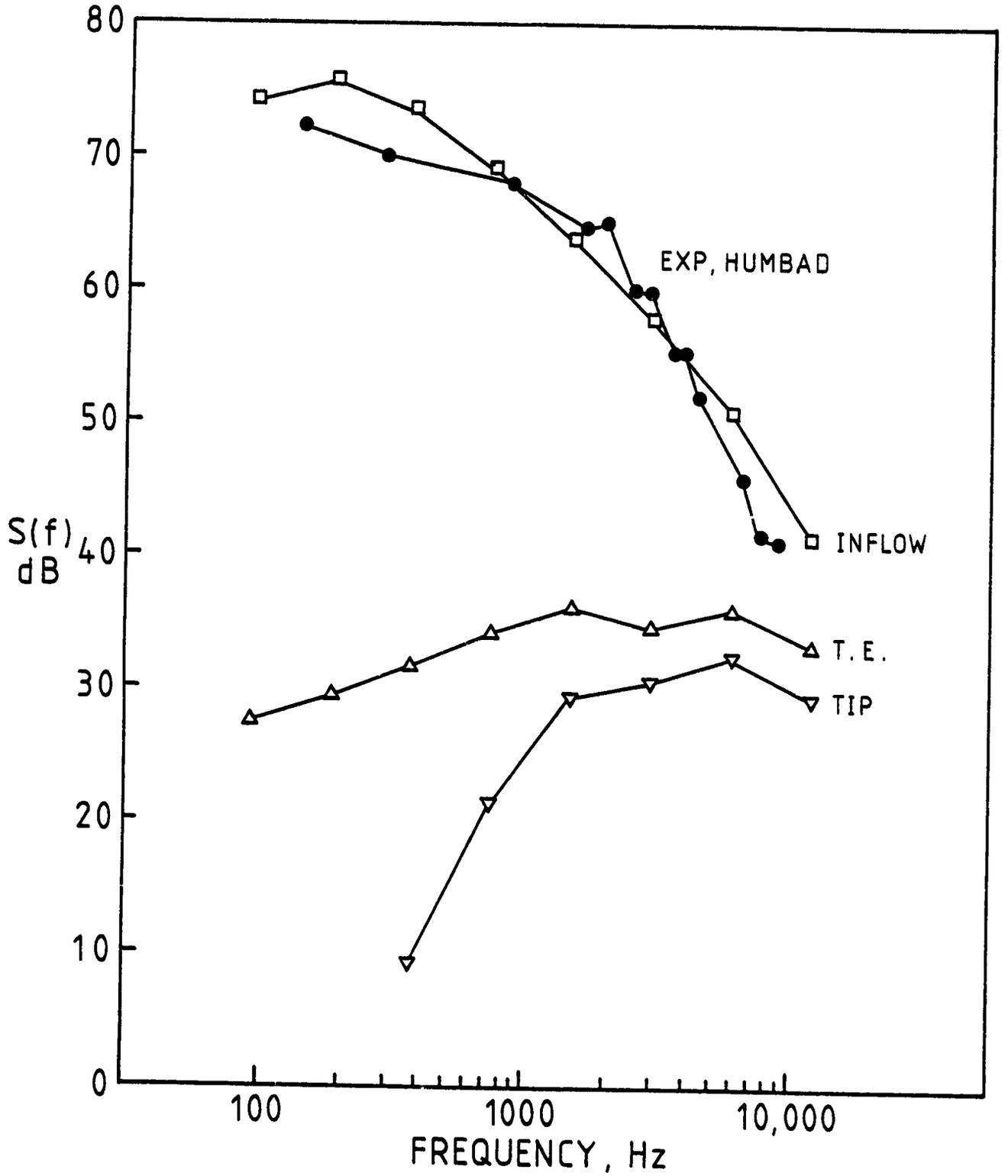

Figure 33 Comparison of Predictions for Model Rotor, Experiment of Humbad and Harris (19), Large Grid, 2000 RPM

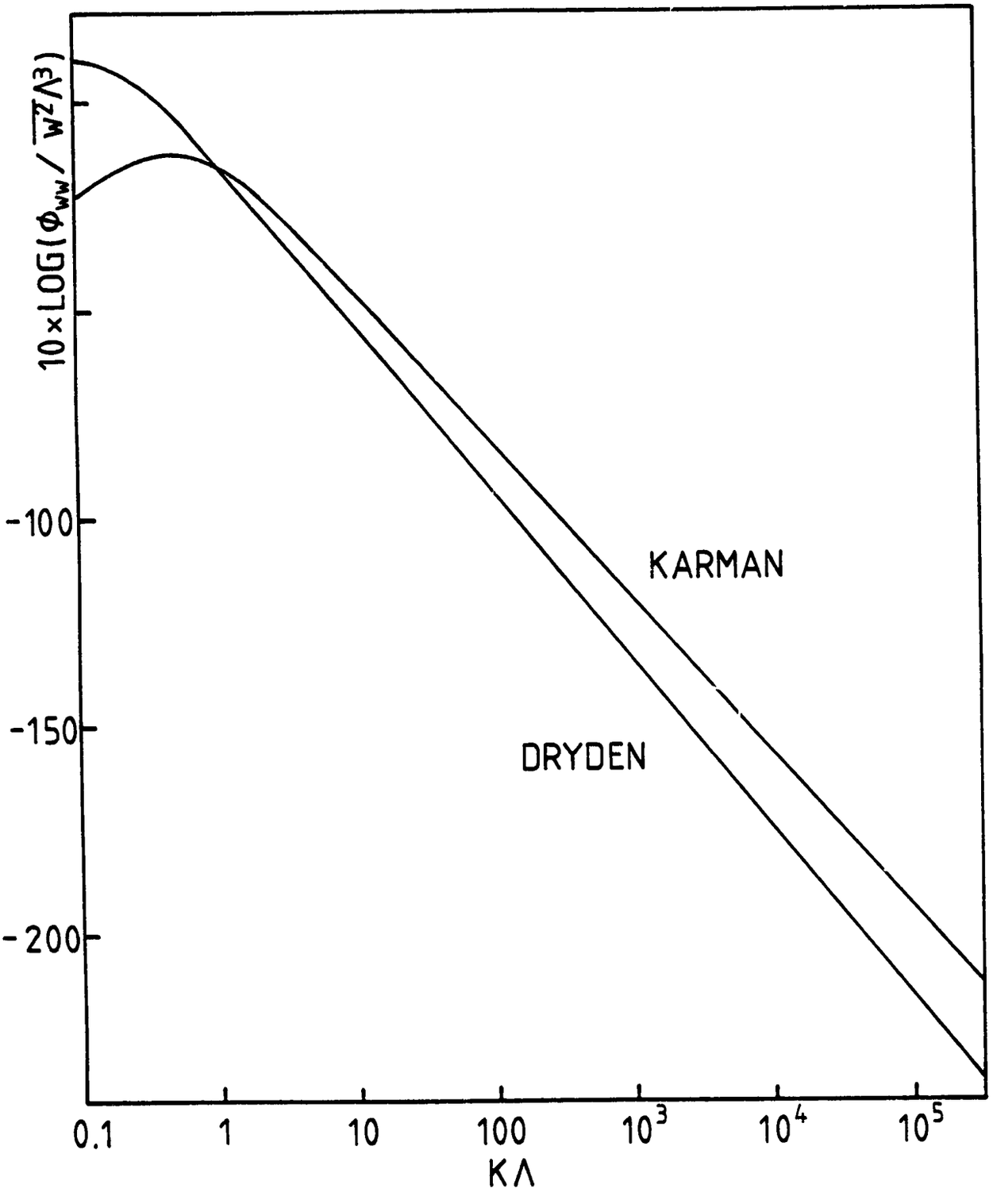

Figure 34 Comparison of Von Karman Spectrum and Dryden Spectrum Models of Atmospheric Turbulence

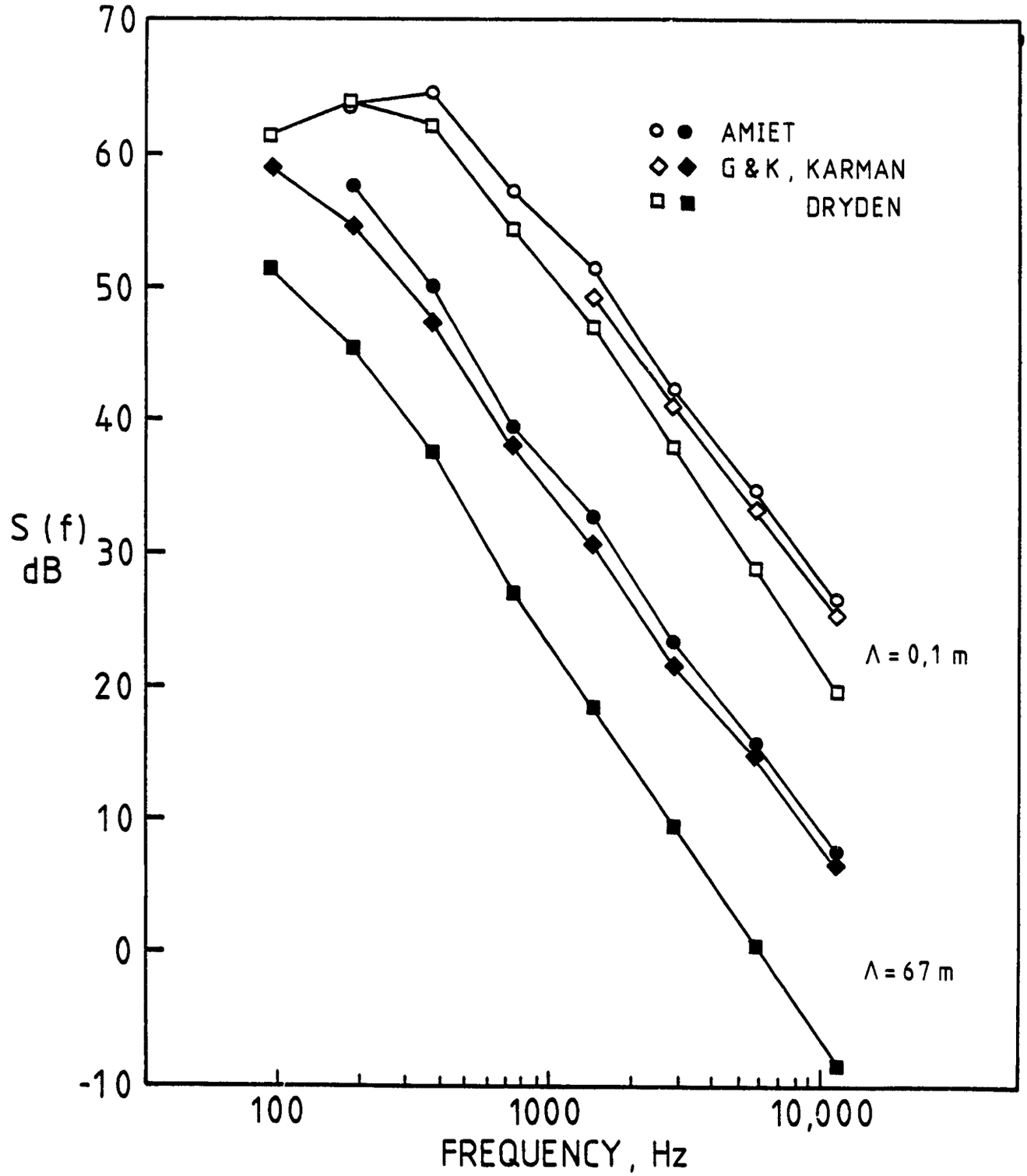

Figure 35 Effect of Turbulent Integral Scale on Rotor Inflow Turbulence Noise calculations, UH-1, $\phi = -90°$, $\sqrt{\overline{w^2}} = 1$ m/s

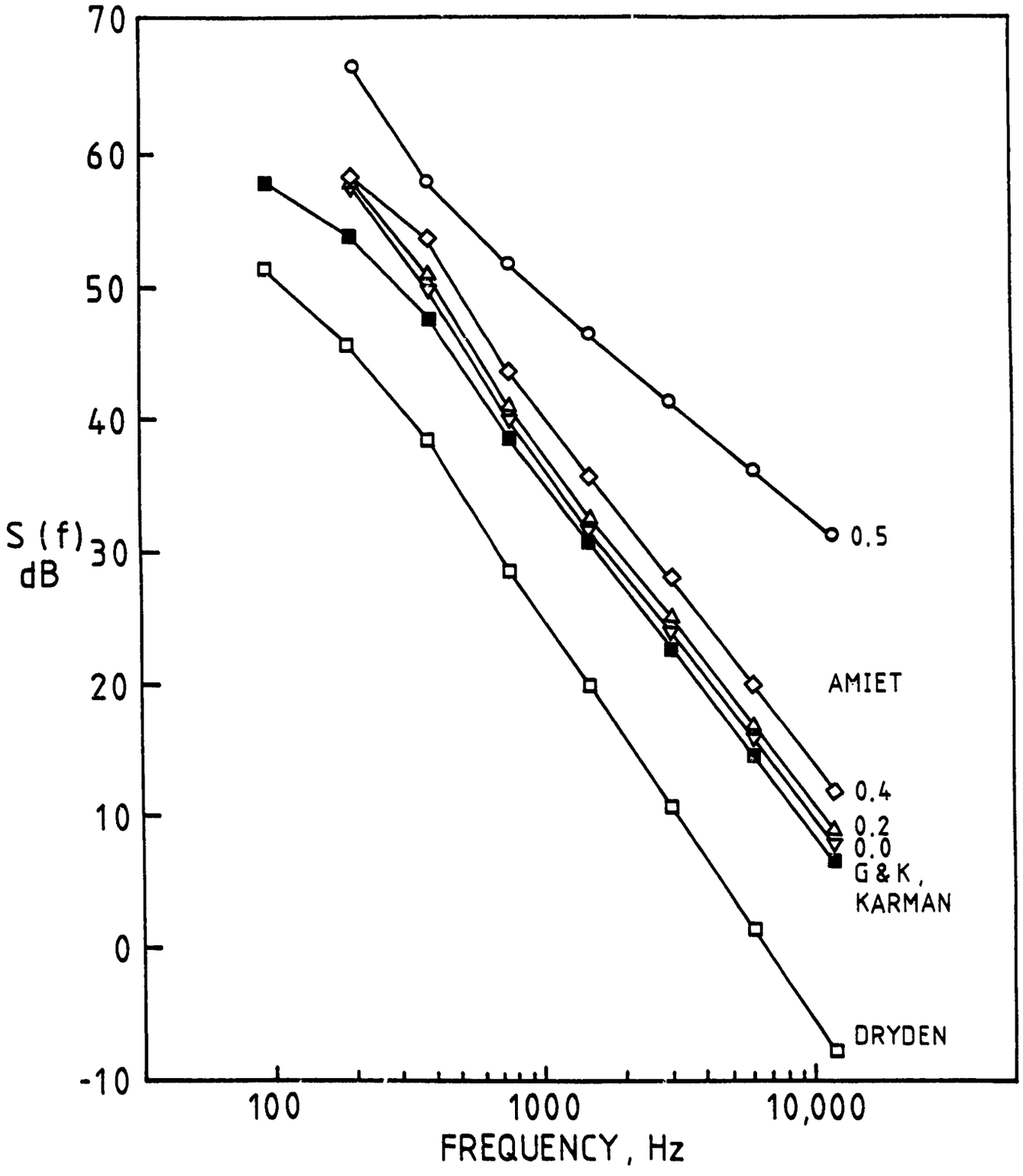

Figure 36 Effect of advance ratio on rotor inflow turbulence noise
Calculations UH-1, ϕ = -60°, Λ = 67 m, $\sqrt{w^2}$ = 1 m/s

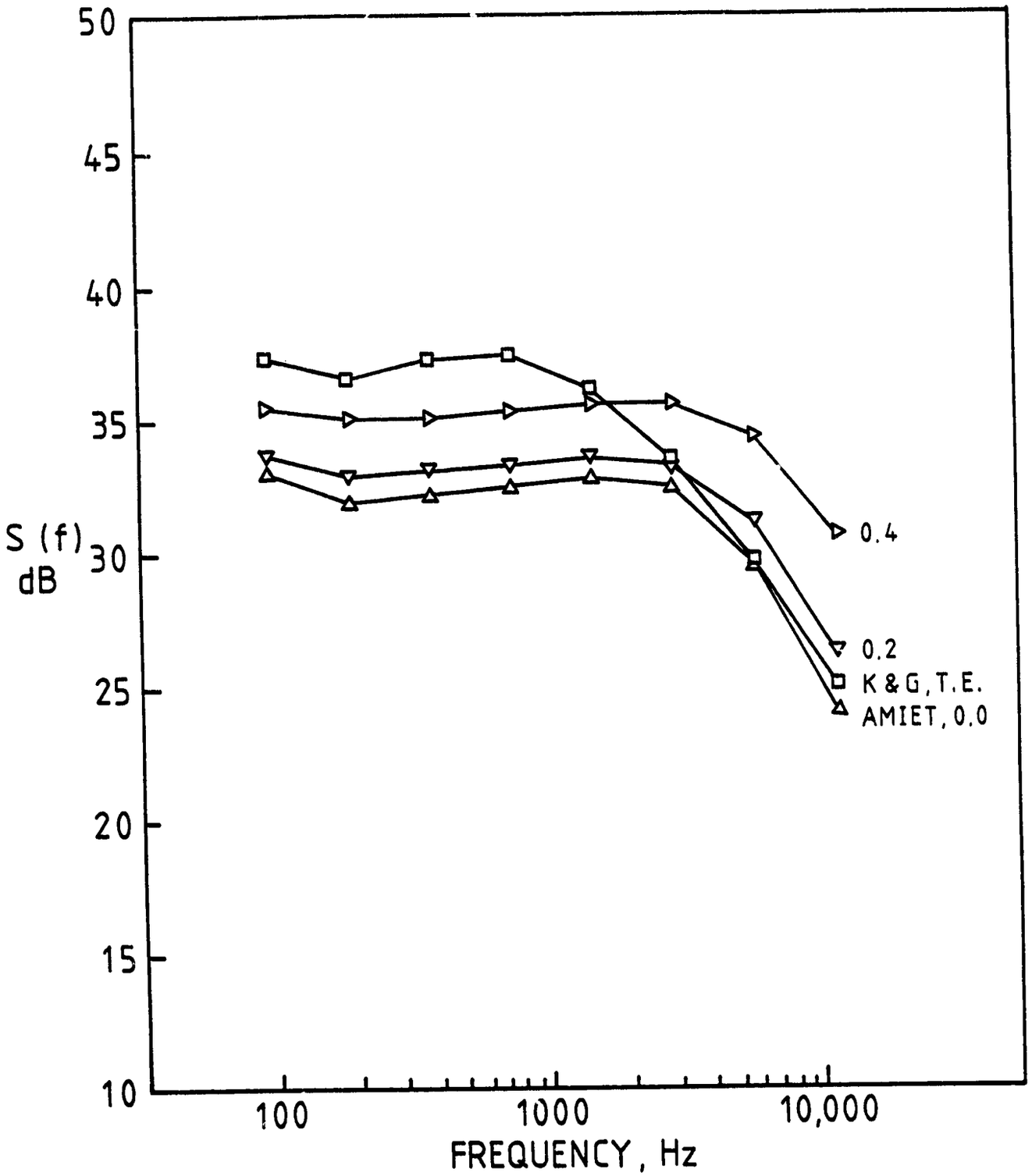

Figure 37 Effect of Advance Ratio on Rotor Trailing Edge Noise Calculations, UH-1, $\phi = -90°$

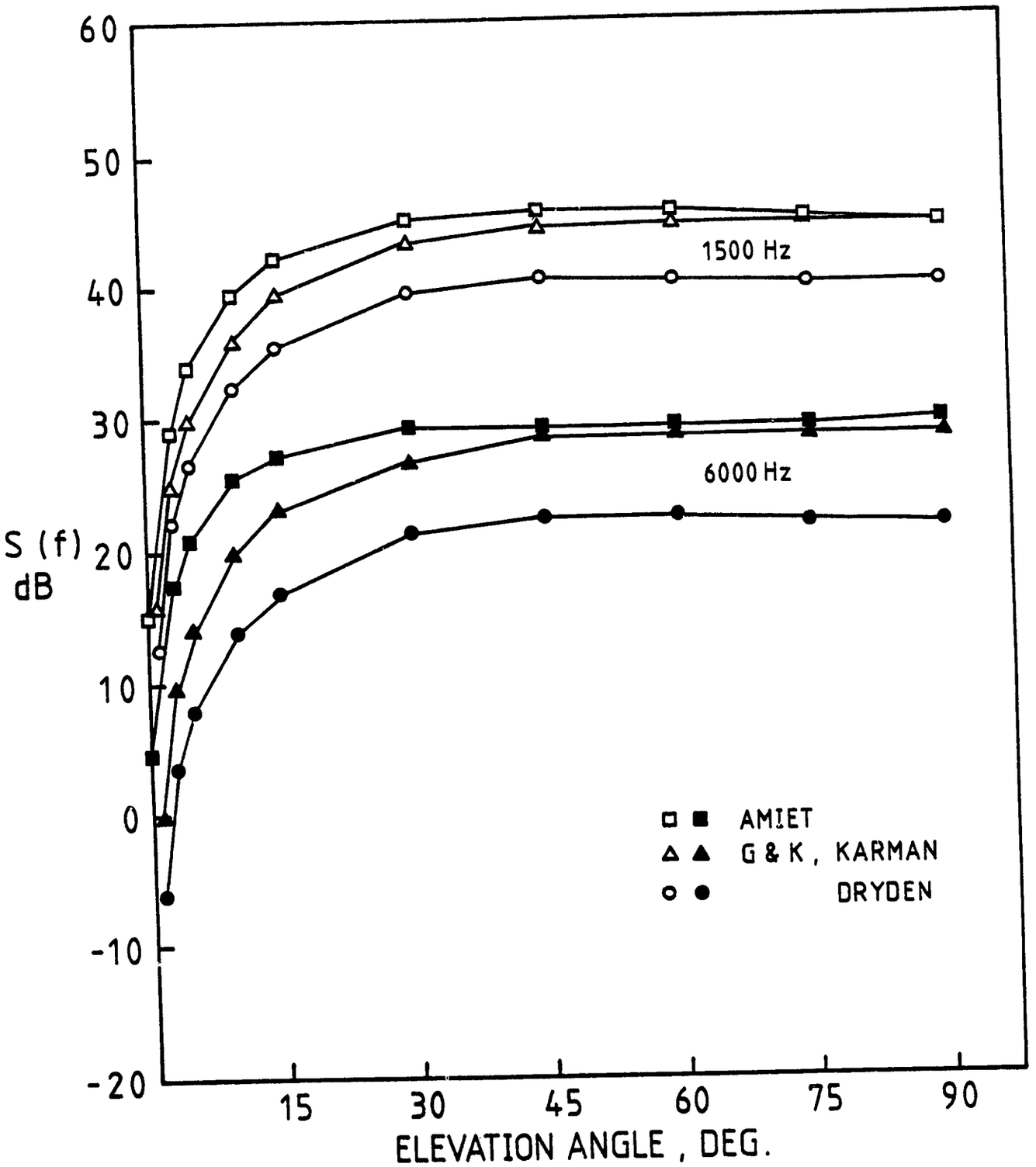

Figure 38 Directionality of Inflow Turbulence Noise for Both 1500 Hz, S55 Full Scale Rotor as in Leverton's Experiment (55), Λ = 0.57 m, $\sqrt{\overline{w^2}}$ = 1 m/s

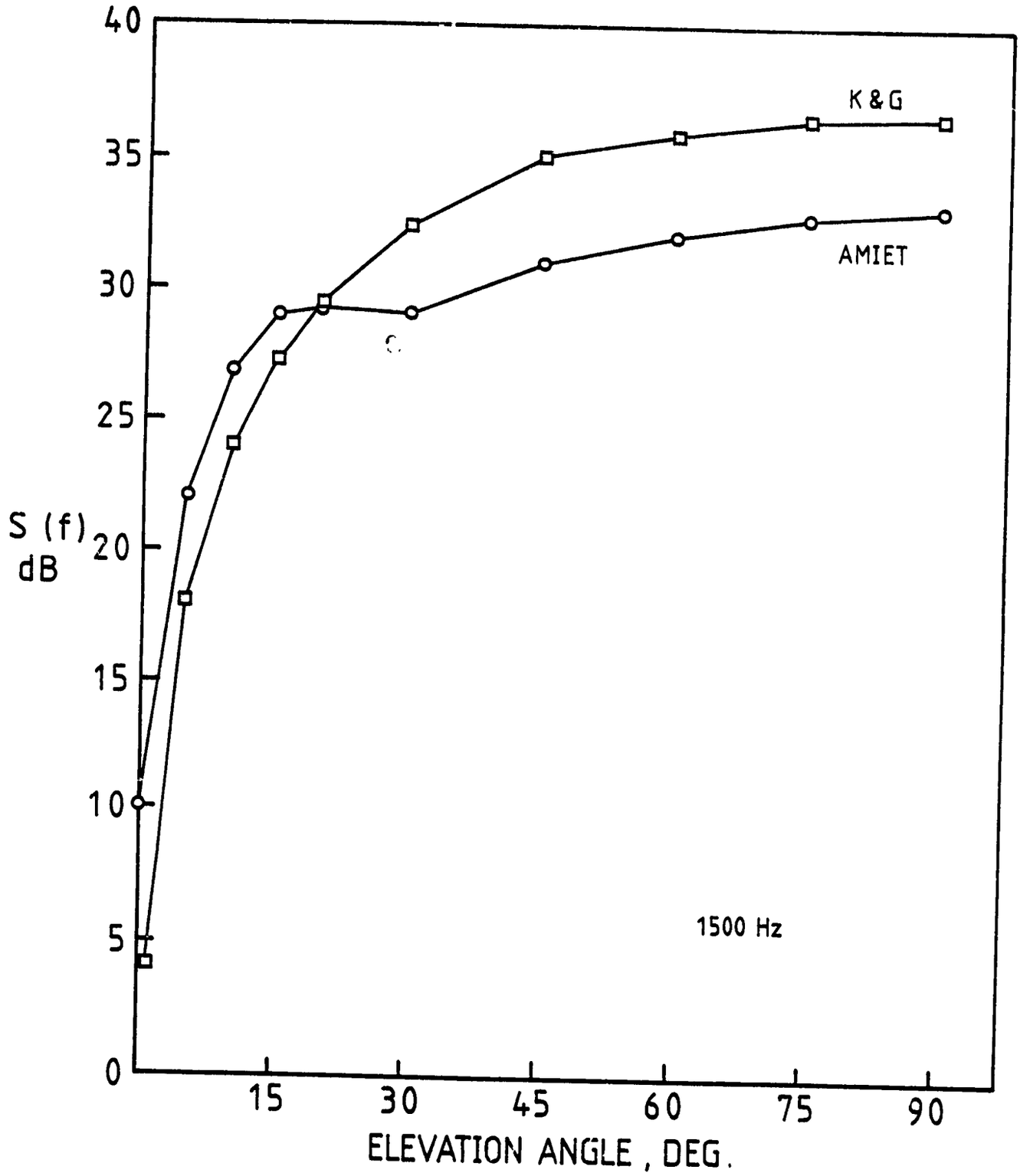

Figure 39 Directionality of Rotor Trailing Edge Noise, 1500 Hz, Same Rotor Used as in Figure 38

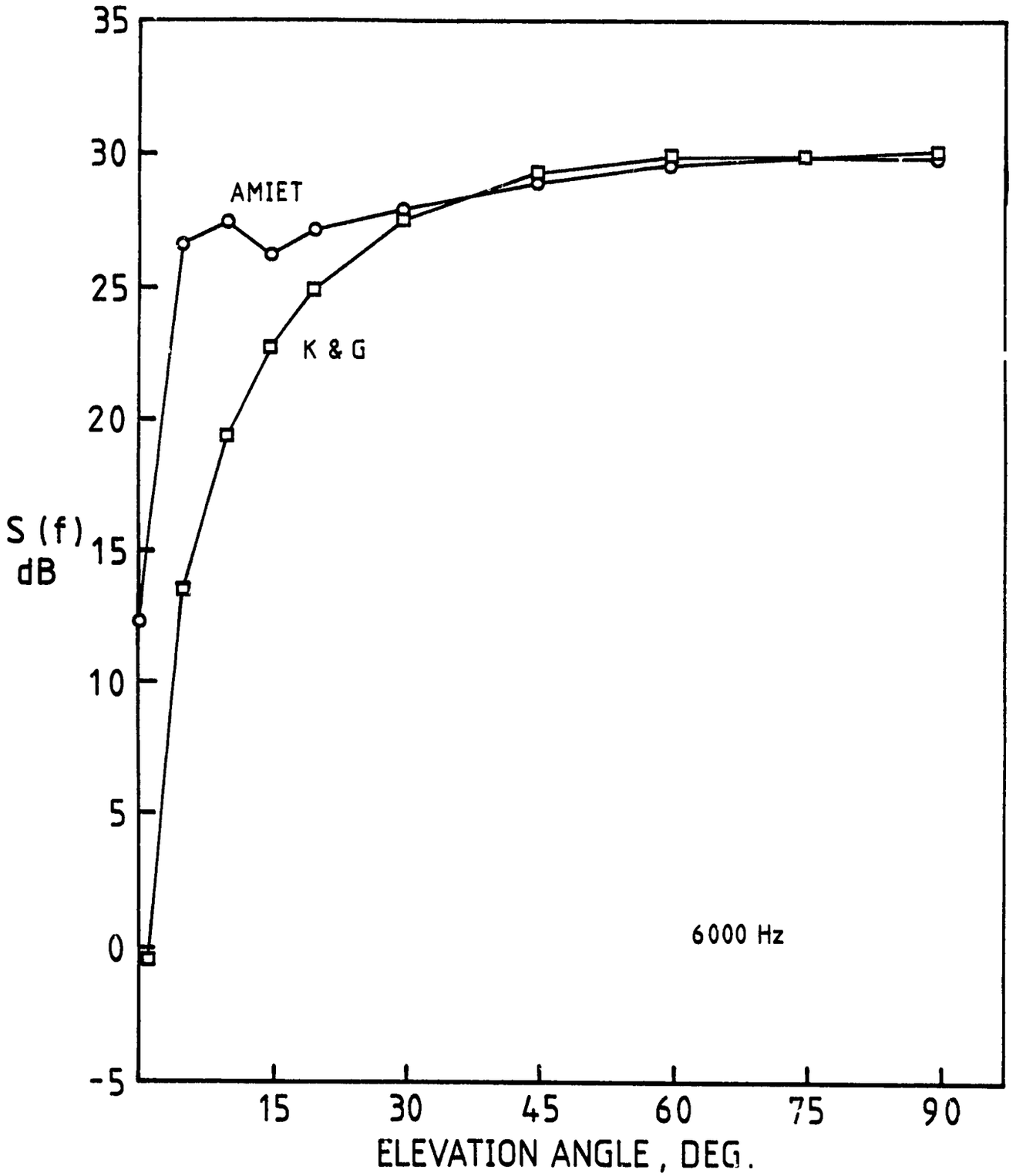

Figure 40 Directionality of Rotor Trailing Edge Noise, 6000 Hz, Same Rotor Used as in Figure 38

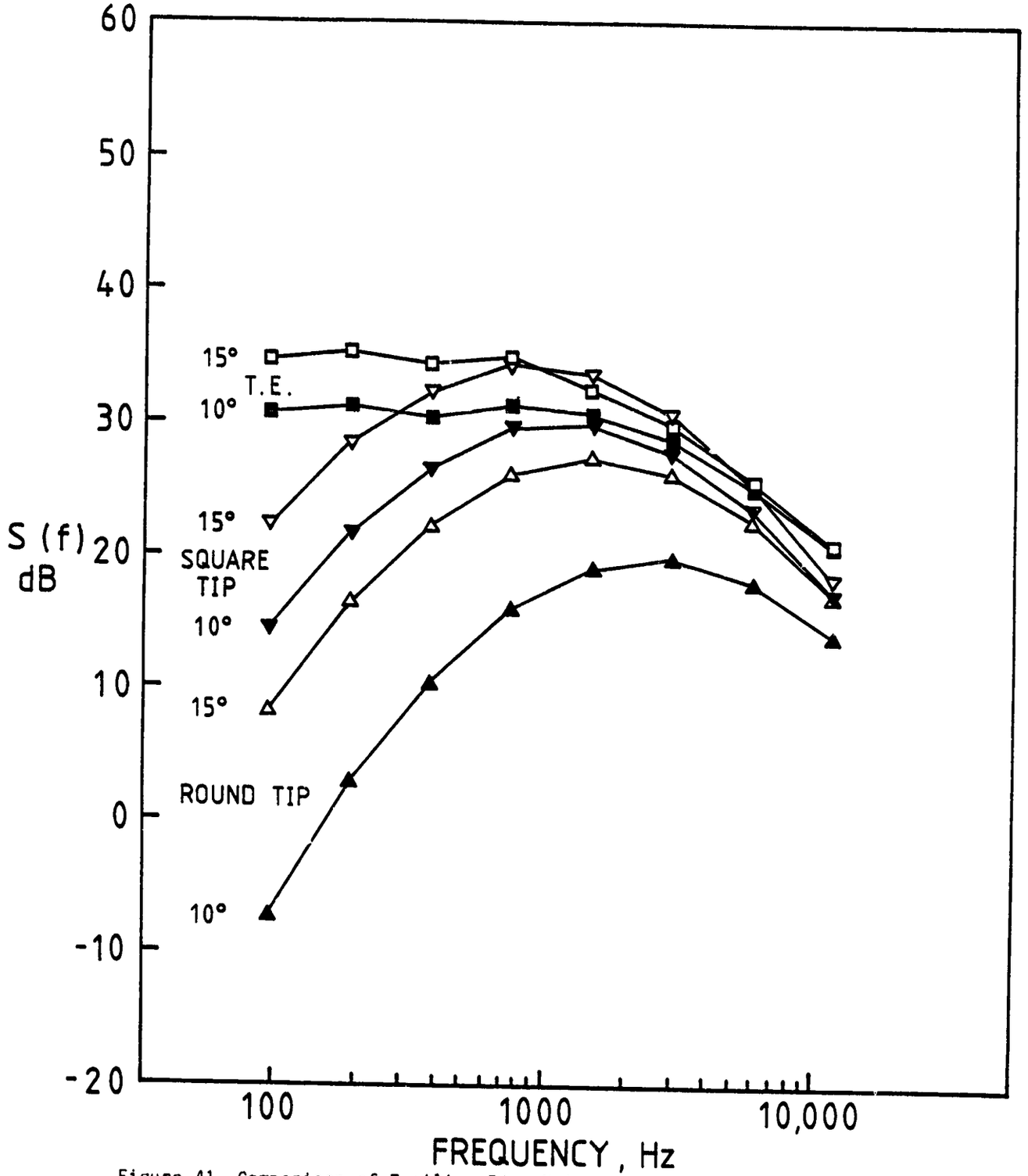

Figure 41 Comparison of Trailing Edge Noise and Tip Vortex Noise (with Different Tip Shapes) Calculations for 10° and 15° Rotor Pitch, UH-1, $\phi = -27°$

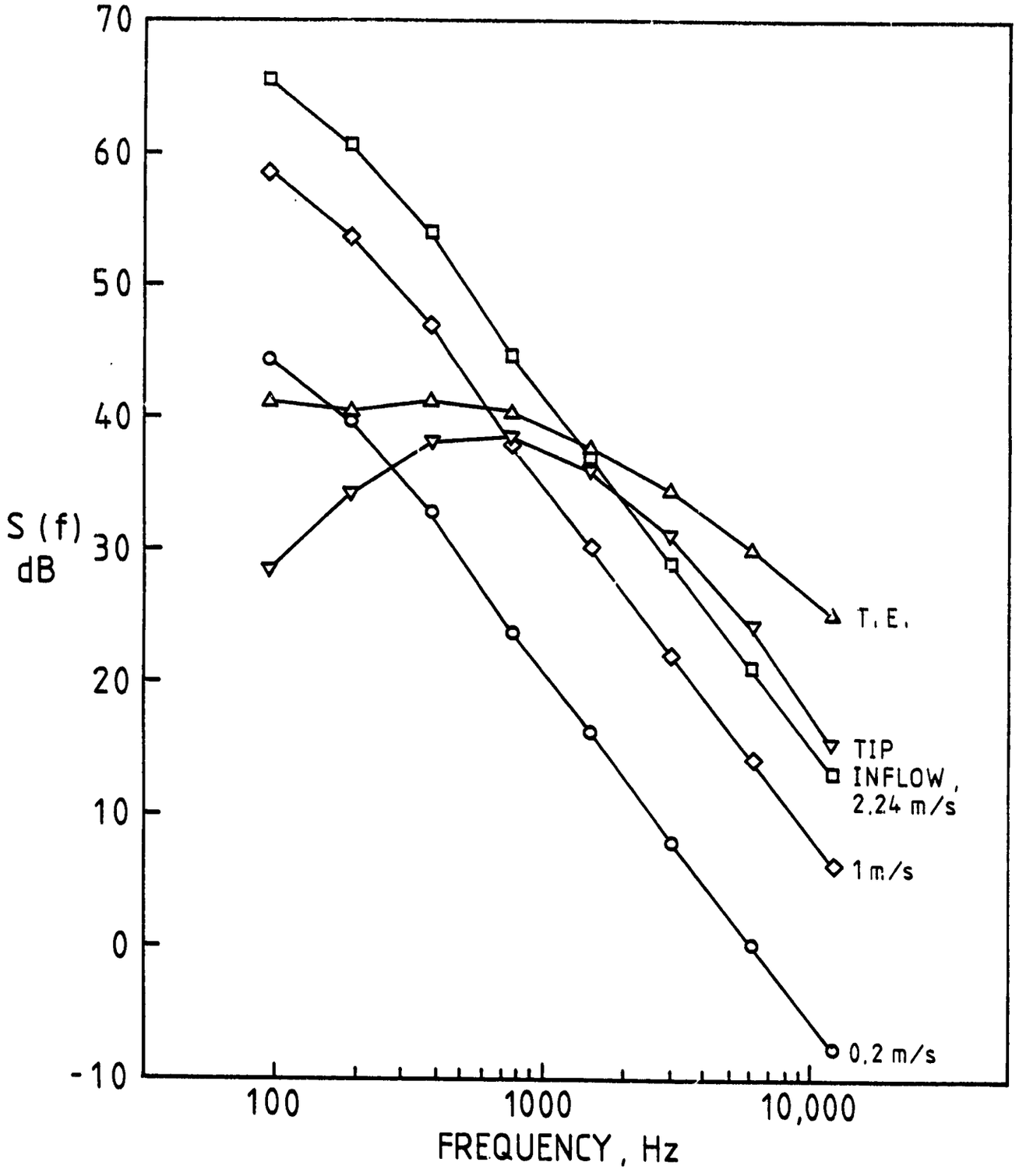

Figure 42 Noise Calculations for UH-1 Helicopter's Main Rotor, r = 74.8 m, ϕ = -78.5°, Λ = 67 m

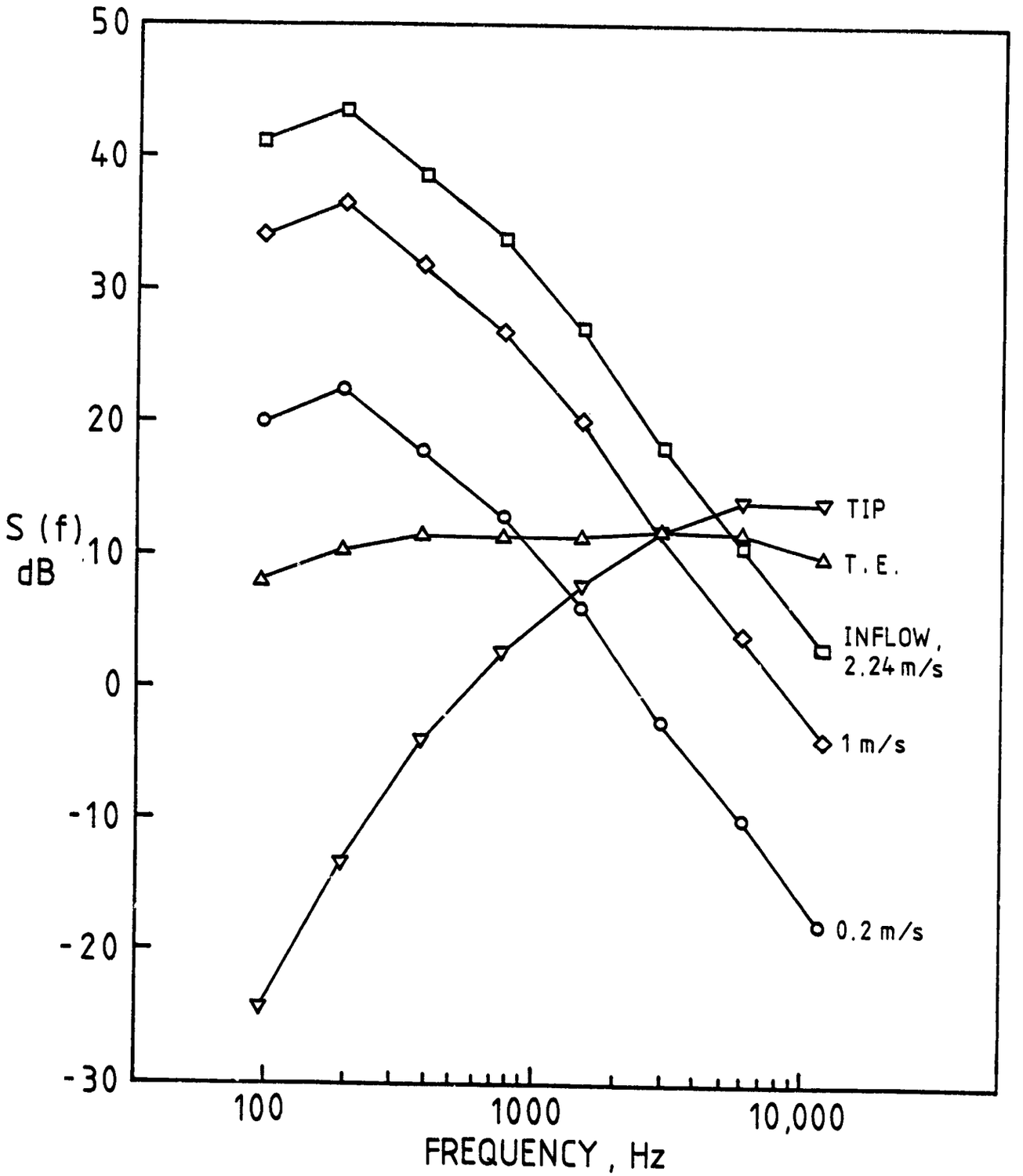

Figure 43 Noise Calculations for UH-1 Helicopter's Tail Rotor, Same Conditions as in Figure 42

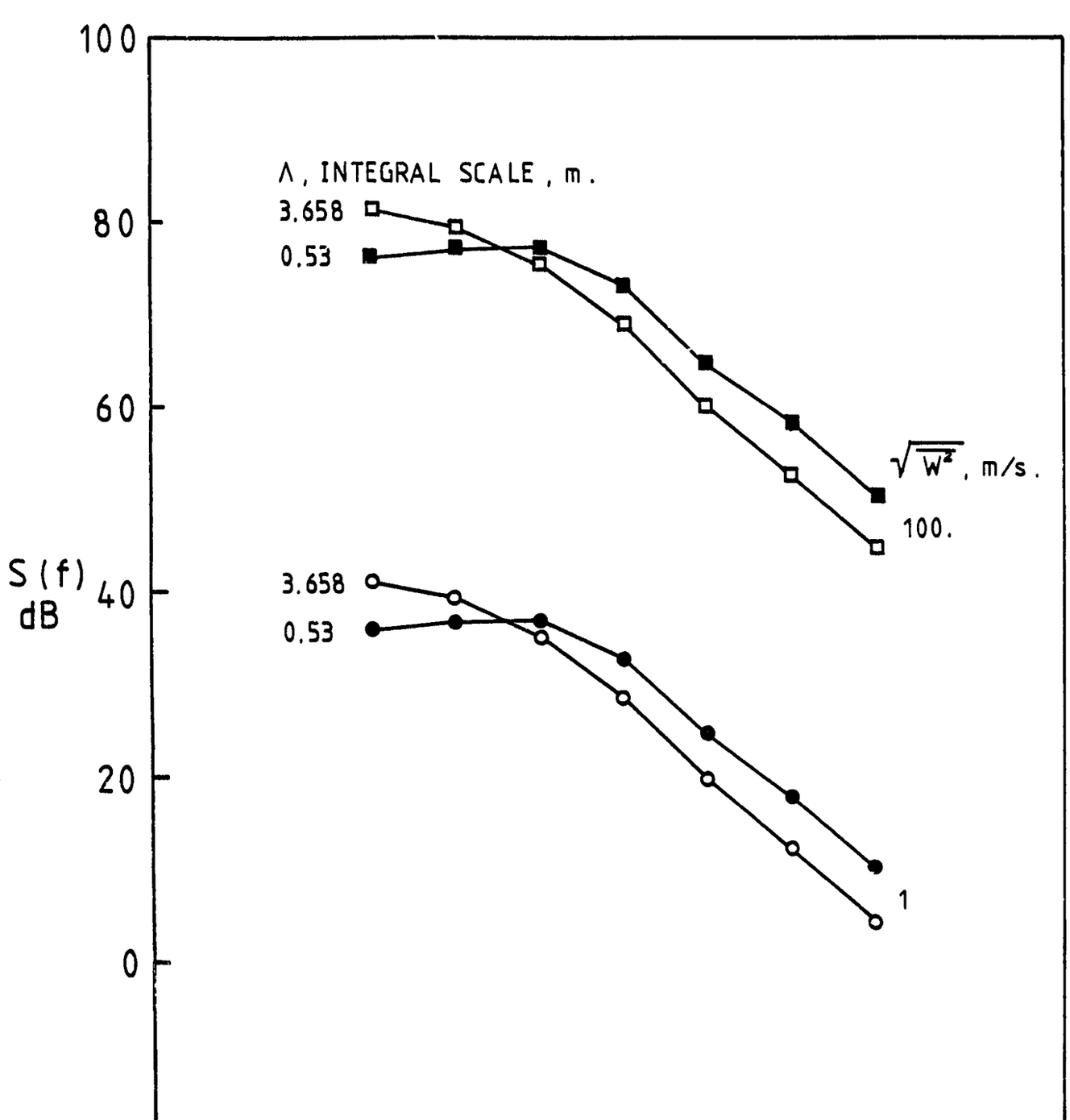

Figure 44 Effect of Main Rotor Wake Being Ingesting by the Tail Rotor, UH-1; Various Assumptions for Turbulent Intensity and Scale

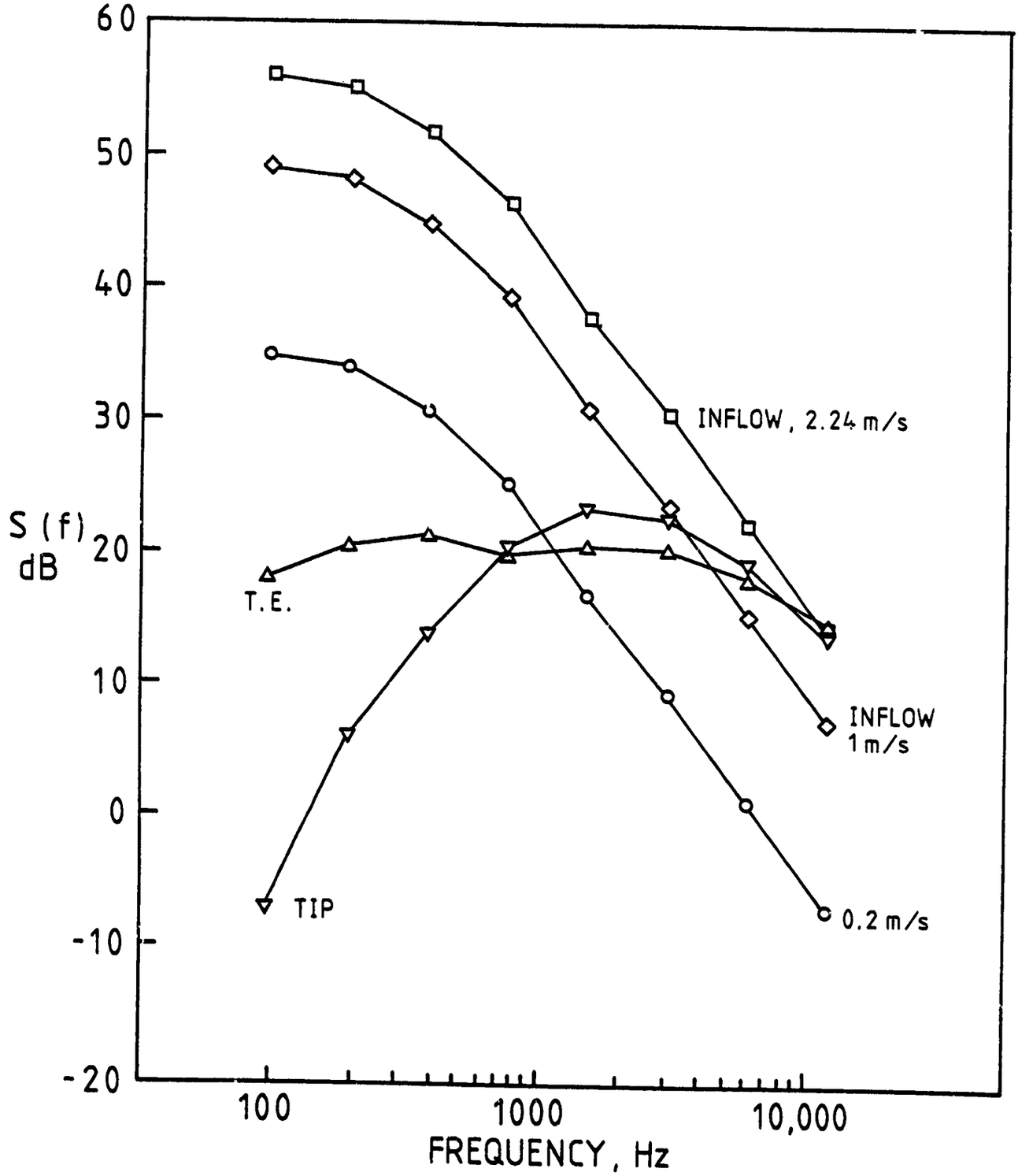

Figure 45 Noise Calculations for a Typical Light Aircraft Propeller, Static on Ground $\phi = -90°$, $\Lambda = 2$ m, 4° Angle of Attack

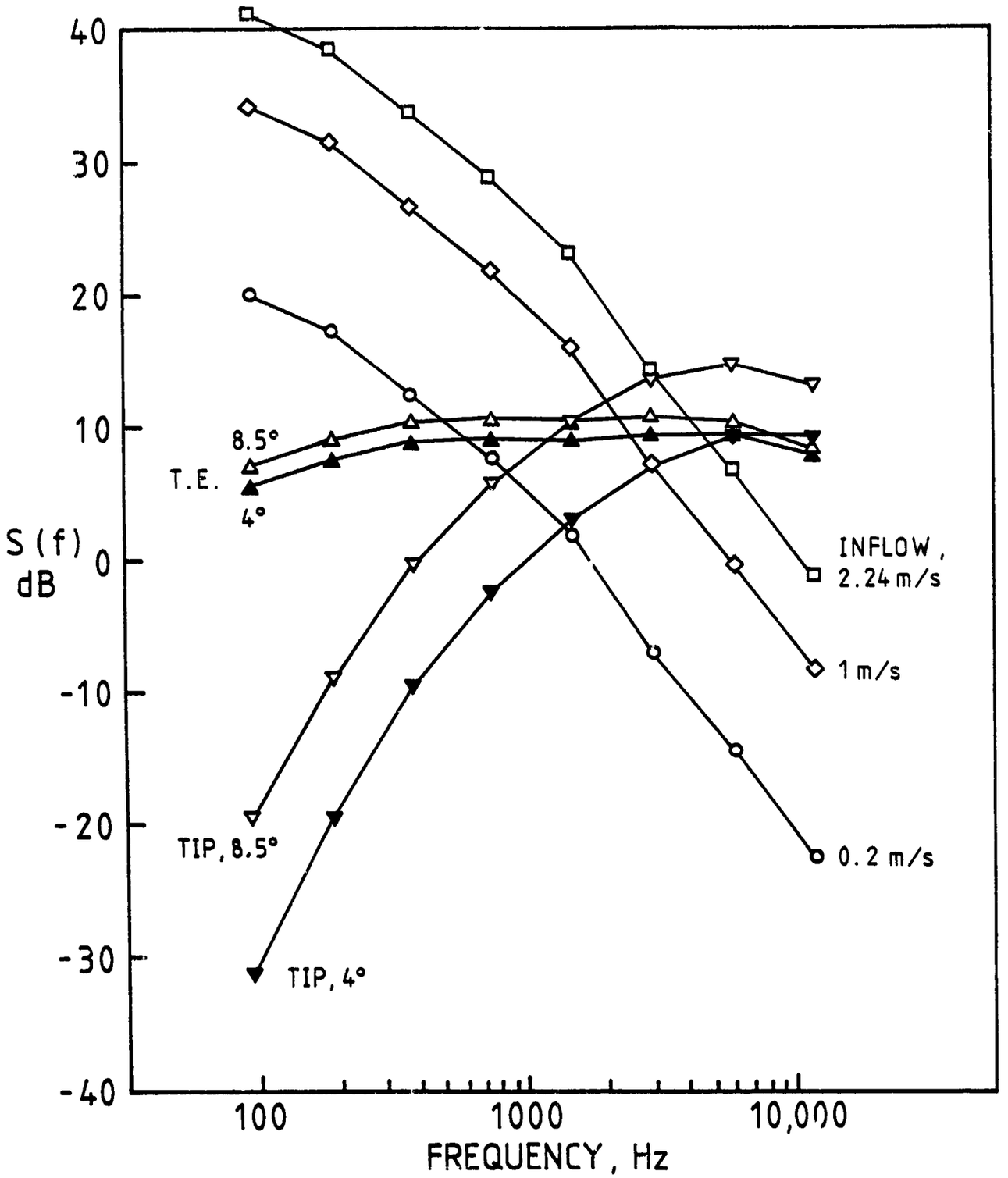

Figure 46 Noise Calculations for a Typical Light Aircraft Propeller, Fly-over, r = 74.8 m, ϕ = -78.5°, Λ = 67 m, 4° and 8.5° Angle of Attack

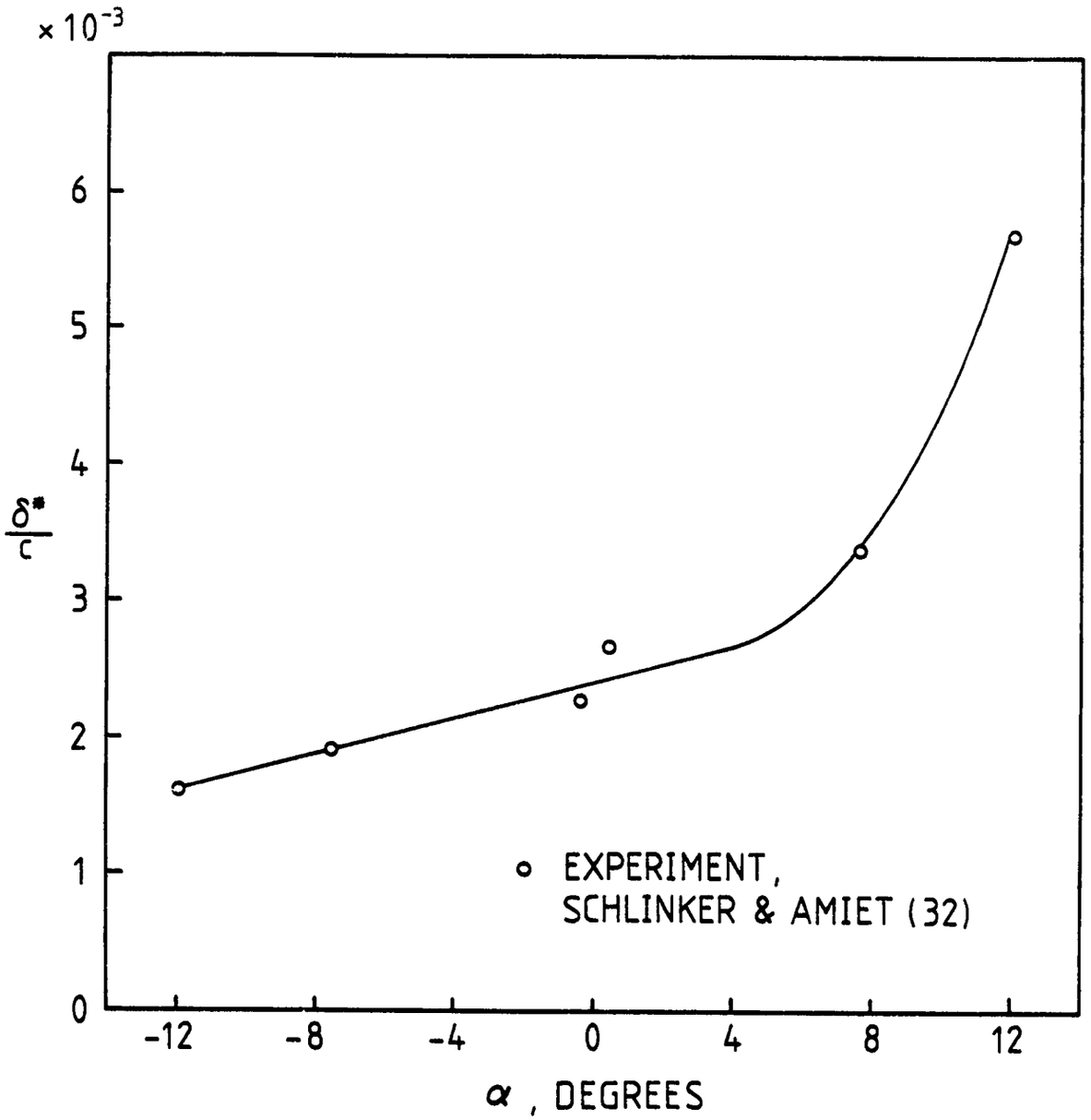

Figure A-1 Variation of δ^* with α

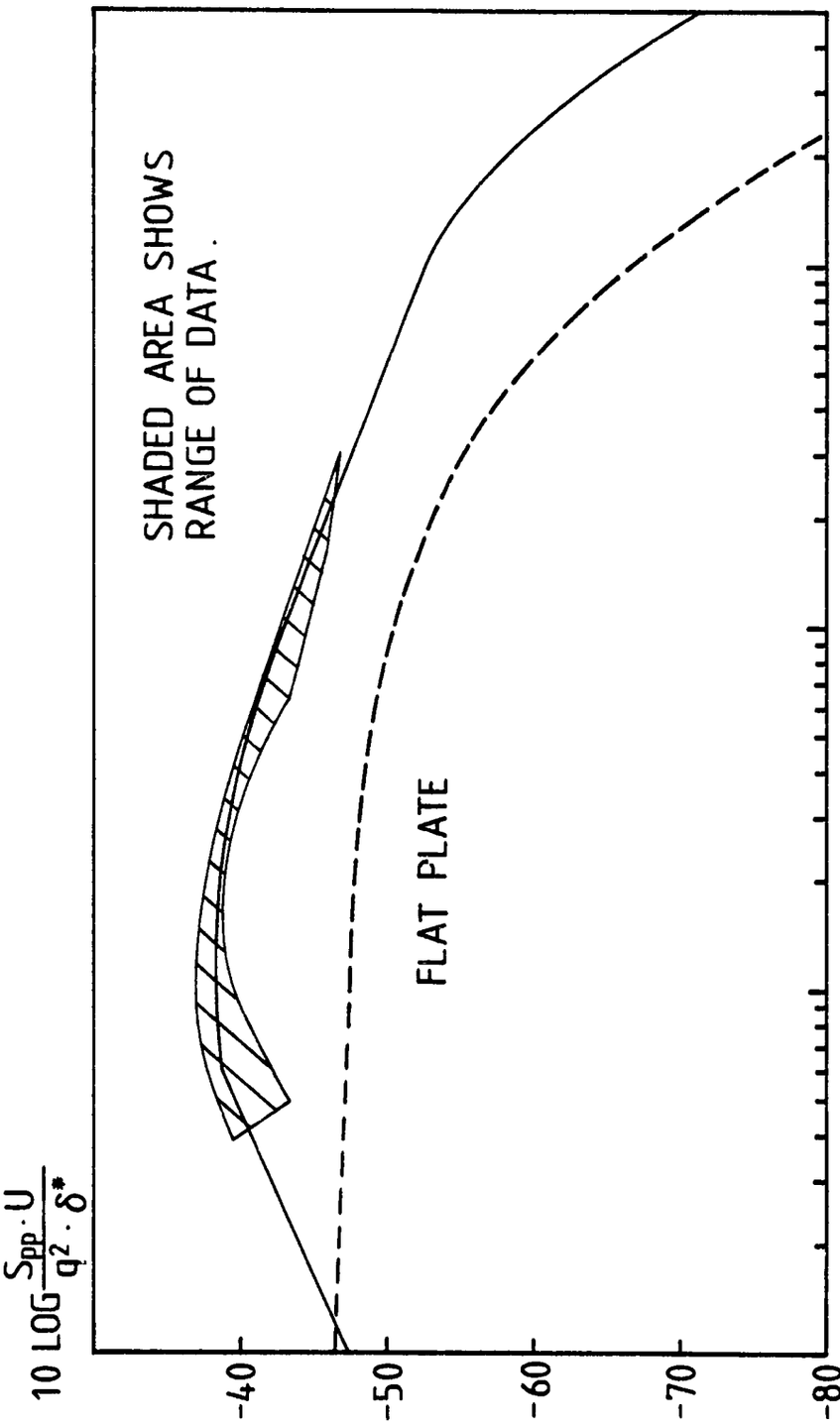

Figure A-2 Plots of $S_0(\tilde{\omega})$ versus $\tilde{\omega}$

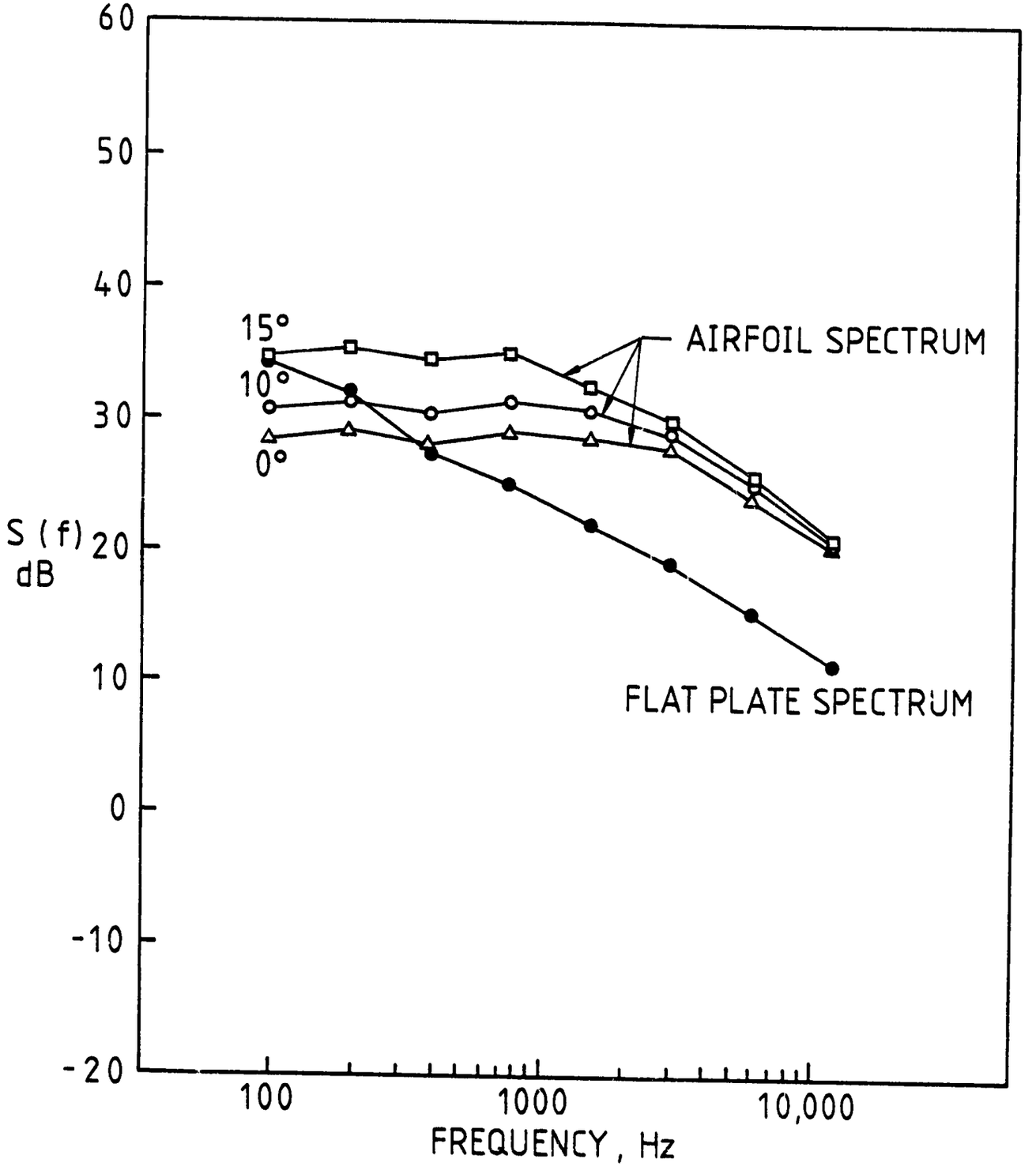

Figure A-3 Effect of Rotor Pitch on Trailing Edge Noise, UH-1, ϕ = -27°

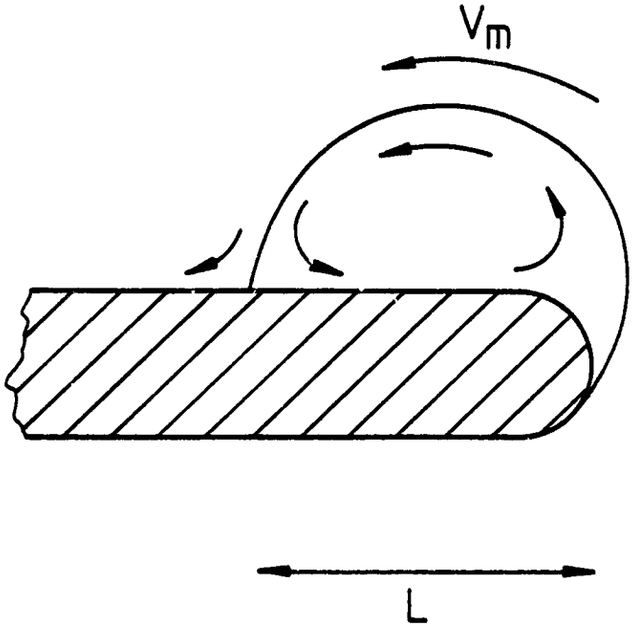

Figure B-1 Cross Flow Plane Model or Tip Flow Relating it to Two-Dimensional Separated Flow

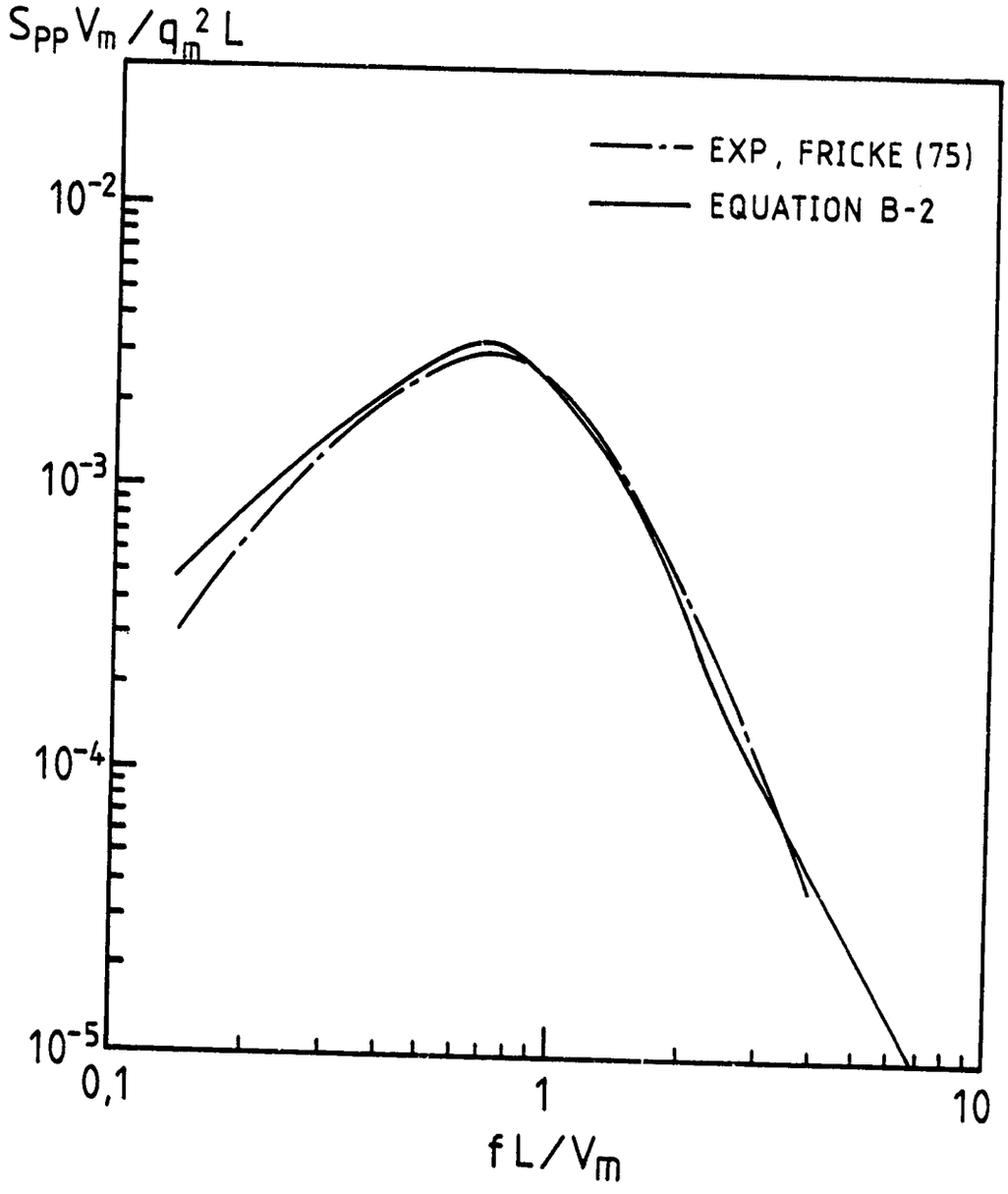

Figure B-2 Normalized Spectrum of Fricke and Stevenson (75) and Equation B-2 Fit to It

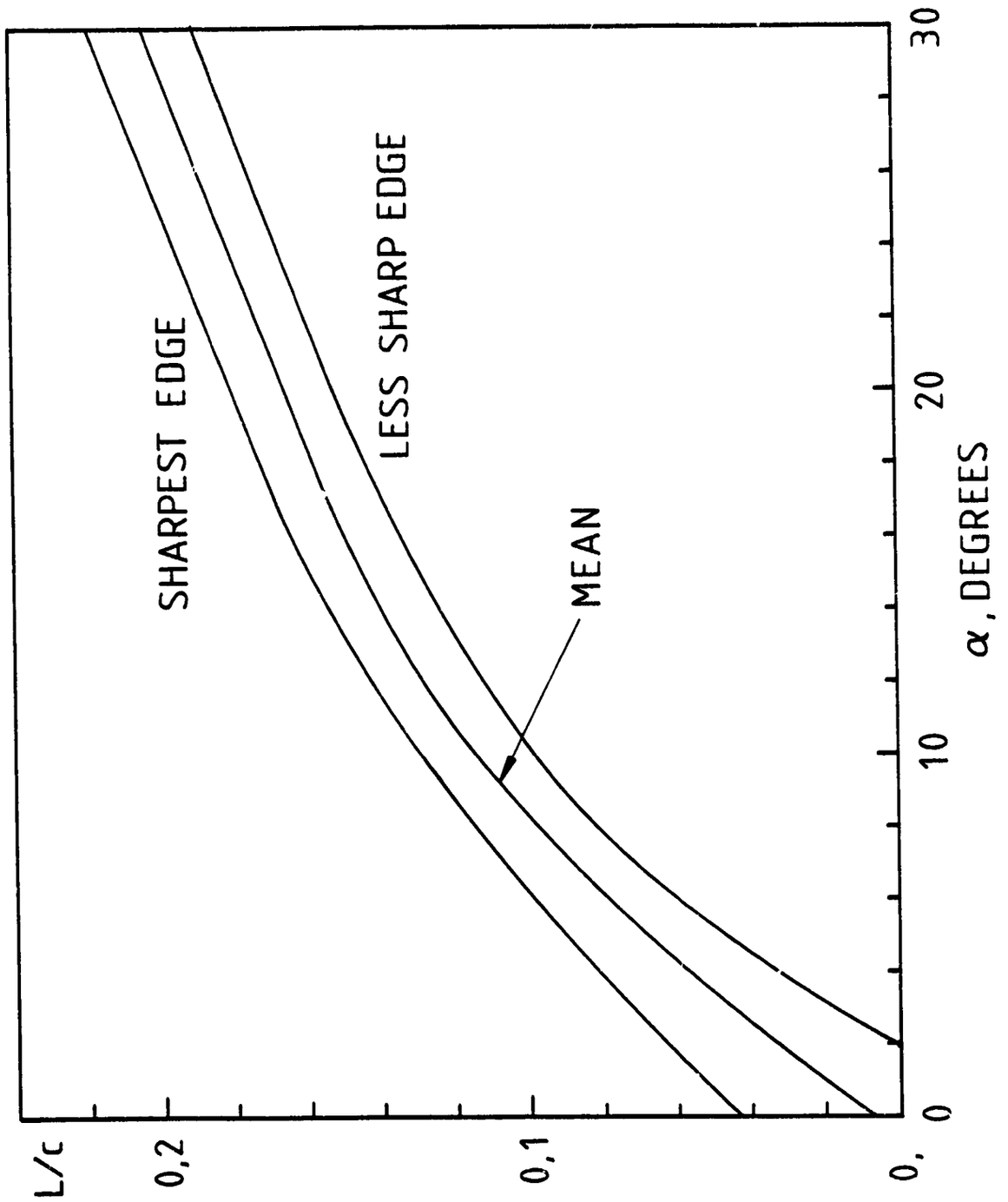

Figure B-3 Lateral Extent of Separatoin for Delta Wings Versus Angle of Attack

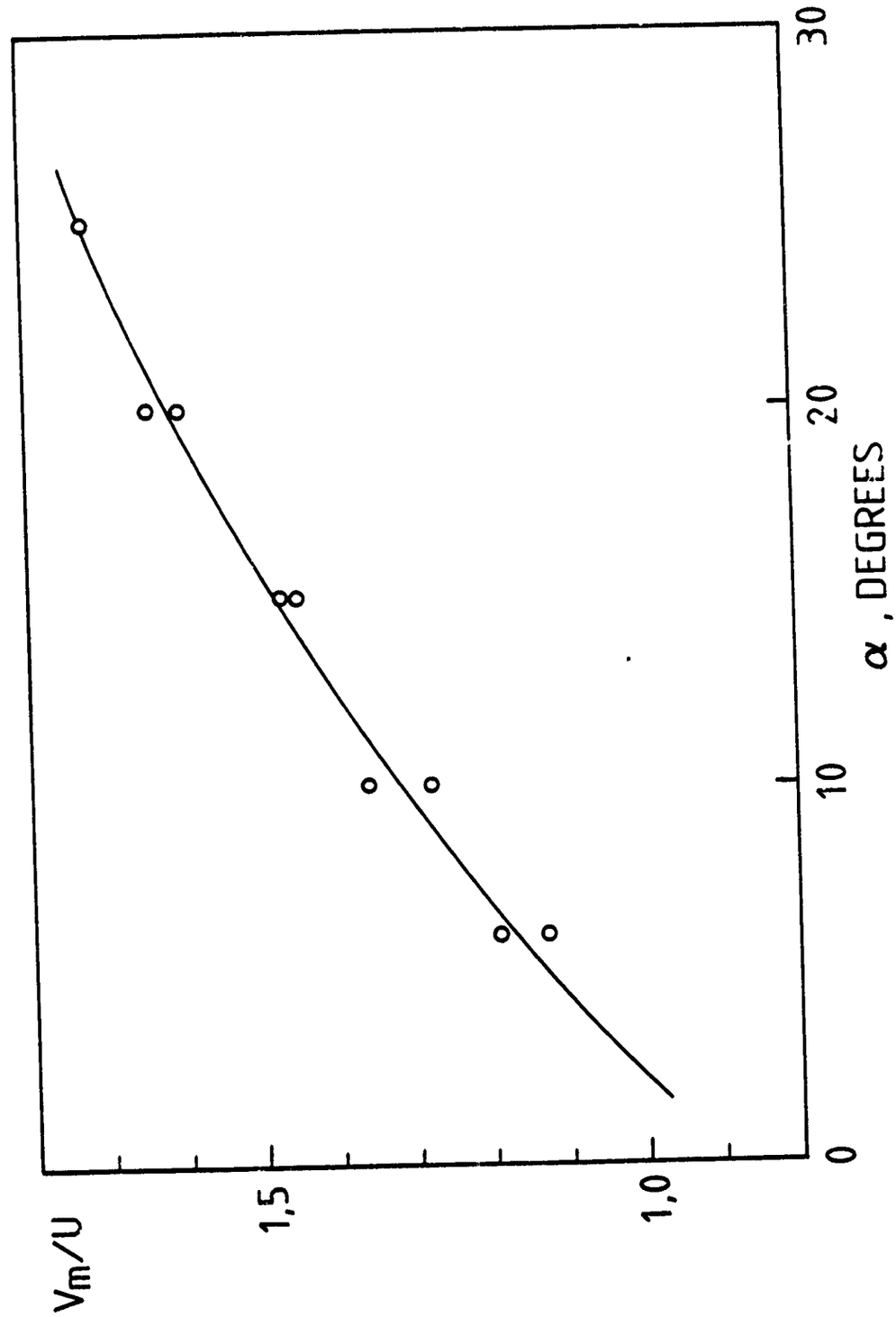

Figure B-4 Maximum Velocity Magnitude Ration for Delta Wings Versus Angle of Attack

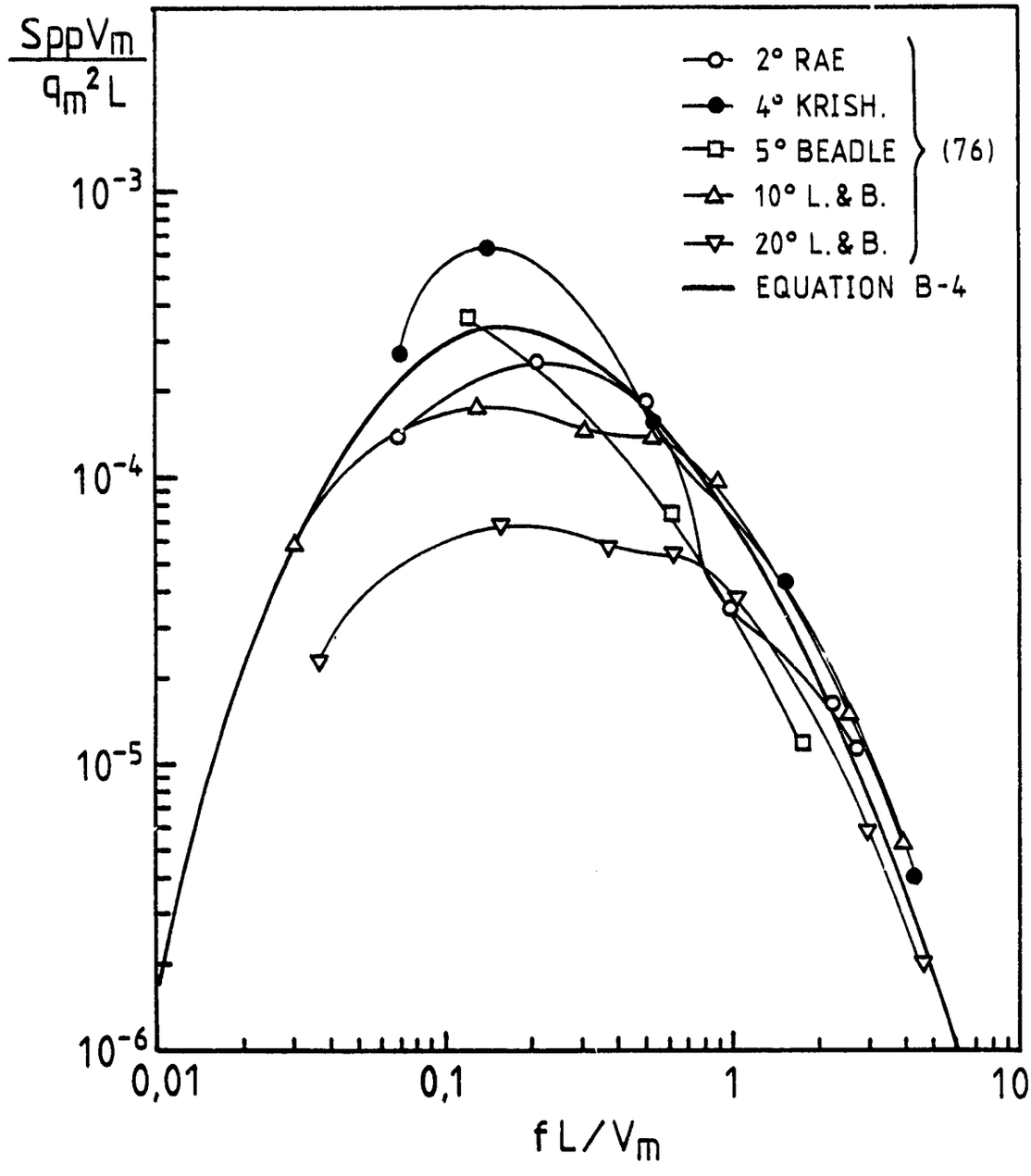

Figure B-5 Normalized Spectra from Richards and Fahy (76) and Equation B-4 Fit to Them

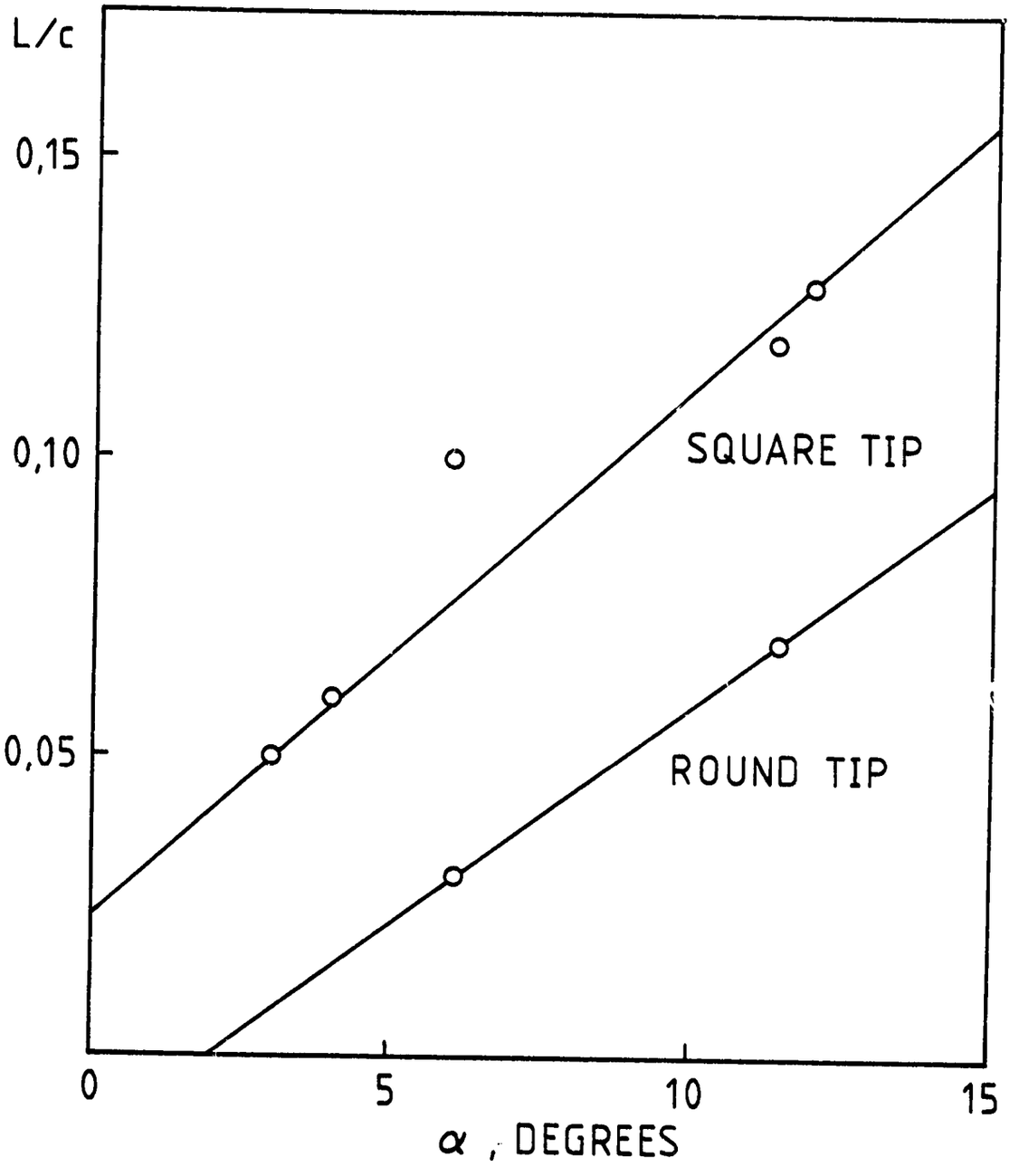

Figure B-6 Lateral Extent of Separation on Tips Versus Angle of Attack

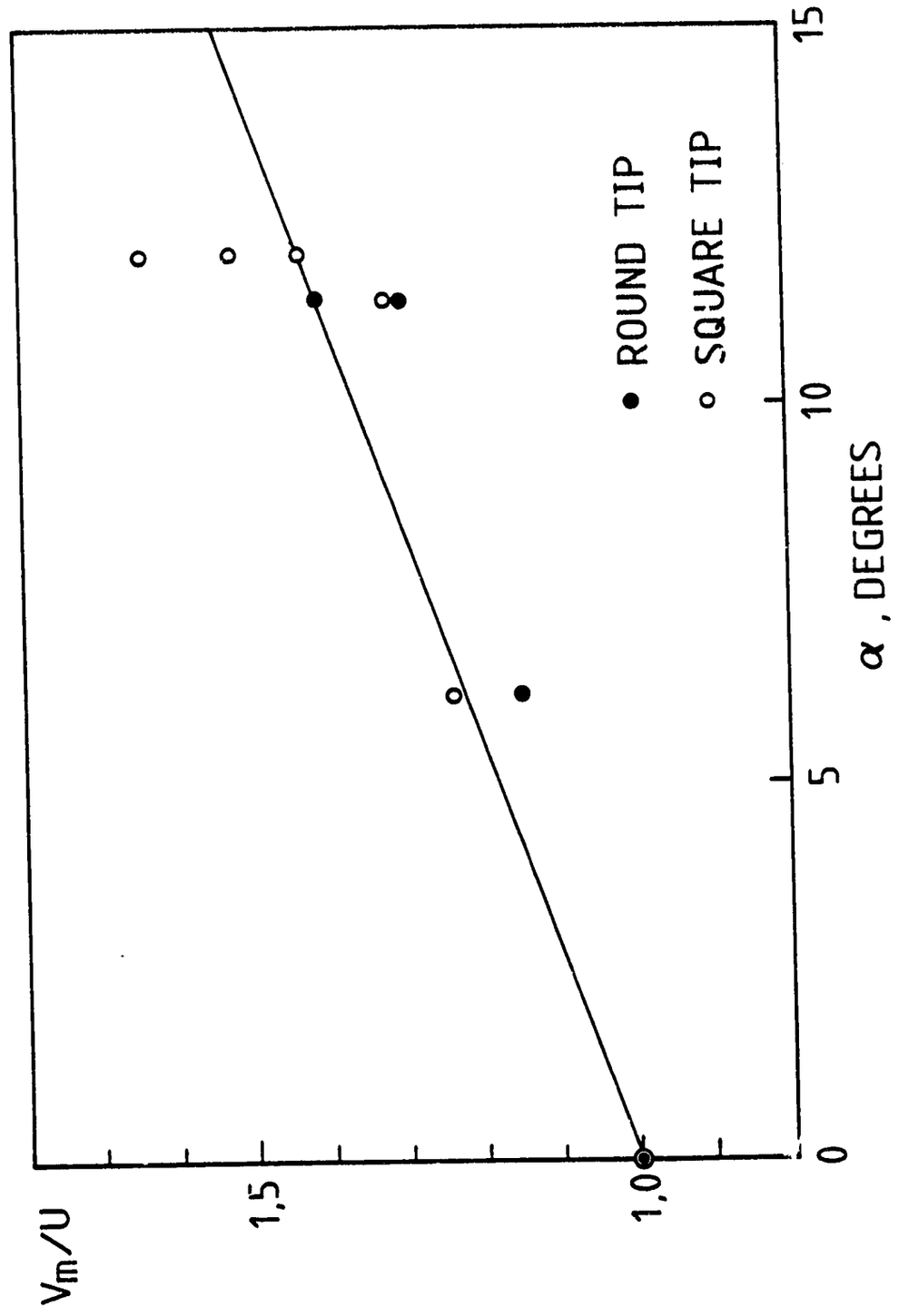

Figure B-7 Maximum Velocity Magnitude Ratio for Tips Versus Angle of Attack

END DATE
Jun 15, 1984